University of Eastern Piedmont "Amedeo Avogadro"
Department of Translational Medicine

PhD course in Food, Health, and Longevity
PhD cycle: XXXV

IMPACT OF THERAPY INDUCED SENESCENCE IN CANCEROUS AND NON-CANCEROUS CELLS

SSD: MED/06

A Dissertation Submitted for the Degree of Doctor of Philosophy

Candidate: Feba Mariam Varughese

Coordinator: Prof. Antonia Follenzi

Supervisor: Prof. Alessandra Gennari

The process of scientific discovery is, in effect, a continual flight from wonder.

-Albert Einstien

Wear gratitude like a cloak and it will feed every corner of your life.

-Rumi

Table of Contents

Summary

Cellular Senescence is an irreversible state of replicative arrest characterized by upregulation of cyclin-dependent kinase inhibitors. Over recent years, compelling evidence supports that senescent cell accumulation negatively influences longevity by driving age-related conditions, including cancer. In this perspective, a better characterization of the function as well as the clearance of senescent cells might provide an important cue to generate innovative strategies for age-related pathologies and extend healthy lifespan.

In Section I, we mainly assessed whether the circulating CD3 positive T senescent cells, MDSCs, blood based IIBs and plasma metabolites have any predictive role in response to NAT in operable BC patients, in terms of pCR and that might be helpful for early identification of those patients who are unlikely benefit from NAT. The CD3+CD4-CD8- DN T cells were isolated from PB by Ficoll stratification at baseline and after NAT, before surgery. The relative expression of p16 and p21 were used to characterize T-cell senescence, by RT-PCR. Further, we characterized sub-populations of MDSCs only at baseline among pCR and RD groups using Flow Cytometry. Then, assessed some inflammatory markers on blood such as SII and PIV at two timepoints. Finally, the plasma associated metabolomics analysis was performed at baseline and stratified patients based upon pCR achievement. From June 2020 to January 2023, ninety patients have been enrolled. Out of 90 patients, only 60 patients were included for final analysis. Of these, 25 (42%) were Triple Negative, 22 (37%) HER2-positive and 13 (21%) Luminal B. 33/60 (55%) achieved pCR. No significant difference observed in p16 and p21 expression at baseline and after NAT in patients who achieved pCR. Notably, patients with RD had a statistically higher significance in p16 and p21 expression after NAT. Further, verified the predictive role of MDSCs, M-MDSCs, PMN-MDSCs, LOX1+PMN-MDSC, blood based IIBs like SII and PIV. Unfortunately, above mentioned factors did not have any significant association with pCR. Interestingly, untargeted metabolomic analysis on patient's plasma represented 25 molecules carrying predictive value in terms of NAT response. These preliminary results suggest that the increase of circulating senescent T-cells and PB based IIBs after NAT is correlated with a worse response to treatment. Moreover, our data on metabolic analysis demonstrated specific plasma metabolomic changes associated with pCR response

resulting the definition of algorithms and interventional trials set the basis to predict therapy response and build a circulating 'pCR-likely' profile, respectively.

In Section II, we utilized an invitro normal cell lines to induce TIS and characterized SASP depending upon the treatment regimens. CDK4/6i can lead non-malignant cells to a poorly characterized senescent state. An interesting aspect of CDK4/6i is their immunomodulatory and immunogenic effect. The immunomodulatory effect of CDK4/6i in chemotherapy-induced nonmalignant senescent cells remains elusive. The rationale of this project is to determine the functional role of CDK4/6i-induced senescence and SASP nature after the doxorubicin treatment alone or in combination with abemaciclib in non-malignant cells in invitro models. We induced senescence in normal cell lines such as MDFs, 3MR, BJ and hTERT RPE-1 using doxorubicin alone and in combination with abemaciclib and validated senescence induction using SA- β-gal and EdU staining. By RT-PCR, we analysed not only the senescence biomarkers but also some p53 and NFkB targets to characterize SASP nature after treatment. Then performed cancer cell proliferation assay, co-culture experiments, and analysed conditioned media using IncuCyte®Zoom live- cell analysis system. Our results indicated that senescence was successfully induced in all cell lines treated with both groups. Notably, NF-κB-Associated Secretory Phenotype (NASP) was observed only in doxorubicin alone treated condition. Further, our data based on IncuCyte experiments suggested that reduction of cancer cells proliferation in the presence of doxorubicin plus abemaciclib and abemaciclib alone treatment were neither dependent on senescent status nor cell type. Finally, observed the proliferation of MDAMB231 and BT549 were less in the CM of abemaciclib alone treated conditions in both BJ and RPE cell lines indicating that abemaciclib treatment might manifests distinctive SASP components.

In conclusion, the two studies on therapy-induced senescence presented in this thesis indicated that TIS may produce increased immune activity and reduced toxicity associated side effects based upon the treatment regimens. A final and perhaps the most important thing is to figure out the key knowledge gaps in this emerging field to improve treatment outcomes for cancer patients.

Riepilogo

La senescenza cellulare è uno stato irreversibile di arresto replicativo caratterizzato dalla sovraregolazione degli inibitori della chinasi ciclina-dipendente. Negli ultimi anni, prove convincenti sostengono che l'accumulo di cellule senescenti influenza negativamente la longevità guidando condizioni legate all'età, incluso il cancro. In questa prospettiva, una migliore caratterizzazione della funzione e dell'eliminazione delle cellule senescenti potrebbe essere uno strumento per generare strategie innovative per le patologie legate all'età e prolungare la durata della vita.

Nella Sezione I, abbiamo valutato principalmente se le cellule senescenti T CD3 positive circolanti, le MDSC, gli IIB basati sul sangue e i metaboliti plasmatici abbiano un ruolo predittivo in risposta al NAT nei pazienti operabili con BC, in termini di pCR e che potrebbero essere utili per l'identificazione precoce di quei pazienti che difficilmente traggono beneficio dalla NAT. Le cellule T CD3+CD4-CD8-DN sono state isolate da PB mediante stratificazione Ficoll al basale e dopo NAT, prima dell'intervento chirurgico. L'espressione relativa di p16 e p21 è stata utilizzata per caratterizzare la senescenza delle cellule T, mediante RT-PCR. Inoltre, abbiamo caratterizzato le sottopopolazioni di MDSC solo al basale tra i gruppi pCR e RD utilizzando la citometria a flusso. Quindi, abbiamo valutato alcuni marcatori infiammatori nel sangue come SII e PIV in due time points. Infine, l'analisi della metabolomica associata al plasma è stata eseguita al basale e nei pazienti stratificati in base al raggiungimento della pCR. Da giugno 2020 a gennaio 2023 sono stati arruolati novanta pazienti. Su 90 pazienti, solo 60 pazienti sono stati inclusi per l'analisi finale. Di questi, 25 (42%) erano tripli negativi, 22 (37%) HER2-positivi e 13 (21%) Luminal B. 33/60 (55%) hanno ottenuto pCR. Nessuna differenza significativa osservata nell'espressione di p16 e p21 al basale e dopo NAT nei pazienti che hanno raggiunto pCR. In particolare, i pazienti con RD avevano un significato statisticamente più elevato nell'espressione di p16 e p21 dopo NAT. Inoltre, abbiamo verificato il ruolo predittivo di MDSC, M-MDSC, PMN-MDSC, LOX1+PMN-MDSC, IIB basati sul sangue come SII e PIV. Sfortunatamente, i fattori sopra menzionati non hanno avuto alcuna associazione significativa con pCR. È interessante notare che l'analisi metabolomica non mirata sul plasma del paziente rappresentava 25 molecole con valore predittivo in termini di risposta NAT. Questi risultati preliminari suggeriscono che l'aumento delle cellule T senescenti circolanti e delle IIB

basate su PB dopo NAT è correlato con una risposta peggiore al trattamento. Inoltre, i nostri dati sull'analisi metabolica hanno dimostrato specifici cambiamenti metabolomici plasmatici associati alla risposta pCR, risultanti dalla definizione di algoritmi e prove interventistiche, che hanno posto le basi per prevedere la risposta terapeutica e costruire un profilo circolante "pCR-associato", rispettivamente.

Nella Sezione II, abbiamo utilizzato linee cellulari normali in vitro per indurre TIS e caratterizzato SASP a seconda dei regimi di trattamento. CDK4/6i può portare le cellule non maligne a uno stato senescente scarsamente caratterizzato. Un aspetto interessante di CDK4/6i è il loro effetto immunomodulatore e immunogenico. L'effetto immunomodulatore di CDK4/6i nelle cellule senescenti non maligne indotte dalla chemioterapia rimane ancora non chiaro. Il razionale di questo progetto è determinare il ruolo funzionale della senescenza indotta da CDK4/6i e della natura SASP dopo il trattamento con doxorubicina da solo o in combinazione con abemaciclib in cellule non maligne in modelli in vitro. Abbiamo indotto la senescenza in linee cellulari normali come MDF, 3MR, BJ e hTERT RPE-1 utilizzando la doxorubicina da sola e in combinazione con abemaciclib e l'induzione della senescenza convalidata utilizzando la colorazione SA-β-gal e EdU. Mediante RT-PCR, abbiamo analizzato non solo i biomarcatori di senescenza, ma anche alcuni target p53 e NFkB per caratterizzare la natura SASP dopo il trattamento. Quindi abbiamo eseguito il test di proliferazione delle cellule tumorali, gli esperimenti di co-coltura e ha analizzato i terreni condizionati utilizzando il sistema di analisi delle cellule vive IncuCyte®Zoom. I nostri risultati hanno indicato che la senescenza è stata indotta con successo in tutte le linee cellulari trattate con entrambi i gruppi. In particolare, il fenotipo secretorio associato a NF-κB (NASP) è stato osservato solo nella condizione trattata con doxorubicina da sola. Inoltre, i nostri dati basati sugli esperimenti IncuCyte hanno suggerito che la riduzione della proliferazione delle cellule tumorali in presenza di doxorubicina più abemaciclib e il solo trattamento con abemaciclib non dipendevano né dallo stato senescente né dal tipo di cellula. Infine, la proliferazione osservata di MDAMB231 e BT549 era inferiore nel CM delle condizioni trattate da solo con abemaciclib in entrambe le linee cellulari BJ e RPE, indicando che il trattamento con abemaciclib potrebbe manifestare componenti SASP distintivi.

In conclusione, i due studi sulla senescenza indotta dalla terapia presentati in questa tesi hanno indicato che il TIS può produrre un aumento dell'attività immunitaria e una riduzione degli effetti collaterali associati alla tossicità in base ai regimi di trattamento. Un'ultima e forse la cosa più importante è capire le principali lacune di conoscenza in questo campo emergente per migliorare i risultati del trattamento per i malati di cancro.

List of abbreviations

BC	Breast Cancer
AJCC	American Joint Committee on Cancer
ER	Estrogen Receptor
PgR	Progesterone Receptor
HER2	Human Epidermal growth factor Receptor 2
TNBC	Triple-Negative Breast Cancer
GEP	Gene Expression Profiling
CDK	Cyclin-dependent kinase
HE	Haematoxylin -Eosin
BRCA1	Breast Cancer gene1
BRCA2	Breast Cancer gene2
PIK3CA	Phosphatidylinositol-4,5-bisphosphate 3-kinase catalytic subunit alpha
PI3K	Phosphatidylinositol-3 kinase
PB	Peripheral Blood
HR	Hormone Receptor
PTEN	Phosphatase and tensin homolog
CDH1	E-cadherin
FDA	Food and Drug Administration
OIS	Oncogene- Induced Senescence
mTOR	Mammalian Target of Rapamycin
SASP	Senescence-Associated Secretory Phenotype
TMZ	Temozolomide
DDR	DNA Damage Response
UPR	Unfolded Protein Response
RAS	Rat Sarcoma
E2f1	E2F Transcription Factor 1
Nf1	Neurofibromatosis type 1

CDK4	Cyclin-dependent kinase 4
CDK6	Cyclin-dependent kina se 6
RB	Retinoblastoma Protein
RB1	Retinoblastoma tumor susceptibility gene
ATM	Ataxia-Telangiectasia Mutated
CDK	Cyclin-Dependent Kinase
CHK	Checkpoint Kinase
SA-β-Gal	Senescence-Associated Beta-Galactosidase
TNF-a	Tumor Necrosis Factor-alpha
IFN-g	Interferon-gamma
MDSCs	Myeloid Derived Suppressor Cells
Tregs	Regulatory T cells
PMN-MDSCs	Polymorphonuclear MDSCs
M-MDSCs	Monocytic-MDSCs
NK	Natural killer cells
HLA-DR	Human Leukocyte Antigen-DR isotype
MLPGs	Monocyte-Like Precursors of Granulocytes
LOX1	Lectin-Like Oxidized Low-Density Lipoprotein Receptor 1
IL-4Rα	Interleukin-4 Receptor alpha
PGE 2	Prostaglandin E 2
TGF-β	Transforming growth factor-β
COX-2	Cyclooxygenase-2
DN T	Double-Negative T cells
FAO	Fatty Acid Oxidation
TCA	Tricarboxylic acid
IIBs	Immune-Inflammatory Biomarkers
NLR	Neutrophil-to-Lymphocyte Ratio
PLR	Platelet-to-Lymphocyte Ratio
SII	Systemic Immune-inflammation index

PIV	Pan-Immune-inflammation Value
P	Platelets
N	Neutrophils
L	Lymphocytes
DCIS	Ductal Carcinoma In Situ
LCIS	Lobular Carcinoma In Situ
IDC	Invasive Ductal Carcinoma
ILC	Invasive Lobular Carcinoma
NAT	Neoadjuvant therapy
pCR	Pathological Complete Response
PET	Positron emission tomography imaging
NMR	Nuclear magnetic resonance spectroscopy
MS	Mass-spectrometry
EDTA	Ethylenediaminetetraacetic Acid
PBMCs	Peripheral blood mononuclear cells
FACS	Fluorescence-Activated Cell Sorter
MACS	Magnetic Activated Cell Sorting
PBS	Phosphate Buffered Saline
RPLP0	Ribosomal Protein Lateral stalk subunit P0
UPL	Universal Probe Library
GC	Gas chromatography
TOFMS	Time-of-flight mass spectrometry
RD	Residual disease
CKIs	Cyclin-dependent Kinase Inhibitors
TMS	Trimethylsilyl derivatives
RT-PCR	Real time PCR
CDK2	Cyclin-dependent kinase 2
CHK2	Checkpoint kinase 2
TIS	Therapy-Induced Senescence

EMA	European Medicines Agency
MBC	Metastatic breast cancer
NF-κB	Nuclear Factor κB
MDFs	Mouse dermal fibroblasts
Igfbp3	Growth Factor Binding Protein3
Lif	Leukemia inhibitory factor
IL1alpha	Interleukin-1 alpha
IL6	Interleukin6
CXCL1	C-X-C Motif Chemokine Ligand 1
CCL2	C-C Motif Chemokine Ligand 2
mRFP	monomeric Red Fluorescent Protein
LUC	Renilla luciferase
tTK	thymidine kinase
NASP	NF-κB- Associated Secretory Phenotype
CuAAC	Copper-Catalyzed Azide-Alkyne cycloaddition
RCU	Red object intensity
SAHF	Senescence-Associated Heterochromatin Foci
CM	Conditioned medium
EdU	5-ethynyl-2'-deoxyuridine
MHC-I	Major Histocompatibility Complex class I
CEBPβ	CCAAT/enhancer-inding protein-β

Section I

Chapter1: Introduction

IMPACT OF IMMUNOSENESCENCE IN RESPONSE TO NEOADJUVANT CHEMOTHERAPY IN EARLY BREAST CANCER PATIENTS.

1.1 Breast Cancer (BC)

1.1.1 Breast tissue: Physiological structure & function

The mammary gland is a common denominator of all animals of the class 'Mammalia'. Mammary gland or breast is an organ of ectodermal origin, composed of two compartments: glandular and stromal. The glandular compartment is made up of lobules and ducts whereas, stromal compartment consists of fat tissue and connective tissue that surrounds the glandular compartment.

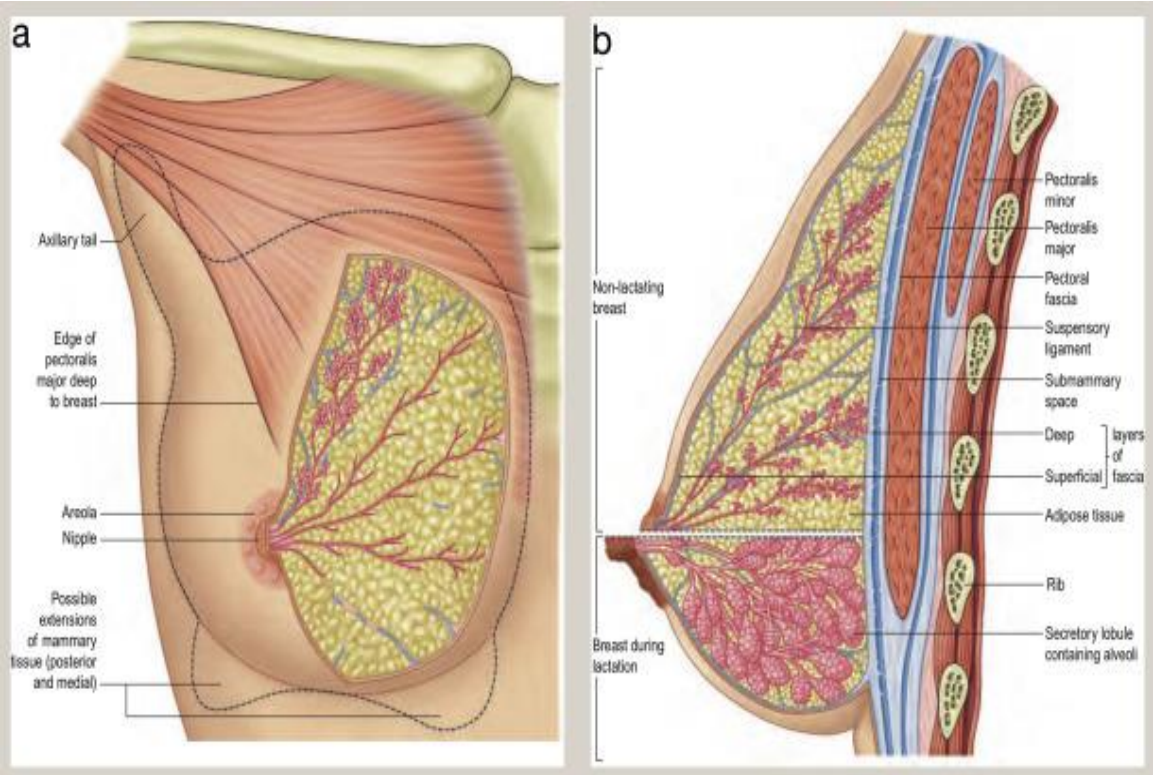

Figure1: Human breast anatomy (a) and changes in breast structure during lactation (b) [Adapted from Standring, S. Gray's anatomy, 41st edition, 2016. Edinburgh: Elsevier].

Most cancers of the breast arise from the cells which form the lobules and terminal ducts. Blood vessels along with the lymph nodes, immune cells and nerve endings are located throughout the breast (figure1).

Anatomically, the mature breast is located within the anterior thoracic wall, lying atop the pectoralis major muscle. The breast tissue extends horizontally (side-to-side) from the edge of the sternum (the firm flat bone in the middle of the chest) out to the midaxillary line (the center of the axilla, or underarm). With the onset of puberty, the breast completes most of its development after birth in response to various hormonal influences. It develops additionally during pregnancy for the process of lactation.

1.1.2 Breast tissue: Pathophysiological structure & function

Breast cancers can be divided into two main groups based upon its cellular origin: carcinomas and sarcomas. Most breast cancers are carcinomas, emerge from the epithelial components (ductal or lobular carcinoma) whereas sarcoma develops from the stromal components of the breast. Intriguingly, sarcomas are rare making up less than 1% of all breast cancers. In accordance with their pathological characteristics, breast cancer can either a non-invasive (cancer has not spread beyond the layer of tissue, usually in early stage of breast cancers) or invasive (involves cancers that have spread within the breast only, or to nearby lymph nodes and tissues).

1.1.3 Epidemiology

Mammary carcinogenesis is a multifactorial disease caused by an interaction between genetic predisposition and environmental exposures. Globally, breast cancer is the most common cancer, accounting for 12.5% of all new female cancer cases each year as per the estimation of American Cancer Society. A total of 390,700 cancer incidence (except skin cancers other than melanoma) were reported in Italy in 2022 (in 2020 they were 376,600), with an increase of 14,100 new cases. The new diagnoses were 205,000 and 185,700 among men and women respectively. Among different types of cancers, breast cancer (55,700 cases, +0.5% compared

to 2020) was the most common malignant neoplasm in 2022, followed by colorectal cancer (48,100, +1.5% in men and +1.6% in women), lung (43,900, +1.6% in men and +3.6% in women), prostate (40,500, +1.5%) and bladder (29,200, +1.7% in men and +1. 0% in women) [Massimo Di Maio et al., 2022]. Besides being most frequent type, breast cancer is also the leading cause of cancer-associated death in women worldwide.

1.1.4 Staging and molecular classification of Breast cancer

The American Joint Committee on Cancer (AJCC) TNM system is most often used to assign the stage of cancer. Breast cancer stage is usually determined from a number on scale ranging from 0 to IV where, stage 0 describing non-invasive cancers that remain within their original location and stage IV representing invasive cancers that have spread outside the breast to other parts of the body.

Staging was calculated based on three clinical characteristics such as T, N, and M where, T is the size of the cancer tumor and whether it has grown into nearby tissue, N stands whether there is cancer in the lymph nodes and M denotes whether the cancer has spread to other parts beyond the breast.

The T category describes the primary tumor:

- TX means the tumor can't be assessed.
- T0 means there isn't any evidence of the primary tumor.
- Tis means the cancer is in situ (the tumor has not started growing into healthy breast tissue).
- T1, T2, T3, T4: These numbers depend on the size of the tumor and the extent to which it has grown into neighboring breast tissue. Higher the T number, the larger the tumor.

The N (lymph node involvement) category describes whether or not the cancer has reached nearby lymph nodes:

- NX means the nearby lymph nodes can't be assessed.
- N0 means nearby lymph nodes do not contain cancer.

- N1, N2, N3: These numbers are based on the number of lymph nodes involved and how much cancer is found in them. The higher the N number, the greater the extent of the lymph node involvement.

The M (metastasis) category explains whether/or not cancer presents in other body parts beyond the primary site:

- MX stands metastasis can't be assessed.
- M0 stands for no distant metastasis.
- M1 stands for distant metastasis.

The breast cancer classification continues to evolve, with the integration of new knowledge from research being translated into clinical practice. A novel immunohistochemical (IHC) panel was identified by Cheang etal [Cheang MCU etal.,2008] which consists of six IHC markers, could recapitulate the biologic subgroups of breast cancer derived from gene expression profiling (GEP). Later, summarized the IHC diagnosing criteria of the intrinsic classification as follows: (1) luminal A: ER^+ and/or PR^+, $HER2^-$, and low Ki-67 (<14%); (2) luminal B: ER^+ and/or PR^+, $HER2^+$ or $HER2^-$, and high Ki-67 (>14%); (3) $HER2^+$: ER^-, PR^-, and $HER2^+$; and (4) basal-like (BLBC): ER^-, PR^-, $HER2^-$ (triple negative), plus CK $5/6^+$, and/or $EGFR^+$[Schnitt S J.,2010].

1.1.5 Patient diagnosis

An era of personalized medicine is ushering in a paradigm shift in the diagnosis and treatment of breast cancer from a one-size-fits-all approach. Breast cancer is typically diagnosed through screening or a symptom that necessitates a diagnostic exam, such as pain or a palpable lump. A mammogram and a breast ultrasound are usually recommended to analyse the breast lump. If suspicious, a biopsy may also be advised. One of the standard methods for predicting the prognosis of BC is the grading of haematoxylin -eosin (HE) stained histopathology images.

1.1.6 Standard of care

Advances in science and technology have a significant emphasis on early diagnosis and therapy resulted in life changing interventions in breast cancer and improved the quality of breast cancer care. The gold standard treatment for breast cancer usually includes total mastectomy followed by axillary dissection (surgery) and radiotherapy, in combination with chemo or other drug therapies either before (neoadjuvant) or after (adjuvant) surgery [Punglia RS etal.,2008]. The number of breast cancer survivors has increased since the standard-of-care has ameliorated dramatically. However, this increase is associated with increasing rates of reappearance of cancer [Pan H etal.,2017]. In parallel, there is an increased utilization of neoadjuvant chemotherapy (NAT), among breast cancer patients (17–79%) based upon their biologic subtype, which is determined by the expression of estrogen receptor (ER), progesterone receptor (PR), and human epidermal growth factor receptor 2 (HER2) as they have been validated as prognostic and predictive biomarkers for therapy with higher pathological complete response (pCR) in different subtypes of breast cancer [Murphy BL etal.,2018]. Contrary to patients who did not receive NAT (primarily anthracycline-based therapy), the recurrence rate is higher in some subtypes of breast cancer patients who received NAT, which raises the intriguing possibility of cellular responses to chemotherapy. Thus, there is an avid need for the identification of novel mechanisms involve in disease recurrence and the better understanding might pave the way for an effective anticancer therapy, associated with high survival rates.

1.2 Tumor heterogeneity

Tumor heterogeneity is one of the hallmarks of malignancy. Differences in the genetic and epigenetic alterations due to clonal and cellular diversity, and/or proteomic properties of the tumor is thought to be a reason of heterogeneity of breast cancer (figure2). Mounting evidence indicated that both inter and intra tumoral heterogeneity occur due to number of cancer-cell-intrinsic and extrinsic parameters. These parameters together lead to cancer cell proliferation, apoptosis, metastasis, and leading to markedly variable clinical course and response to treatment modalities.

1.2.1 Intertumoral heterogeneity of Breast Cancer

The Intertumor heterogeneity occurs in tumor tissues among different patients or different metastases. About 5 to 10% of all patients with breast cancer carry a hereditary predisposition [Rhei E etal.,1998]. The germline mutation in the BRCA1 or BRCA2 gene (nearly 50%) is the most common cause of hereditary breast cancer and is associated with early-onset breast cancer [Kuchenbaecker KB etal.,2017]. Both BRCA1 and BRCA2 are tumor suppressor genes involve in DNA repair.

There are other high penetrance genetic mutations responsible for the elevated risk of breast cancer. PIK3CA is one of the most dysregulated among PI3K genes, PIK3CA activated events comprise up to 47% of luminal A (HR+/HER2–), 39% of HER2-enriched, 33% of luminal B (HR+/HER2+), and 8–25% of basal-like/triple negative breast cancer subtypes [González-Angulo A.M etal., 2011; Martínez-Sáez O etal.,2020]. Besides that, PTEN related Cowden's syndrome, p53 related Li Fraumeni syndrome, CDH1 related diffuse hereditary gastric cancer syndrome, PALB 2 (partner and localizer of BRCA2 gene) related breast cancer [Tischkowitz M etal.,2010]. Besides that, intra tumoral heterogeneity is observed with coexistence of cancer subpopulations, that differ in their genetic, phenotypic, or behavioural characteristics within the individual tumor and between the individual tumor and its metastasis site in the same patient.

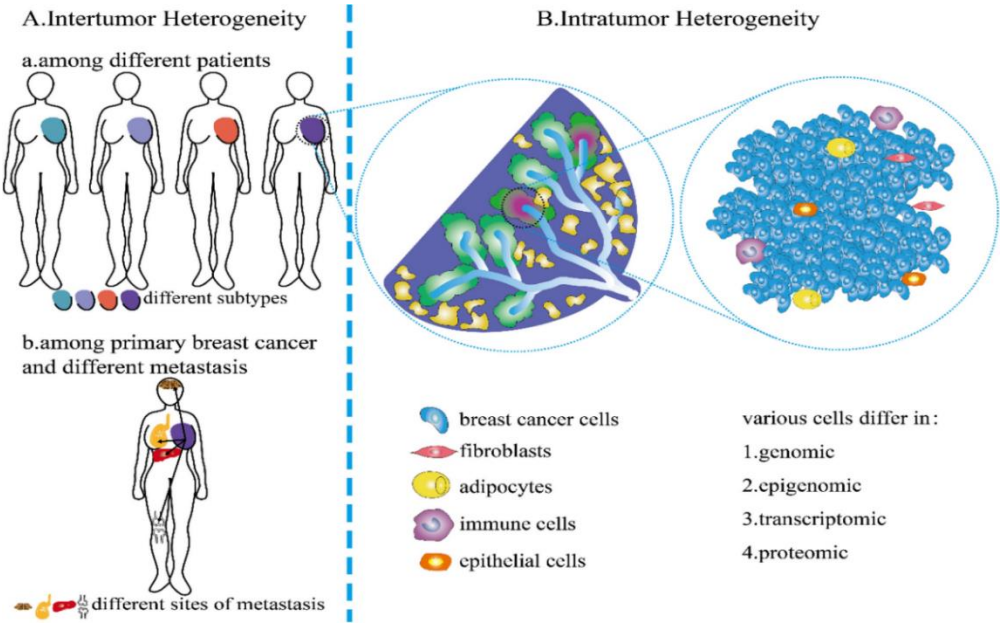

Figure2: Heterogeneity of breast cancer. **(A)** Intertumoral heterogeneity: **a** different patient with different breast cancer subtypes; **b** patients with primary breast cancer with different metastasis site

among different subtypes. **(B)** Intratumor heterogeneity: variation in different cell types within a tumor [Adapted from Liantao Guo etal.,2023].

1.3 Treatments for Breast Cancer

The breast cancer treatment has improved dramatically over the past decades, from a strict surgical approach to a multidisciplinary one, including local and systemic therapies. Local treatment of breast cancer consists of surgery with or without radiation therapy to the breast and nearby lymph nodes whereas, systemic cancer therapy includes chemotherapy (ie, conventional or cytotoxic chemotherapy), antihormone therapy and targeted therapies [Kreienberg R etal.,2012]. In women with breast cancer, several types of surgical procedures are done including a lumpectomy and modified mastectomy. Local therapy modalities are typically used for palliation in the metastatic setting [Waks AG etal.,2019].

Systemic therapy is usually administered after surgery as adjuvant therapy, but it may also be given before surgery as neoadjuvant therapy (NAT). Patients diagnosed with high-risk non-metastatic breast cancer, including locally advanced and inflammatory breast cancer, are usually treated with upfront chemotherapy, in the form of NAT followed by surgery. This treatment has been demonstrated to decrease tumor burden and increase breast conservation rate [Mieog J S etal.,2007]. Simultaneously, as the response to NAT can be evaluated, there is possibility to modify regimens to increase rates of pathological complete response (pCR). Intriguingly, pCR has been supported by the FDA as a surrogate end point for the accelerated approval of new drugs tested in the neoadjuvant setting in randomized clinical trials [FDA.,2022]. In neoadjuvant settings, most are anthracycline or taxane-based therapies. For HER2-positive tumors, usually includes a combination of chemotherapy and HER2-targeted therapy drugs trastuzumab (Herceptin) and pertuzumab (Perjeta). Pembrolizumab (Keytruda), immunotherapy drug along with chemotherapy used in neoadjuvant therapy in triple negative breast cancer.

Besides, the positive side of systemic therapy such as determination of chemosensitivity, reduction of tumour volume and downstaging of surgical requirement. Concerns are still existed includes local control after downsized surgery and the delay of local treatment in patients with tumours resistant to chemotherapy.

1.4 An overview of senescence

Senescence (from the Latin word “senex”, meaning growing old) is a proliferative arrest due to excessive intracellular or extracellular damage [Hooten N etal.,2017]. Cellular senescence was first described by Leonard Hayflick and Paul Moorhead in 1961, as a limited dividing ability of cultured human fibroblast cells. This phenomenon, termed replicative senescence, is dependent on telomere shortening as primary cells divide. In fact, replicative senescence is one type of cellular senescence. Lately, a wide range of intrinsic and extrinsic insults have been identified able to trigger ‘premature senescence’ including oncogenic activation, mitochondrial dysfunction, oxidative or genotoxic stress, irradiation, and chemotherapeutic agents [Kuilman T etal.,2010]. Earlier, authors had hypothesized that it could plays role in organismal aging [L. Hayflick.,1965]. Since then, numerous studies showed that senescence is a highly complex phenotype and induced in multiple physiological processes such as embryonic development [Muñoz-Espín etal., 2013], wound healing [Jun and Lau, 2010], tissue repair [Krizhanovsky etal., 2008], and paradoxically, age-related pathologies including cancer [Muñoz-Espín and Serrano, 2014; Pérez-Mancera etal., 2014].

In general, senescence is a cell fate specifically to a progression of complex changes culminating in the loss of proliferative potential (which may be reversed in some circumstances), the inhibition of cellular apoptosis, chromatin alterations, metabolic and phenotypic changes with secretion of a plethora of factors collectively referred as senescence-associated secretory phenotype (SASP). The nature of SASP is highly dependent on the cell type, degree and duration of stimuli that triggered senescence induction. Thus, SASP includes proinflammatory and immune-modulatory cytokines and chemokines, growth factors and matrix-remodeling proteases. Mainly, SASP is initiated through NF-κB and p38 MAPK signaling and is maintained in an autocrine fashion by interleukin 1α [Salminen A etal.,2012] and SASP have impact on the adjacent cells and extracellular matrix and contributes to age-related tissue degeneration.

Based on the size and duration of the stimulus, senescence can be categorized as acute or chronic senescence. Acute senescence is a short-term process, often triggered in response to physiological process, such as wound healing, embryological development, or tissue

remodelling [Davaapil H etal.,2017] whereas, chronic senescence is occurred because of prolonged senescent stimulus, leading to the occurrence of several diseases such as arthritis, neurodegenerative disease, diabetes, and cancer [Xu M etal.,2018].

Historically, induction of senescence considered as an endogenous evolutionary homeostatic mechanism to prevent malignant transformation [Rodier etal.,2011]. Consistently, the presence of senescent cells has been observed within premalignant tumors [Michaloglou etal.,2005; Bennecke M etal.,2010].

1.4.1 Senescence: beneficial and detrimental roles

Senescence plays a key cell-intrinsic mechanism of tumor suppression through enhancing immune surveillance and reducing malignant cells proliferation. In cancer, oncogene-induced senescence (OIS) was first characterized as a protective barrier against tumor progression, in addition to apoptosis [Collado etal., 2007; Michaloglou etal., 2005]. Of note, senescent cells generally express an anti-apoptotic program [Childs etal., 2014]. Depending on the context, SASP components can recruit and/or activate immune cells to target the clearance of senescent cells collectively called, senescence surveillance. The immune cell types responsible for the immune surveillance vary depending on the pathological conditions. Inhibition of mTOR (using rapamycin) hampers the SASP production and reduces the immune cell infiltration, thus impairing senescence surveillance and tumor suppression [Tasdemir etal., 2016]. Interestingly, senescent cells can also be induced by chemotherapeutic agents such as TMZ, doxorubicin and cisplatin can trigger therapy induced senescence (TIS) [Demaria etal., 2017]. However, accumulation of senescent cells can contribute age-related diseases including cancer.

Besides the positive effects of senescence, there are also negative consequences. Increasingly, cellular senescence is considered as an in vivo response in cancer patients to various anticancer therapies. Most anti-cancer therapies have an impact on the physiological effect of organism, which leads to the accumulation of senescent cells in the tumor environment. In the hematopoietic context, few senescent cancer cells can escape the senescent state and acquire de novo self-renewing properties which further increases tumor aggressiveness (Milanovic etal., 2018). While cells undergoing oncogene induced senescence

(OIS) and therapy induced senescence (TIS) can be efficiently cleared by immune cells, they can also evade immune clearance and persist (Michaloglou etal., 2005). In this case, chronic senescence takes place and promotes tumorigenesis via the production of a pro-tumorigenic SASP. Moreover, senescence in cancer is ambiguous and even controversial due to its hallmark-promoting capabilities.

1.4.2 Senescence in cancer: mechanism of action

There are several regulatory signalling pathways involve in the induction of senescence under appropriate conditions include the cell cycle and its regulatory machinery, the DNA damage response (DDR) pathway, the regulation of apoptosis, and the unfolded protein response (UPR) [Pluquet O etal.,2015]. In turn, initiation of senescence induction occurs even through different oncogenic insults such as Ras, E2f1, Akt, Cyclin E, loss of tumor suppressor genes (Pten, Nf1) and high levels of ROS. The p53/p21CIP1 and p16INK4A/Rb pathways are mainly involve in TIS via DDR [Collado etal., 2005; Michaloglou etal., 2005]. The cell cycle inhibitor p16Ink4a exerts CDK4/CDK6 mediated inactivation of RB to block the transition of cell cycle(figure3). This mechanism occurs either alone or in combination with p53/p21CIP1 pathway depending on stress or cell of origin. The research evidence indicates that p21 is often upregulated first and p16Ink4a later, possibly representing distinct phases on the path from early to full senescence [Van Deursen JM.,2014]. Also, senescence may impact on these same pathways via positive or negative feedback loops as well as other intracellular pathways and extracellular processes, such as the immune modulation, inflammation, regulation, and maintenance of the extracellular matrix, and angiogenesis [Coppe JP etal.,2006]. Many of these pathways are also involved in the process of cancer development, suppression, progression, recurrence, and response to therapies.

In cancer, senescence plays a vital role in tumor suppression by enhancing immune surveillance and reducing the progression and invasion of tumor cells and is exploited in anticancer therapies. However, numerous studies demonstrated its pro-tumorigenic activity [Kuilman etal., 2008]. It is now accepted that senescence is a “double-edged sword” that can paradoxically prevent or promote tumor progression in a context-dependent manner [Sieben

et al., 2018]. To date, the interactions between senescence and cancer are complex and poorly understood.

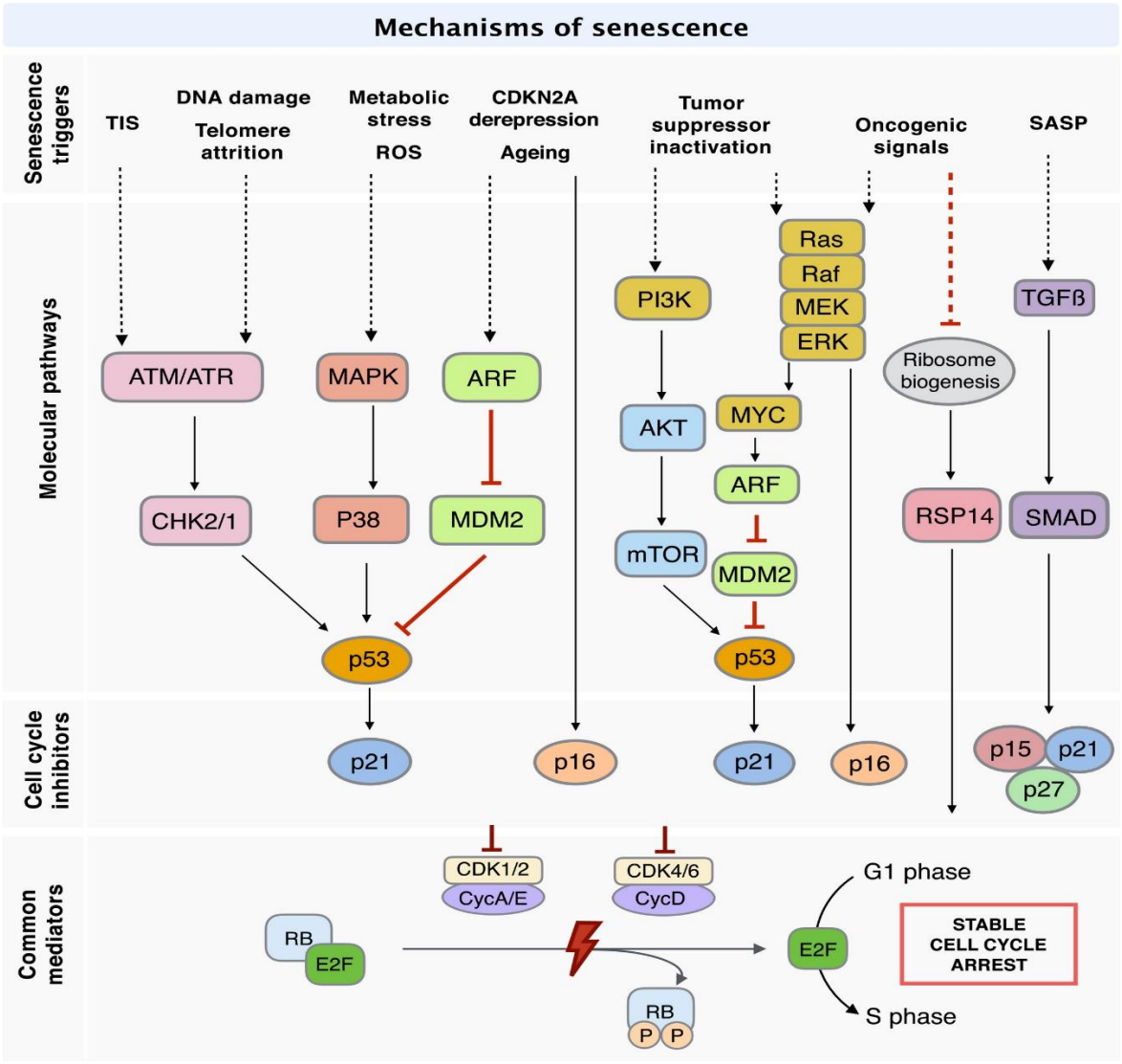

Figure3: Diagrammatic representation of signalling pathways involve in senescence induction in cancer. The activation of DNA damage response that imposes cell-cycle arrest through the p53-p21 axis while ARF and p16 upregulation due to ageing and CDKN2A de-repression block cell-cycle transition via both the p53-p21 and p16 axis. Abbreviation: ATM, ataxia-telangiectasia mutated; CDK, cyclin-dependent kinase; CHK, checkpoint kinase [Adapted from Hui-Ling Ou etal.,2020].

1.4.3 Targeting cellular senescence in cancer patients'

Though senescence induction may prevent cell proliferation, long-term senescence may promote tumorigenesis, mainly through SASP, which may result the proliferation of neighbouring non-senescent cells and/or provoke immune escape. Therefore, targeting senescent cells and eliminating the deleterious aspect of senescence may be a potential

strategy for cancer therapy. However, it's a challenging task due to no universal markers for senescent cells yet.

The senescence-associated beta-galactosidase (SA-β-Gal) activity is widely used marker and often considered as gold standard for identifying senescent cells [Debacq-Chainiaux F etal.,2009]. Despite of this, SA-β-Gal activity was not a universal marker for cellular senescence [Dimri G P etal.,1995] due to its expression in certain cell types and not all senescent cells express SA-β-Gal [Lee B Y etal., 2006]. Of note, SA-β-Gal detection is only possible in fresh snap-frozen tissue samples [Evangelou K etal., 2017], thus limits its use in a clinical context.

Detection of cancer cells or cancer-specific circulating material in patient fluids by means of liquid biopsy is a comprehensive and an emerging field in oncology with early detection of cancer or tumor recurrence, monitors cancer therapies, determine therapeutic targets and clinical implications for personalized medicine [Alix-Panabières C etal.,2021]. In contrast to tissue biopsy or surgical samples, liquid biopsies can be obtained repeatedly to track the evolution of the tumor's molecular profile, which may lead to drug resistance, and not impacted by sampling bias or tumor heterogeneity [Siravegna G etal.,2017].

1.4.4 Senescence induction in Breast cancer treatment

Studies to better figure out the molecular mechanisms regulating the senescence are becoming more and more clinically relevant. Accumulating evidence suggests that senescence may be a key effector mechanism of many types of anticancer therapies, such as chemotherapy, radiotherapy, and endocrine therapies, both directly and via bioactive molecules released by senescent cells, activate immune surveillance. However, senescence may contribute to reduced patient resilience to cancer therapies and leads to disease recurrence after cancer therapy.

Depending upon the severity of chemotherapy induced DNA damage, either occurs cell death via the DNA damage response (DDR), or trigger a non-lethal DDR, leads to acute or chronic senescence [Van Deursen JM.,2014]. Of note, induction of senescence or cell death occurs, based upon the functional tumour suppressor genes, such as p53 or p16INK4A to control cell

behaviour [Te Poele RH etal.,2002]. There is increasing evidence reported that chemo (radio) therapy able to induce T cell senescence in various cancer types including breast cancer [Onyema OO etal.,2015]. One of the explanations is that senescent T cells are non-proliferative cells, resistant to chemo (radio)therapy as a result accumulate after several cycles of chemo(radio) therapies [Arina A etal.,2019]. Another explanation is that DNA-damage caused by chemo(radio)therapies can induce T cell senescence which impair cytotoxicity and the production of TNF-a and IFN-g, which may further lead to a poor response [Bruni E etal.,2019].

1.5 Inflammation in cancer

Inflammation has been demonstrated to not only initiates immune response but also cause immune surveillance. The interaction between the processes of inflammation and the host's immune system plays a key role in progression, invasion, metastasis as well as responses to therapies [Grivennikov SI etal.,2010].

In 1863, Virchow hypothesized that the origin of cancer was at sites of chronic inflammation, in part based on his hypothesis that some classes of irritants, together with the tissue injury and ensuing inflammation they cause, enhance cell proliferation. Although it is now clear that proliferation of cells alone does not cause cancer, sustained cell proliferation in an environment rich in inflammatory cells, growth factors, activated stroma, and DNA-damage-promoting agents, certainly potentiates and/or promotes neoplastic risk.

The acute inflammatory response is the first line of defense against external infection or injury, promoting innate and adaptive immune responses. However, if the acute inflammation does not resolve in time, it could be transformed into chronic inflammation [Mantovani A etal.,2008]. There is convincing evidence that chronic inflammation induces immunosuppression with many immunosuppressive cells (myeloid derived suppressor cells (MDSCs), Treg cells, etc.) which inhibits both adaptive and innate immune reactions in different human disorders including cancer [Wang D etal.,2015].

1.5.1 Myeloid Derived Suppressor cells (MDSCs)

The generation of immune suppressive cells like MDSCs, one of the strategies of immune system to protect the host from the deleterious effects of inflammation through suppressing the activity of CD4+ T cells, CD8+ T cells and NK cells [Suzuki E etal.,2005]. MDSCs are heterogeneous cells composed of immature cells (macrophages, granulocytes, and dendritic cells) with potent immunosuppressive activity, widely distributed in the spleen, peripheral blood, and tumor sites [Ostrand-Rosenberg S etal.,2009]. Emerging data highly emphasized that increased levels of MDSCs are dramatically related to cancer development and poor prognosis in patients with breast, colorectal, and lung cancers and hematologic malignancies [Yang Z et al.,2020; Hao Z etal., 2021]. The presence of MDSCs was first reported in the blood of head and neck cancer patients and they were identified as Lin−CD33+CD15+CD34+ cells [Pak AS etal.,1995]. Several markers have been used to characterize MDSC populations in cancer patients. Broadly, human MDSCs are categorised into two sub-groups, polymorphonuclear (PMN-MDSC) and monocytic (M-MDSC) according to their origin from granulocytic and monocytic lineages, respectively [Veglia F etal.,2021]. The phenotypes of human PMN-MDSCs and M-MDSCs are defined as $CD11b^{+}$ $CD14^{-}$ $CD15^{+}$ and $CD11b^{+}$ $CD14^{+}$ $HLA\text{-}DR^{-/low}$ $CD15^{-}$ respectively [Vuk-Pavlović S etal.,2010]. A recent study identified a new group designated as monocyte-like precursors of granulocytes (MLPGs) [Mastio J etal.,2019]. In addition, several other markers have been associated with the MDSCs phenotype, such as CD49d, LOX1 and IL-4Rα [Haile LA etal.,2010].

1.5.2 MDSCs in cancer progression

MDSCs are present at low frequencies in healthy individuals, but rapidly increase in pathological conditions such as autoimmune disease, bacterial or fungal or viral infections as well as in cancer [Daker E etal.,2015; Wu H etal.,2016]. In recent years, many studies proved that MDSC-induced immune tolerance facilitates cancer progression and metastasis, few other reported that MDSC expansion might be beneficial, restraining potentially damaging inflammation. Generally, PMN-MDSCs are predominantly expanded population in most cancers [Kumar V.,2016]. The proportion of MDSC subsets vary with tumour type and clinical staging of the disease. For example, PMN-MDSC population outnumber M-MDSC in breast cancer, but this proportion is reversed in prostate cancer [Gabrilovich DI.,2017]. In clinical

scenario, MDSC sub-classification is essential, as these subsets have different mechanism of activation and immunosuppression among different types of cancer. A lot of studies have been reported about the interaction between MDSCs and T cells. MDSCs utilize a variety of mechanisms to inhibit T cell function by downregulating the pro-inflammatory cytokines, such as IL-12 and prostaglandin E_2 (PGE_2) [Huang S etal.,2019]. The accumulation of MDSCs in peripheral tissues in cancer is well known along with their pro-tumor role in tumor progression. More specifically, MDSCs are known to produce reactive oxygen species, nitric oxide, arginase, IL-10, TGF-β, and COX-2 to inhibit the proliferation and function of immune cells including T cells (figure4). Moreover, the involvement of molecular and signaling pathways in the generation of MDSCs from myeloid precursors in disease conditions, including cancer is not completely understood.

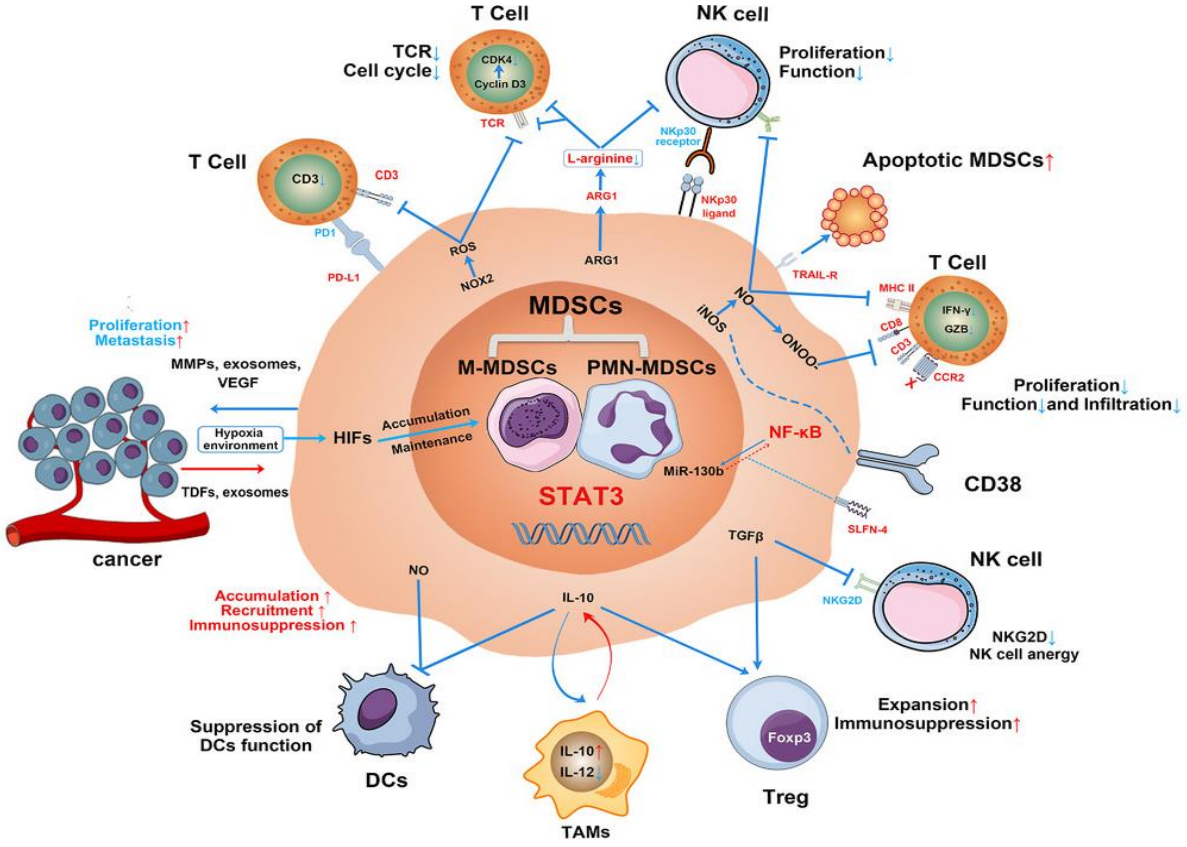

Figure4: Schematic representation of myeloid-derived suppressor cells in cancer [Adapted from Cheng Cui etal.,2021].

1.6 CD3+CD4-CD8- (Double-Negative) T Cells in cancer

There is ample evidence demonstrated the role of $CD3^+CD4^-CD8^-$ double-negative (DN) T cells, a rare population in peripheral blood, involve in inflammation, immune disease, and cancer. DN T cells involve in both innate and adaptive immune functions, differing from conventional $CD4^+$ and $CD8^+$ T cells and, shares functions with differentiated effector T cells in different settings [Yang L etal.,2021]. In addition, they act as Treg cells, cytotoxic T in distinct pathological conditions, which are closely linked with human disorders(figure5). In human breast cancer [Georgiannos SN etal.,2003; Carlomagno C etal.,1995], several studies have attributed an important role to DN T-lymphocytes, as well as cytokines produced by them. The evidence suggest that T-lymphocytes might cooperate with tumor cells favouring tumor development and progression. The better understanding of the heterogeneity and functions of DN T cells may help to develop DN T cells as a potential therapeutic tool for inflammation, immune disorders, and cancer.

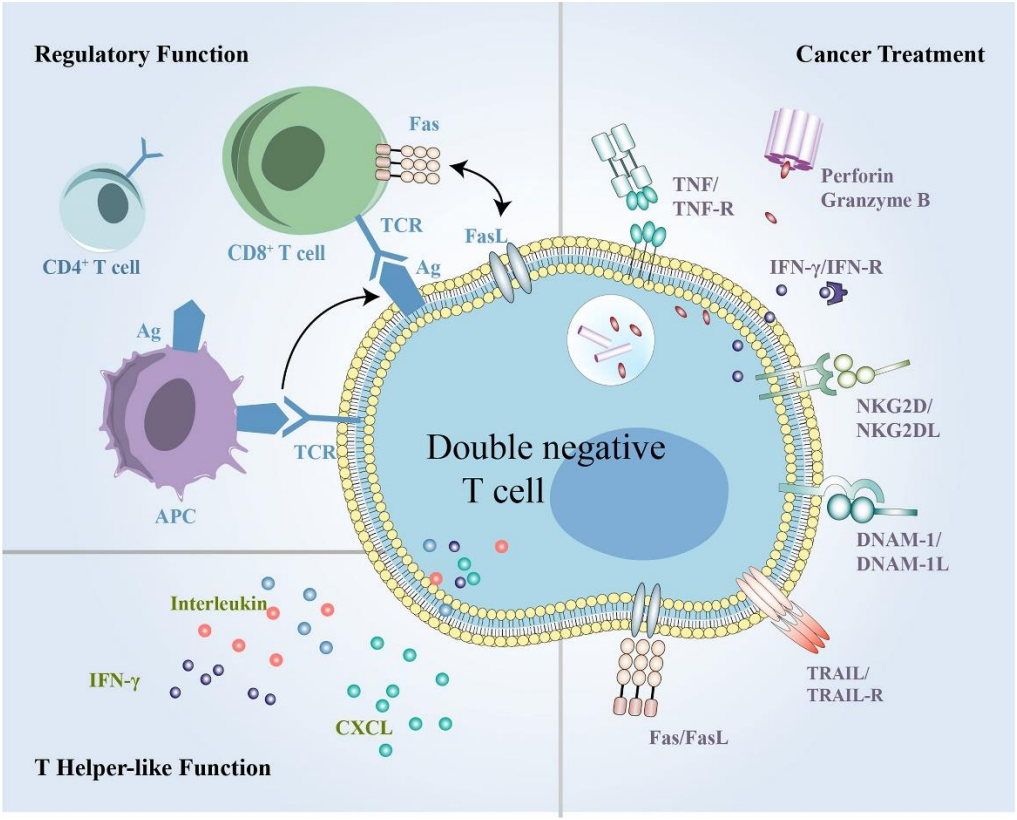

Figure5: The multifunctional DN T cells, which exert both regulatory and helper-like functions under different pathological conditions. DN, double-negative [Adapted from Zhiheng Wu et al., 2022].

The regulation of immune cell metabolism provides insight into cellular mechanisms influencing immune cell fate and function. The metabolically quiescent T lymphocytes (T cells) circulate between lymph nodes and peripheral tissues in search of antigens in healthy individuals. The activation of T cell encounters metabolic programs compatible with their functional demands. The stimulation of the T cell antigen receptor (TCR) is required for the initiation of the T cell activation, those stimulation promotes signaling through the ERK/MAPK pathways and calcium flux, the PI3K-AKT-mTOR axis by CD28 signaling, and both pathways together engage the NF-κB pathway [Smith-Garvin JE etal., 2009]. Of note, signaling pathways fundamental for the T cell activation, differentiation, and effector functions, are closely linked to changes in the cellular metabolic programmes. The important six metabolic pathways such as glycolysis, fatty acid oxidation (FAO), fatty acid synthesis, tricarboxylic acid (TCA) cycle, amino acid metabolism, and the pentose phosphate pathway play a crucial role in immunometabolism especially, in T cells.

1.6.1 Alteration in T cell metabolism with senescence

The changes in senescent cell metabolism have been extensively reviewed recent years and it displays a unique metabolic signature. Senescence occurs in tissues as well as in the immune system but the interaction between this is poorly understood. Despite the loss of proliferative capacity, senescent cells are metabolically active. Senescent T cells are pro-inflammatory, displays effector functions, secrete large amounts of cytokines and are highly cytotoxic (Henson SM etal., 2012). For instance, senescent fibroblast generated by replicative senescence and radiation, which shift their energy production to glycolysis (James et al., 2015) similar like cancer cells. Subsequently, glycolysis ensures rapid biosynthesis to meet the high metabolic demands of those senescent cells. Emerging evidence suggests that inducing T cell senescence is a key strategy used by malignant tumours to evade immune surveillance.

1.7 Peripheral immune-inflammatory biomarkers in cancer

In peripheral blood, circulating inflammatory immune cells mainly involve neutrophil, lymphocyte, monocyte, and platelet [Gao Y etal.,2018]. Systemic inflammation has been

demonstrated to be closely associated with chemoresistance and prognosis of a series of solid tumors. In recent years, studies on immune-inflammatory biomarkers (IIBs), compared with traditional tumor-related biomarkers showed immense potential in the prognosis of breast cancer. It has been proven that blood-based IIBs as independent prognostic factors in breast cancer, such as neutrophil-to-lymphocyte ratio (NLR) and platelet-to-lymphocyte ratio (PLR). The abovementioned indicators sometimes, limit the prediction power of the prognosis due to the complex interaction between the tumor and host immune system [Nikolaou K et al.,2013].

A new comprehensive blood-based IIBs such as systemic immune-inflammation index (SII) and pan-immune-inflammation value (PIV) involve neutrophil, platelet, and lymphocyte counts and neutrophil, platelet, monocyte, and lymphocyte count, has been proven to be a strong predictor of survival outcomes with better performance than other well-known IIBs in patients with solid cancers [Fuca G etal.,2020]. SII is an index that is calculated by using the formula SII = (P x N)/L, where P, N, and L correspond to platelets, neutrophils, and lymphocytes, respectively. PIV is determined by considering the peripheral blood's platelet, neutrophil, lymphocyte, and monocyte counts; PIV = = (P x N x M)/L. Accumulating evidence noted that SII has been used to evaluate the balance between inflammatory factors and immune status of patients with cancer before the start of therapy [Zhang K etal.,2019; Murthy P etal.,2020]. Additionally, SII is also linked with prognosis of cancer in many cancer types including BC, although the results are controversial [De Giorgi U etal.,2019]. So far, these parameters have not been validated in a larger cohort to predict patient's response to chemotherapy.

1.8 Metabolomic profiling in cancer

Metabolomics includes a quantitative analysis of all metabolites and illustrate the association between metabolites and physio-pathological changes in an organism [Johnson CH etal.,2016]. Unlike genomics and proteomics, the focus of metabolomics is on the downstream products of genes and proteins, which allows more accurate identification of disease-associated changes that have occurred, rather than predictions [Rinschen MM etal.,2019].

At present, the pathogenesis of BC has not been fully demonstrated. Emerging evidence suggests that metabolites might be a key driver in the occurrence and development of BC. For instance, high levels of glutamine, tryptophan, γ-glutamyl-threonine, phenylalanine, 5-aminovaleric acid, or 5-aminovaleric acid was associated with increased risk of BC [[Lécuyer L etal 2018]. Another study exemplified those high levels of glucose, creatinine, glutamine, arginine, lysine, and valine to be closely linked with high risk for BC [Lécuyer L etal 2019]. Moreover, Metabolomics is still a research lab-based technique due to the technological and computational limitations make the translation into clinical practice a difficult task.

Chapter2: Objectives

Cellular senescence is a key effector mechanism of several types of anticancer therapies, both directly and via bioactive molecules released by senescent cells that may stimulate an immune response. TIS has been extensively established in many preclinical models, the induction and potential role of senescence in cancer patients receiving antineoplastic treatment is still under investigation. Antineoplastic drugs, such as anthracyclines, taxanes, and some platinum derivatives have been shown to achieve long-term clinical remissions in cancer patients partially by stimulating innate and adaptive immune cells [Bernal-Estevez DA etal.,2018]. However, the effect of neoadjuvant chemotherapy (NAT) on the phenotype of T cell senescence induced and whether this allows the early detection of patients who are unlikely benefit from treatment is not fully understood.

To assess these effects, we decided to conduct a non-interventional observational study to figure out the impact of circulating senescent T-cells, as predictive factors of response in patients with operable BC treated with NAT, according to biological subtypes. Moreover, we evaluated the peripheral blood levels of MDSC subpopulations, blood based IIBs and plasma metabolomics to identify cancer-associated changes in BC patients, in terms of pCR.

To this purpose we:

- Investigated by RTPCR the relative expression of senescence markers p16 and p21 in circulating CD3+CD4-CD8- double-negative (DN) T cells of patients, before and after NAT,
- Evaluated the percentage of circulating MDSCs and its subsets, by FACS analysis, at baseline and assessed whether it has impact on pCR status,
- Validated some blood based IIBs such as SII and PIV in BC patients before and after NAT,
- Performed an untargeted metabolomic investigation in patients' plasma at baseline (before NAT), in collaboration with Prof. Marcello Manfredi's laboratory.

Chapter3: Materials and Methods

3.1 Study Participants and clinical evaluation

The study participants were accrued between June 2020 and January 2023 at the Oncology department of Azienda Ospedaliero-Universitaria(A.O.U.) Maggiore DellaCarità, University of Eastern Piedmont, Novara. All patients provided written informed consent to participate in the study before any sample collection. The key inclusion criteria were as follows: (i) patients aged ≥ 18 years at initial treatment, (ii) pathological confirmation of breast cancer diagnosis by core needle biopsy prior to NAT treatment, (iii) consent for NAT and surgery in our hospital, (iv) complete clinical recorded information and follow-up data, (iv) peripheral blood samples obtained within one week prior to NAT initiation and right after the NAT finished, (v) absence of side effects upon therapy administration, (vi) patients who received one of the following NAC prior to surgery: (anthracycline and paclitaxel), (anthracycline, paclitaxel and carboplatin) or (anthracycline, paclitaxel and trastuzumab or/and pertuzumab) and (vii) ability to understand and sign an informed consent. The key exclusion criteria were as follows: (i) Patients ≤ 18 years of age, (ii) patients with distant metastasis, (iii) patients who had undergone previous radiotherapy, chemotherapy, or major surgery for BC and not suitable for NAT, and (iv) inability to understand and/or sign an informed consent. The clinicopathological data were collected from the patients' medical records.

3.2 PBMC preparation and plasma collection from PB of BC patients

Peripheral whole blood samples (15ml) were taken from potential candidates for NAT, both at baseline (PRE) and at the end of treatment, before surgery (POST), collected into Vacutainer EDTA (ethylenediaminetetraacetic acid) tubes (BD Bioscience, Milan, IT) from the Oncology department of Azienda Ospedaliero-Universitaria (A.O.U.) Maggiore Della Carità, University of Eastern Piedmont, Novara and processed freshly in Center for Translational Research and Autoimmune & Allergic Disease (CAAD), University of Eastern Piedmont, Novara. Within 3 hours of blood collection, peripheral blood mononuclear cells (PBMCs) were isolated using Ficoll-Paque (Lympholyte, Miltenyi Biotech Bergisch Gladbach, Germany) density gradient centrifugation for 20 min at 2200 rpm with an acceleration (AC) value of 7 and a break (DC)

value of 0. The isolated PBMCs were washed (twice) and counted using Burker chamber with TURK solution (1:10 dilution). The plasma was collected and stored at −80 °C until further analysis.

3.3 Isolation of CD3+CD4-CD8- DN T cells from PBMCs using MACS beads

The heterogeneous cell suspension was resuspended in appropriate MACS buffer solution (PBS1x, pH7.2, 0.5%FBS and 2mMEDTA) and isolation was based upon a classical positive selection by antibody-dependent Magnetic Activated Cell Sorting (MACS) using CD3 MicroBeads (Miltenyi Biotech Bergisch Gladbach, Germany) according to the manufacturer's protocol. Briefly, PBMCs was mixed with magnetic beads that carry an antigen specific capture antibody (e.g., against CD3) that connects the beads with the cells of interest. The incubation time was for 25 minutes at 4°C. Once incubation was finished, the suspension was loaded onto a column containing a ferromagnetic matrix in a magnetic field, the magnetic bead-labeled cells remain in the column while the unlabeled cells pass. Then, column was washed thrice with MACS buffer. The elution of our cells of interest (CD3+T cells) done by removing the column from magnetic field, placed in a collection tube, and flushed out with MACS buffer using a plunger. That eluted CD3+CD4-CD8- DN T cells were washed, counted, and stained with PE-Cy7 conjugated anti-CD3 (clone: HIT3a, eBioscence) for purity analysis using Flow Cytometer.

3.4 Expression of p16 and p21

The quantification of expression levels of p16 and p21 with RPLPO as reference gene was performed by RT-qPCR analysis on a CFX96 Touch Real-Time PCR Detection System (BIORAD) with 96-well plate capacity, with 500 ng of mRNA from human CD3+ T cells were retrotranscribed with a high-capacity cDNA Reverse Transcription Kit (Applied Biosystem Waltham, MA USA) using manufactures' protocol. The eluted RNA was quantified using NanoDropTM and the purity was assessed by 260/280 ratio. The reaction included as follows: Step1- 25°C (10 min) Step2- 37°C (120 min), Step3- 85°C (5 min) and Step4- 4°C (00). This was followed by qPCR on p16, p21 and RPLPO: the 10 µL reactions included 2.5 µL of cDNA, 5 µL

of Sensifast Probe Lo-ROX kit (BIOLINE, London, UK), 0.1uL of Universal Probe Library (UPL) for p16 (UPL#67) or p21 (UPL#32) or RPLP0 (UPL#1), 2.3uL of nuclease-free water per each sample, 0.1uL of primerset for p16 or p21 or RPLP0 [50µM] and 300 nM for both forward and reverse primers for the respective reactions: p16-FW:GAGCAGCATGGAGCCTTC and RW:CGTAACTATTCGGTGCGTTG; p21-FW:TCACTGTCTTGTACCCTTGTGC and p21-RW:GGCGTTTGGAGTGGTAGAAA; RPLP0-FW:TCTACAACCCTGAAGTGCTTGAT and RW:CAATCTGCAGACAGACACTGG). All samples were run in duplicate on the same plate. The thermo-cycling programme comprised step1- 95°C (7min) 1 cycle, step2- 95°C (5sec) 60°C (30sec) 40 cycles, step3- 37°C (1minute) 1 cycle. The data was collected at the end of the cycle, processed using Bio-Rad CFX Maestro Software (BIORAD) and had examined the relative gene expression using delta-delta Ct (2–ΔΔCt) method.

3.5 MDSC staining

From each sample, 1x106 PBMCs were taken for MDSC phenotyping using Flow Cytometer (BD Bioscience, Milan, IT). FACS tubes with PBMCs were stained with seven surface markers include: CD45 (BUV395), CD33 (APC), HLA-DR (BV605), CD14 (BUV737), CD15(BV510), CD16 (PE-CY) and LOX-1(PE) and were incubated in dark condition at room temperature (RT) for 15 minutes. Then, lysed the cells using 1x lysis buffer (BD biosciences, Milan, IT), followed by 15 minutes' incubation at RT, protected from light. Finally, stained PBMCs were acquired using FlowJo v10.5.3 software.

MDSC subpopulation phenotypes were defined according to Bronte et al as follows:

- M-MDSC: HLA-DR-/low CD33 intermediate CD15- CD14+
- PMN-MDSC: HLA-DR-/low CD33 intermediate CD15+ CD14-
- LOX-1-PMN-MDSC: LOX-1+ HLA-DR-/low CD33 intermediate CD15+ CD14

3.6 Metabolomics GCxGC/TOFMS analysis on BC patient’s plasma

A total of 2 ml of peripheral whole blood was centrifuged to extract 4 vials of 200 µl plasma, which were stored at -80°C. For each patient, a vial was thawed and prepared for

metabolomics analysis as follows: 30µl of plasma was treated with 1 ml of acetonitrile (VWR, Milan, IT) and isopropanol (Scharlab, Barcelona, ES) water solution (3:3:2), with tridecanoic acid (Merck, Darmstadt, DE) at 1 ppm, added as internal standard. The solution was then vortexed and centrifuged at room temperature for 15 minutes at 14.500g, the resulting supernatant was collected and dried in a speed-vacuum. Then, the sample was derivatized by adding 20 µl of Methox at 80°C for 20 minutes, followed by 90 µl of N, O-Bis(trimethylsilyl) trifluoroacetamide (both reagents were purchased from Merck, Darmstadt, DE) at 80°C for 20 minutes, respectively for methoximation and sialylation. For GCxGC/TOFMS metabolomic analysis, 1 ml of derivatized solution was injected in splitless mode at 250°C into a LECO Pegasus BT 4D GCXGC/TOFMS instrument (Leco Corp., St. Josef, MI, USA) equipped with a LECO dual stage quad jet thermal modulator. High-purity helium (99.9999%) was used as a carrier gas. Chromatograms were acquired in total ion current (TIC) mode, and we rejected those peaks with a signal-to-noise value lower than 500. Finally, the ChromaTOF software (ver. 5.51) was utilized for raw data processing, spectral assignments were achieved by matching the results with the NIST MS Search 2.3 library and implemented by FiehnLib. The alignment of chromatographic signals was performed by LECO ChromaTOF Statistical Compare® optimized for Pegasus® 4D.

3.7 Collection of laboratory data for SII & PIV scoring

Complete blood cell counts were retrieved from patients' electronic medical records at baseline and after NAT, before surgery. The calculation formula of each indicator was as follows: SII (systemic immune-inflammation index) = neutrophil count (109/L) × platelet count (109/L) / lymphocyte count (109/L); and PIV (pan-immune-inflammation value) = neutrophil count (109/L) × platelet count (109/L) × monocyte count (109/L)/lymphocyte count (109/L) [Fuca G etal.,2020]. According to the calculation formula mentioned above, the SII and PIV were calculated in Excel, and performed analysis using Graph pad prism 9. These markers were considered in our analyses due to some research evidence demonstrated about pre-diagnostic associations to cancer risk and prognostic significance in cancer patients [Dolan RD etal.,2017].

3.8 Statistical analysis

Statistical analyzes were performed on Prism V9 software (GraphPad). To compare groups (pCR vs RD), we applied non-parametric tests, Mann-Whitney and Kruskal-Wallis tests. In addition, we used the Wilcoxon test for paired samples (Before vs After NAT) to test for statistical differences. P values < 0.05 were considered statistically significant.

3.9 Follow-Up

All patients received a 3-monthly follow-up for two years after surgery, a 6-monthly follow up for the next three years, and then an annual follow-up. Laboratory tests, physical examination (breast and lymph node palpation), breast ultrasonography, liver ultrasound, mammography, and other suitable examinations are used to assess the physical condition of patients at follow-up.

Chapter4: Results

4.1 Clinical and pathological characteristics of the included patients at baseline

The demographic characteristics of our study group at baseline (BC patients=90) are described in Table 1. The study groups showed the table was well matched for most of the demographic and clinical characteristics. Most of the BC participants included in this study has a previous history of cancer in their family.

Characteristics	**Number of patients (%)**
Age (years)	
< 50	42 (47%)
≥ 50	48 (53%)
Gender	
Female	89 (99%)
Male	1 (1%)
Family history	
Present	61 (68%)
Absent	23 (25%)
Unknown	6 (7%)
Histological type of BC	
Invasive ductal carcinoma	82 (91%)
Invasive lobular carcinoma	1 (1%)
Invasive ductal and lobular	6 (7%)
Invasive metaplastic	1 (1%)
BRCA 1/2 mutational status	
BRCA 1/2 wildtype	37 (41%)
BRCA 1/2 mutated	12 (13%)
BRCA 1/2 unknown or not verified	41 (46%)
Tissue marker status	
HER2 status	
Positive (+)	37 (41%)
Negative (-)	53 (59%)
Progesterone receptor (PR)	
Positive (+)	29 (32%)
Negative (-)	61 (68%)
Estrogen receptor (PR)	
Positive (+)	39 (43%)
Negative (-)	51 (57%)

Clinical lymph Node status, n (%)	
N0	44 (50%)
N1	29 (33%)
N2	11 (12%)
N3	4 (5%)
Clinical tumor stage, n (%)	
T1	11 (12%)
T2	49 (56%)
T3	24 (27%)
T4	4 (5%)
Grade, n (%)	
G2	20 (22%)
G3	70 (78%)
Ki67 level, n (%)	
<30%	12 (13%)
≥ 30%	78 (87%)
Body mass index, kg/m2	
< 25	52 (58%)
25-30	27 (30%)
≥ 30	11 (12%)
Molecular subtypes of BC	
Luminal A	1 (1%)
Luminal B	19 (21%)
HER2+	37 (41%)
TNBC	33 (37%)

Table1: Baseline clinical characteristics of the study cohort.

4.2 Pathological complete response (pCR) after NAT.

Ninety women with histologically proven early-stage BC and eligible for preoperative therapy were included in this study. Of those, four patients were deceased while receiving treatment and twenty-six patients were lacking one or more inflammatory markers were excluded from the further molecular analysis. Out of these 90, 60 patients completed the treatment of indicated NAT regimens and surgery with variable pathological responses; 33 (55%) achieved pCR and 27 (45%) still had RD.

Based upon molecular subtype, pCR has been observed as follows:

- Of the 13 luminal B patients, 3 achieved pCR (23.1% of Luminal B; 9.09% of total pCR).
- Of the 22 HER2+ patients, 13 achieved pCR (59.1% of HER2+; 39% of total pCR).

- Of the 25 TNBC patients, 17 achieved pCR (68% of TNBC; 52% of total pCR).

4.3 Evaluation of relative expression of p16 and p21, senescence biomarker by RTPCR

Sixty patients have been tested for T-cell senescence at baseline (PRE) and after NAT (POST), before surgery. The relative expression of p16 and p21 was significantly increased from baseline to surgery (p16: 3.01±5.02 vs 6.00±5.75, p= <0.0001; p21: 4.09±6.26 vs 10.07±12.49, p=0.0002). There was no significant difference in relative expression of p16 and p21 at baseline and after NAT in patients who achieved pCR (p16: 4.23±6.29 vs 5.23±5.60; p=0.08; p21: 4.52±7.24 vs 10.39±12.66; p=0.07). However, patients with residual disease (RD) had a statistically higher significance in p16 and p21 expression after NAT (p16: 1.51±2.03 vs 6.08±5.02; p=<0.0001; p21: 3.55±4.89 vs 8.21±11.05; p=0.003) (figure6). The values are expressed as arbitrary units and mean±SD.

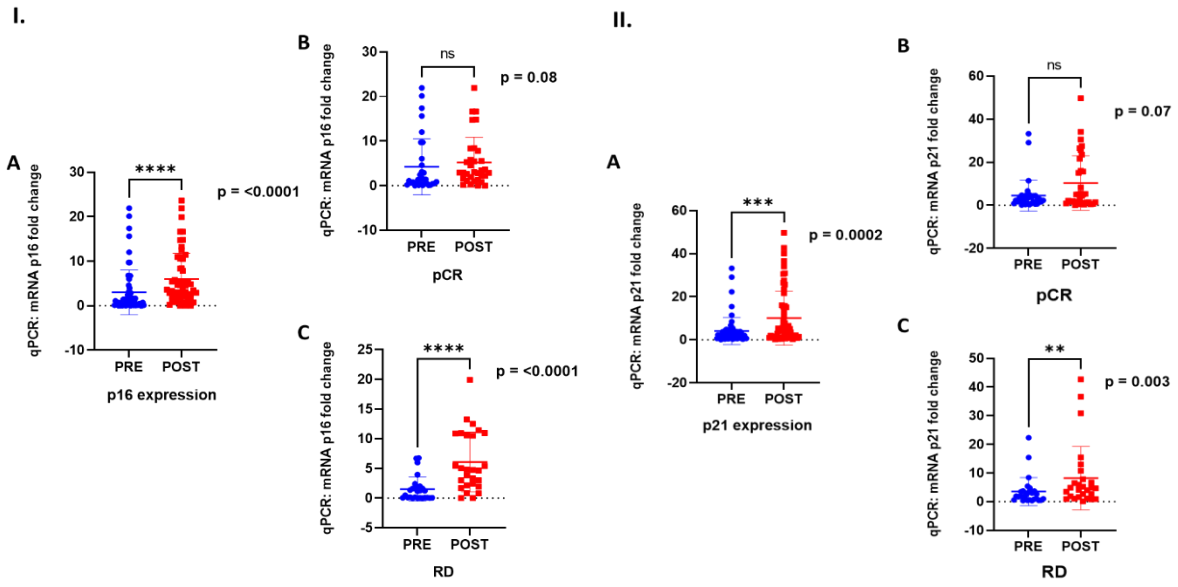

Figure6: **Relative expression of p16 and p21 at two time points: at baseline (PRE) and after NAT (POST)**. (I) expression of p16 and (II) p21 expression.

Then, stratified the patients based upon molecular subtypes (figure7) and no significant difference observed in the expression of both p16 and p21 within BC molecular subtypes

(TNBC, HER2+ and Luminal B), neither at baseline (p16: 2.53±4.19 vs 3.98±6.64 vs 2.29±2.96; p=0.8; p21: 6.05±8.85 vs 2.89±3.46 vs 2.37±1.20; p=0.3) nor after NAT (p16: 5.48±5.92 vs 5.44±5.45 vs 7.99±5.97; p=0.2; p21: 12.06±14.24 vs 6.99±8.81 vs 11.445±14.06; p=0.7).

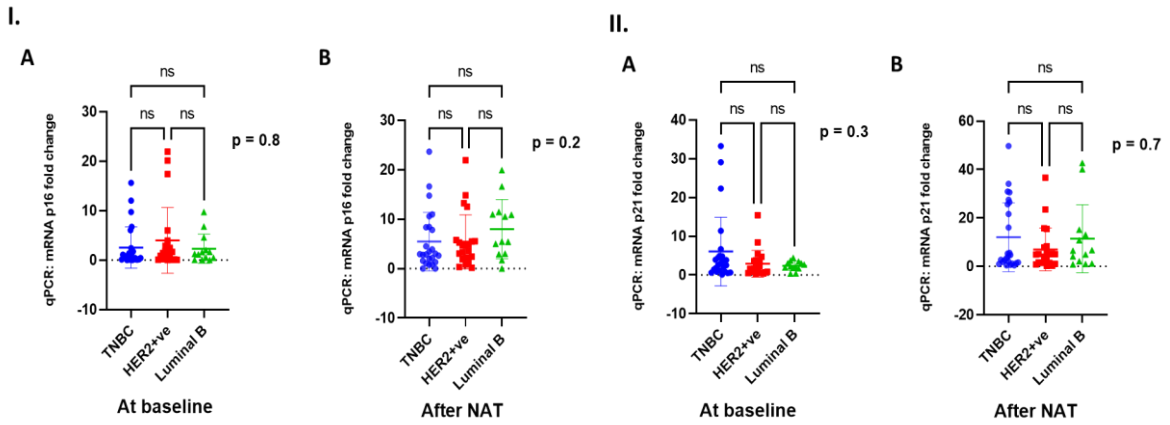

Figure7: **p16 and p21 expression within molecular subtypes of BC**. (I) expression of p16 (A) at baseline and (B) after NAT; (II) expression of p21 (A) at baseline and (B) after NAT.

Furthermore, classified them based upon the pCR status of each patient in response to neoadjuvant chemotherapy (figure8). There was no significant difference in p16 and p21 expression neither at baseline (p16: 4.23±6.30 vs 5.23±5.60; p=0.08; p21: 4.52±7.24 vs 10.39±12.66; p=0.07) nor after NAT (p16: 4.23±6.29 vs 5.23±5.60; p=0.08; p21: 4.52±7.24 vs 10.39±12.66; p=0.07) among both pCR and RD groups.

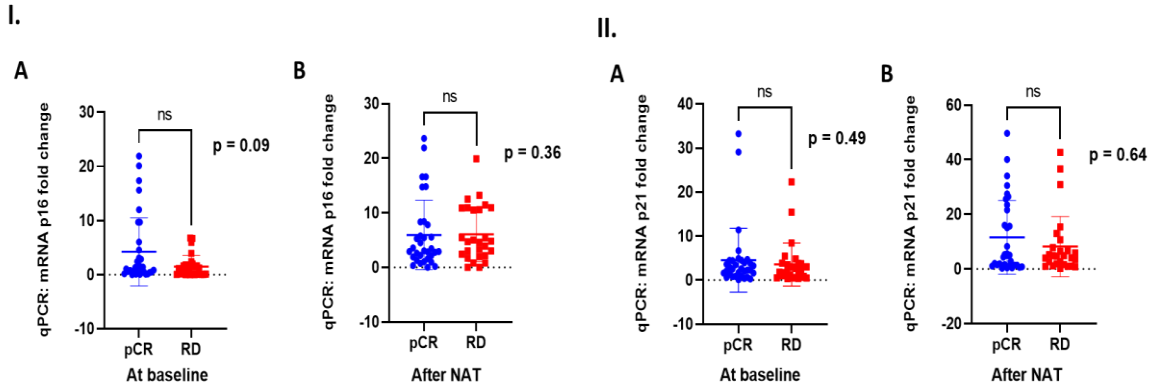

Figure8: **p16 and p21 expression among pCR and RD group at two time points**. (I) expression of p16 (A) at baseline and (B) after NAT; (II) expression of p21 (A) at baseline and (B) after NAT.

4.4 Gate strategy for MDSCs characterization by flow cytometry

The gating strategy started by excluding dead cells through forward (FSC-A) and side scatter (SSC-A), followed by the exclusion of doublets based upon forward side scatter area (FSC-A) and forward side scatter height (FSC-H). SSC-A versus CD45 was used to set the lympho-monocyte gate and later, gated monocytes and subpopulations of MDSCs such as M-MDSCs (HLA-DR-/low, CD14+) and PMN-MDSCs (CD33 intermediate, CD15+). Also, gated LOX1 positive PMN-MDSCS by SSC-A versus LOX-1(figure9).

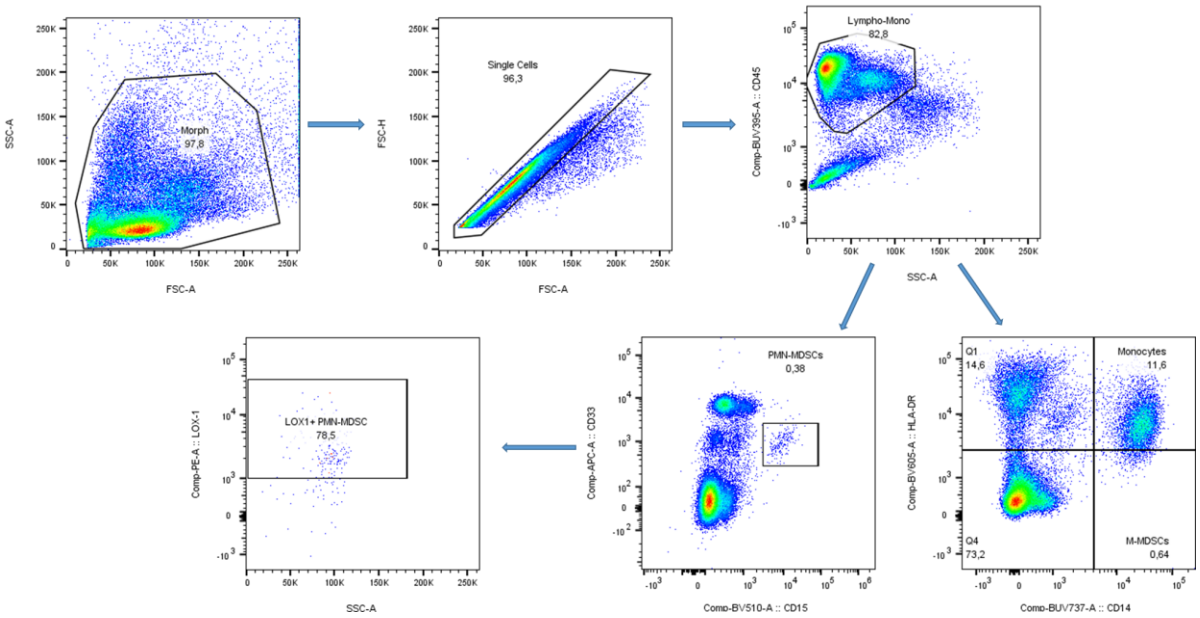

Figure9: Representative flow cytometry of MDSC and its subsets isolation and gating strategy.

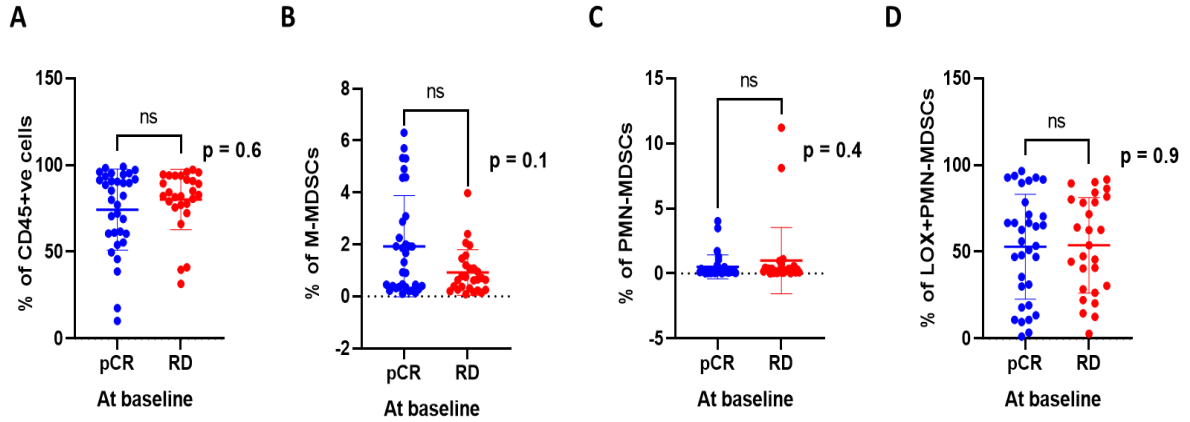

Figure10: The percentage of (A) CD45+ve cells, (B) M-MDSCs, (C) PMN-MDSCs and (D) LOX+PMN-MDSCs among pCR and RD group at baseline (PRE).

There was no significant difference in the percentage of neither M-MDSC nor PMN-MDSCs at baseline in pCR vs RD group of BC patients (figure10).

4.5 Relationship between blood-based inflammatory biomarkers and pCR association.

We examined whether our potential inflammatory biomarkers such as SII (figure11) and PIV (figure12) were associated with pCR status or not. For RD group, SII and PIV were significantly higher (p-values <0.0001 and 0.01, respectively) after NAT. No significant difference was found neither at baseline nor after NAT in both pCR and RD group.

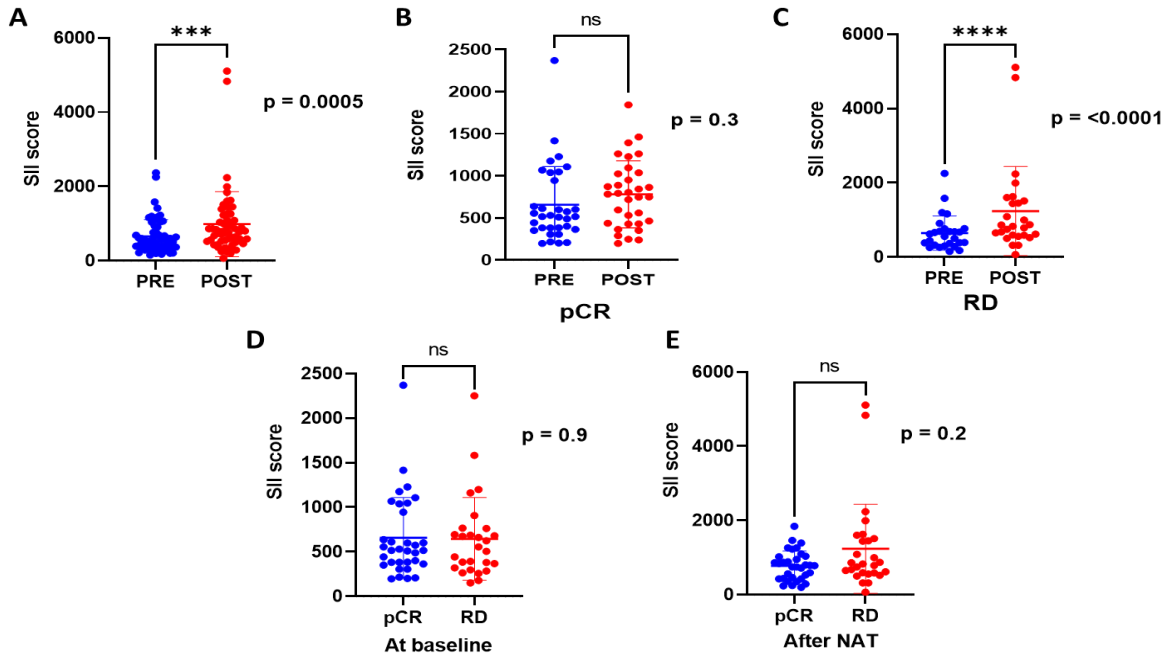

Figure11: Validation of blood based IIB, SII. (A) SII at two time points: at baseline (PRE) and after NAT (POST), SII scoring (B) among pCR vs (C) RD group, SII (D) at baseline and (E) after NAT among pCR and RD group.

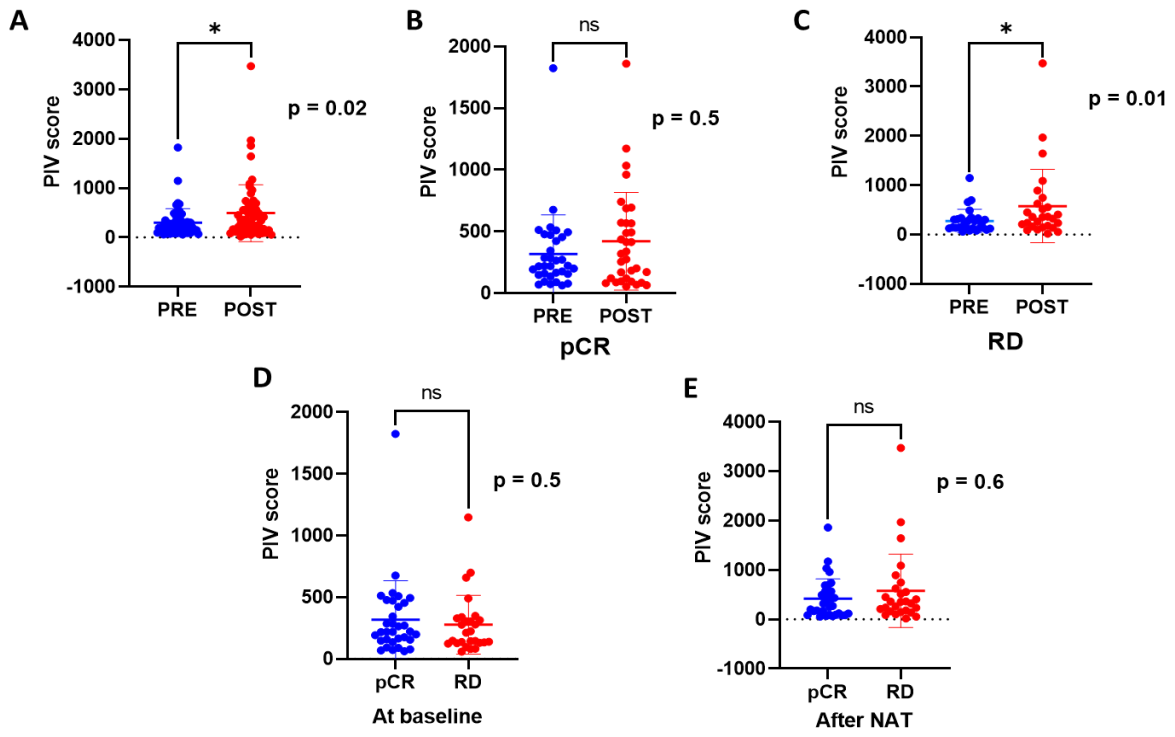

Figure12: Validation of second blood based IIB, PIV. (A) PIV at two time points: at baseline (PRE) and after NAT (POST), PIV scoring (B) among pCR vs (C) RD group, PIV(D) at baseline and (E) after NAT among pCR and RD group.

4.6 Pre-NAC metabolomics analysis and pCR association

In collaboration with Prof. M. Manfredi's group, a metabolomics analysis was done on patient's plasma at baseline. The stratification performed based upon NAT response to figure out whether any potential metabolites were associated with pCR status or not. Interestingly, 25 molecules have been found out with predictive value in response to neoadjuvant treatment (figure13). The patients having RD (Table2) had an upregulation of some unsaturated fatty acids such as (8Z,11Z,14Z)-Icosatrienoate, 9-Decenoic acid and 17-Octadecynoic acid, which promotes inflammation through immune recruitment. On the other hand, Hexadecenoic acid (palmitoleic acid), doconexent and 9(E),11(E)-Conjugated linoleic acid was downregulated, which mainly involve in ferroptosis in tumor, boost chemotherapeutic sensitivity and so on. Also, identified lower levels of circulating monosaccharides such as glucose and glucopyranose among RD group.

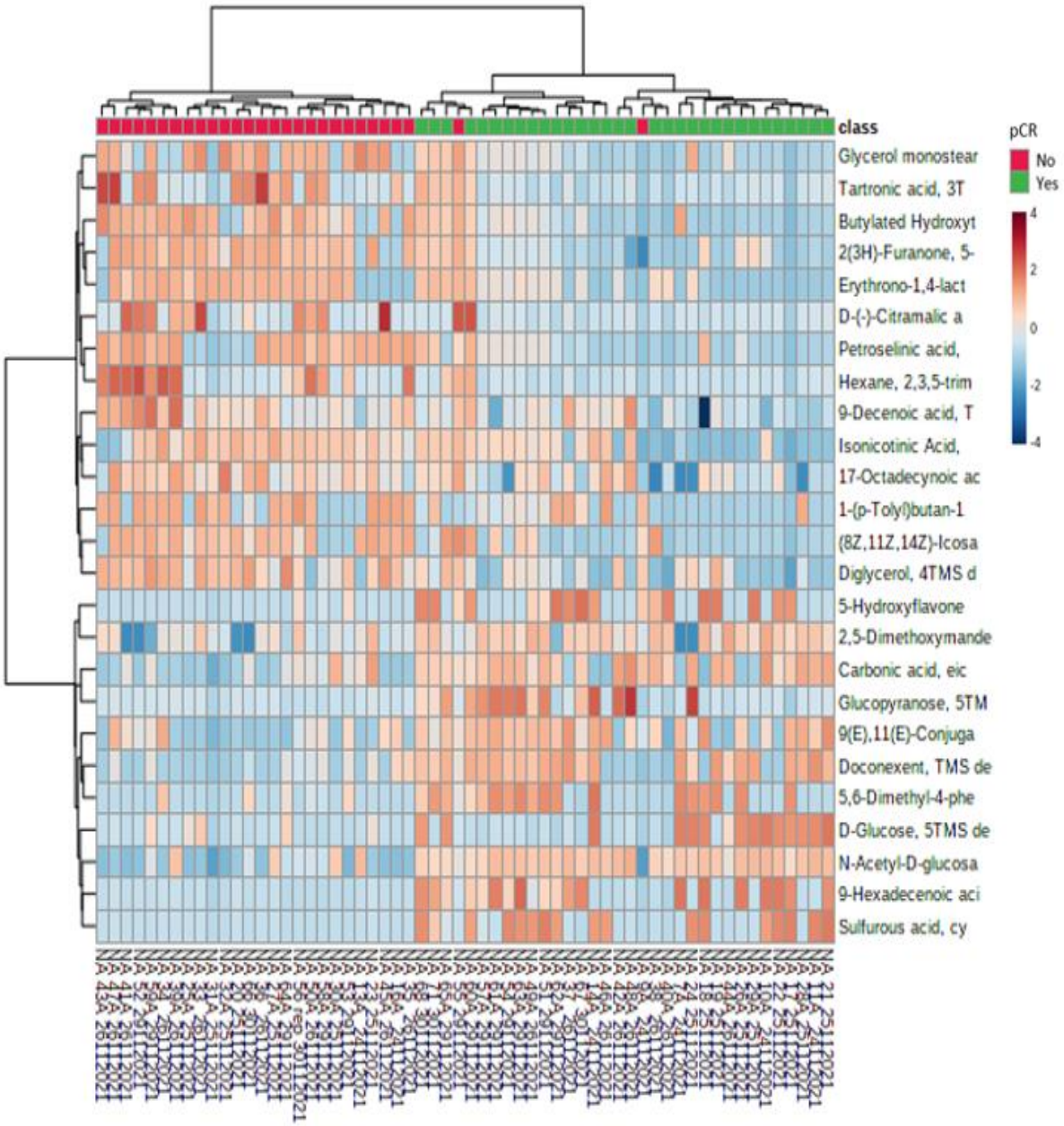

Figure13: Heatmap for metabolite characterization in patients' plasma at baseline, before NAT and their association with pCR response. Each column illustrated each patient. In row 'class' the patient achieved pCR in green in colour and others (RD group) are highlighted with red colour. Each row inside the heatmap was associated with a metabolite, which may be upregulated (bright/warm color) or downregulated (light/cold color).

Top 25 molecules	Mean fold change	Raw p-value	Regulation
Hexane, 2,3,5-trimethyl-	25,07700	0,00004	
Erythrono-1,4-lactone, (Z)-, 2TMS	15,08200	0,00026	
Glycerol monostearate, 2TMS	11,39000	0,00010	
Petroselinic acid, TMS derivative	9,91710	0,00001	
2(3H)-Furanone, 5-dodecyldihydro	8,34770	<0,0005	
Tartronic acid, 3TMS	8,13310	0,00048	
D-(-)-Citramalic acid, 3TMS	7,19670	0,00051	
			Upregulated
Butylated Hydroxytoluene	7,00020	<0,0005	
Diglycerol, 4TMS	5,00380	<0,0005	
1-(p-Tolyl)butan-1-one	4,05300	0,00061	
Isonicotinic Acid, TMS	3,98060	0,00040	
(8Z,11Z,14Z)-Icosa-8,11,14-trienoate, O-TMS	3,47380	<0,0005	
9-Decenoic acid, TMS	2,11350	0,00035	
17-Octadecynoic acid, TMS	2,08980	0,00064	
Sulfurous acid, cyclohexylmethyl hexadecyl ester	0,00001	<0,0005	
9-Hexadecenoic acid, (Z)-	0,00096	<0,0005	
5,6-Dimethyl-4-phenyl-3-cyanopyridine-2(1H)-thione	0,00102	0,00007	
5-Hydroxyflavone	0,00119	0,00017	
D-Glucose, 5TMS	0,01478	0,00060	
Doconexent, TMS	0,01501	<0,0005	Downregulated
Glucopyranose, 5TMS	0,01502	0,00013	
9(E),11(E)-Conjugated linoleic acid, trimethylsilyl ester	0,20185	0,00011	
N-Acetyl-D-glucosamine	0,21955	<0,0005	
2,5-Dimethoxymandelic acid, di-TMS	0,22205	0,00056	
Carbonic acid, eicosyl vinyl ester	0,30438	0,00009	

Table2: Top 25 metabolites and their relative up/down regulation for those patients who did not achieve pCR. Each subgroup (upregulated and downregulated) is organized based on the mean fold change value.

Section II

THE SHORT-TERM EFFECTS OF CDK4/6 INHIBITOR IN THERAPY INDUCED SENESCENCE MODELS

Chapter1: Introduction

1.1 Cellular Senescence: in general

Replicative cells progressively accumulate mutation during organismal aging. Despite of array of repair mechanisms exist, some damage caused by either endogenous or exogenous stressors can be persistent [J.C. Jeyapalan etal.,2007]. Cellular Senescence is one of the defense mechanisms to reduce the impact of these persistent stresses by switching to a dynamic, stable non-proliferative, metabolically active survival state and the acquisition of a senescence-associated secretory phenotype (SASP). The senescence phenomenon was initially described as a limited number of doublings in culture due to telomere erosion and this process is now termed as replicative senescence [Hayflick L etal.,1961]. In addition to the growth arrest of cell division, senescent cells differ from other non-dividing cells (such as quiescent or terminally differentiated cells) characterized by striking phenotypic, structural, and functional changes [Campisi J etal.,2007]. These features include the following: absence of proliferative markers, upregulation of lysosomal senescence-associated β-galactosidase (SAβGAL) activity [Lee BY etal.,2006], altered cell metabolism by mitochondrial dysfunction, expression of tumour suppressors, loss of lamin B1 (a protein of the nuclear lamina) and high level of p16INK4a and/or p21CIP1 [Sherr CJ etal.,1999], and often also of DNA damage markers, nuclear foci of constitutive heterochromatin and prominent secretion of signalling molecules. Although none of these markers is on its own completely specific or universal for all senescence types, there is ample consensus that senescent cells express most of them. So, multiple facultative senescence-associated markers are necessary for the identification of senescence in both cell culture and in vivo.

The irreversibly senescence growth inhibition enforces the idea that senescence response evolved at least in part to suppress the development of cancer. To date, no known physiologic stimuli can stimulate senescence cells to re-enter the cell cycle and the

senescence-associated arrest is stringent. It is established and maintained by at least 2 major tumor suppressor pathways: the proteins p53/p21 and the p16INK4A/retinoblastoma protein (pRb). Indeed, these pathways are now recognized as a formidable barrier to malignant tumorigenesis. There is convincing evidence that senescent cells have been accumulate over the life span of rodents, non-human primates, and humans [Dimri G P etal.,1995].

1.1.2 Cellular senescence in physiology and pathology

Cellular senescence as a trigger of different types of stimuli which reflects its spectrum of roles under different conditions (figure1). In general, transient induction of senescence for the elimination of damaged cells followed by tissue remodelling during normal embryonic development and upon tissue damage is beneficial. Conversely, persistent senescence or the inability to eliminate senescent cells by immune system has detrimental effects. Importantly, aberrant persistence of senescent cells is often associated with tissue dysfunction and pathology. During active tissue repair or in cancer, pro- and anti-senescent therapies contribute to minimize the damage by limiting proliferation and eliminate accumulated senescent cells, to recover tissue respectively.

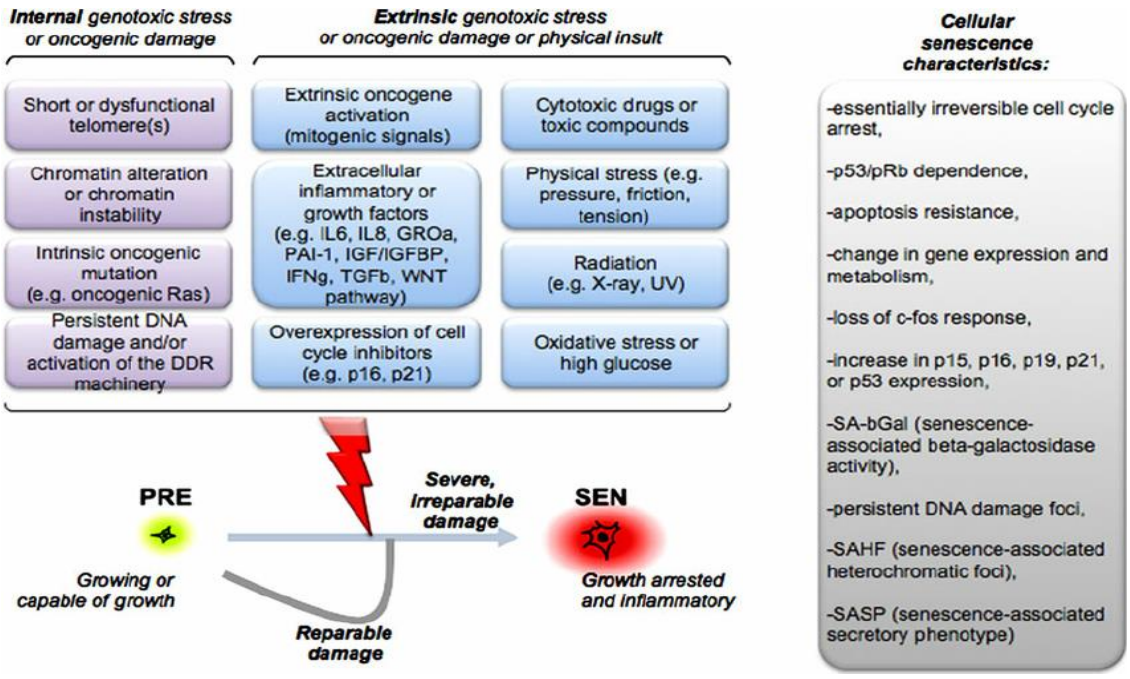

Figure1: Schematic representation of induction of cellular senescence by different stressors.

Genotoxic insults, both internal and external genotoxic stress (left panel) can trigger the cells to enter irreversible growth arrest. Most of these senescence inducers lead to the acquisition of multiple senescence markers (right panel), including SASP factors (PRE: pre-senescent; SEN: senescent) [Adapted from Albert R D etal.,2010].

1.1.3 Cellular Senescence: secretory phenotype

The first evidence of SASP was reported on a gene expression study of inflammation-associated genes in senescent fibroblasts in 1999 [Shelton DN etal.,1999]. SASP is nonspecific and highly heterogeneous secretory program which is predominantly characterized by the secretion of pro-inflammatory cytokines and extracellular matrix-modifying factors and plays an important role in embryonic development, wound healing, tissue repair and aging as well as cancer therapy-evoked insults [Herranz, N etal.,2018; Lee, S etal.,2019]. The nature of SASP is cell type and stimulus dependent. The signaling pathways such as nuclear factor κB (NF-κB), IL-6, cyclic GMP–AMP synthase (cGAS)–stimulator of interferon genes (STING), CCAAT/enhancer-binding protein-βa (CEBPβ), NOTCH, Janus kinase (JAK)–signal transducer and mTOR pathways involved in the generation of SASP Kuilman T etal.,2008; Faget DV etal.,2019]. The SASP influences the surrounding tumor, non-tumor, and immune cells via the paracrine mechanism. Certain SASP components are highly immunogenic and able to potentiate tumor immune surveillance. However, paradoxical pro-tumorigenic roles of senescence via SASP growth factors and inflammatory mediators have been previously demonstrated (Coppe etal., 2010; Gonzalez-Meljem J.M etal.,2018).

In an oncologic context, this conserved mechanism that permanently halts the proliferative capacity of stressed or premalignant cells triggered by stimuli like oncogene activation (oncogene-induced senescence, OIS) [Serrano M etal.,1997], oxidative stress, irradiation, or chemotherapeutic drugs, termed as therapy-induced senescence (TIS) [Kuilman T etal., 2010]. TIS typically arises in response to genotoxic insults. Indeed, conventional anticancer therapies induce senescence leading to tumor regression and increased tumor-specific immune activity [J.A. Ewald etal.,2010]. Therefore, therapy-induced senescence (figure2) serves as an initial antitumor mechanism to prevent further genomic instability [Nardella C etal.,2011]. The senescent cancer cells can also influence the neighboring cancer cells via SASP, thereby contributing to tumor suppression through the recruitment of immune cells and improvement of vasculature for drug delivery [Xue W etal.,2007; Kang TW etal.,2011;

Ruscetti M etal.,2018]. However, endurance of therapy-induced senescent cells in the long term may be detrimental due to pro-inflammatory or/and immunosuppressive microenvironment [Ruhland MK etal.,2021]. Moreover, the SASP can enhance migration and promote metastasis in neighboring cancer cells. Some DNA-damaging therapeutic agents such as doxorubicin [Demaria M et al.,2017; Spallarossa P etal.,2009], cisplatin [Seluanov A etal., 2001], etoposide [Probin V etal.,2006], paclitaxel [Seluanov A etal., 2001] and ionizing radiation causes senescence induction at low doses and apoptosis at high doses. Treatment associated senescent cells can persist and contribute to adverse effects after treatment including cancer progression through SASP.

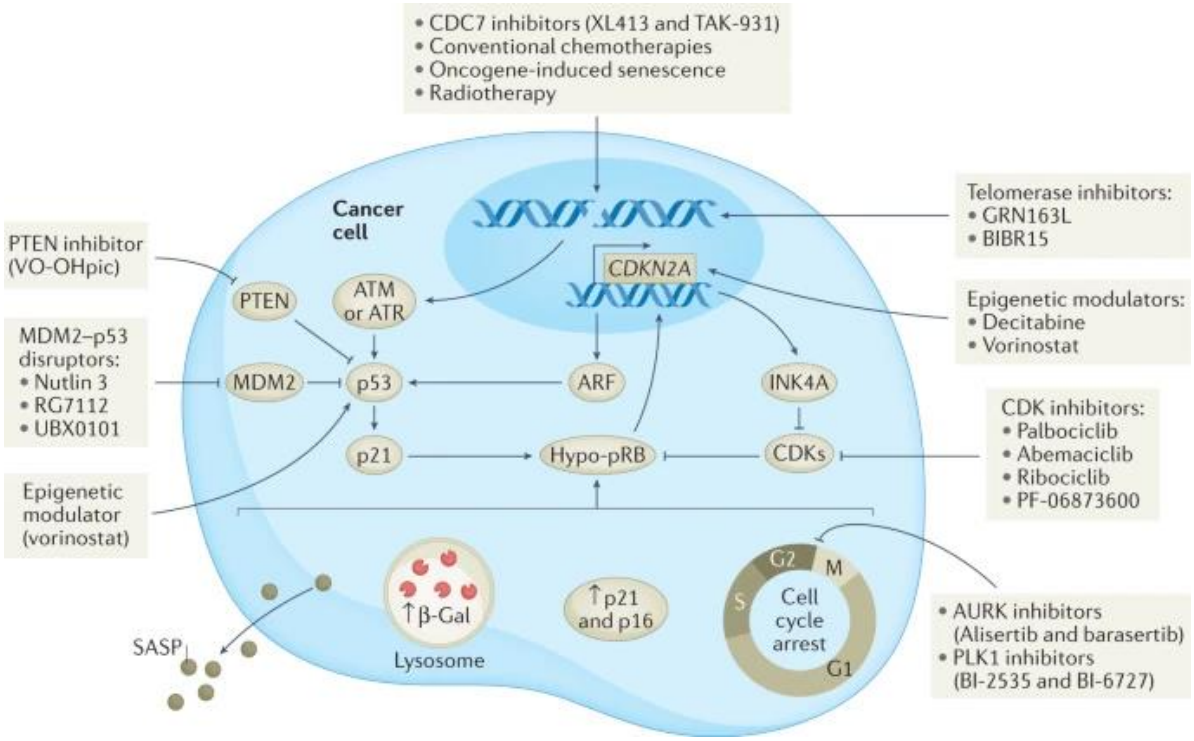

Figure2: Diagrammatic representation of therapies inducing senescence in cancer. The conventional chemotherapies, radiotherapy, and CDC7 inhibitor (XL413 or TAK931) or telomerase inhibitor (GRN163L or BIBR15) treatment cause massive DNA damage, resulted in senescence induction. The CDK4/6 inhibitors namely, palbociclib, abemaciclib or ribociclib also induce CDK inhibition-mediated senescence [Adapted from Wang L etal.,2022].

TIS is heterogeneous in nature, which is also reflected in biomarkers, tissue of origin, cellular plasticity, expression of SASPs, and cell lineage. It can occur not only in cancer cells but also other proliferating stromal cells.

1.2 Overview of cell cycle and its regulators

The mitotic cell cycle regulation is a highly orchestrated process by numerous checks and balances to ensure that division and proliferation is a favored outcome. Progression is mediated by cyclin-dependent kinases (CDKs) and their partner cyclins. Those are crucial players in several mammalian cell cycle transitions from 1990s. CDK act as a major regulatory enzyme in cell cycle through monitoring different phases in cell cycle progression and transcriptional regulation in response to both intracellular and extracellular signals. The cyclin D-Cdk4-6/INK4/Rb/E2F pathway plays a vital role in cell cycle regulation by integrating multiple mitogenic and antimitogenic stimuli. The transition between the different phases of mitotic cell cycle includes sequential activation of several distinct cyclin-dependent kinases (CDKs) whose activity is crucial to this process (figure3).

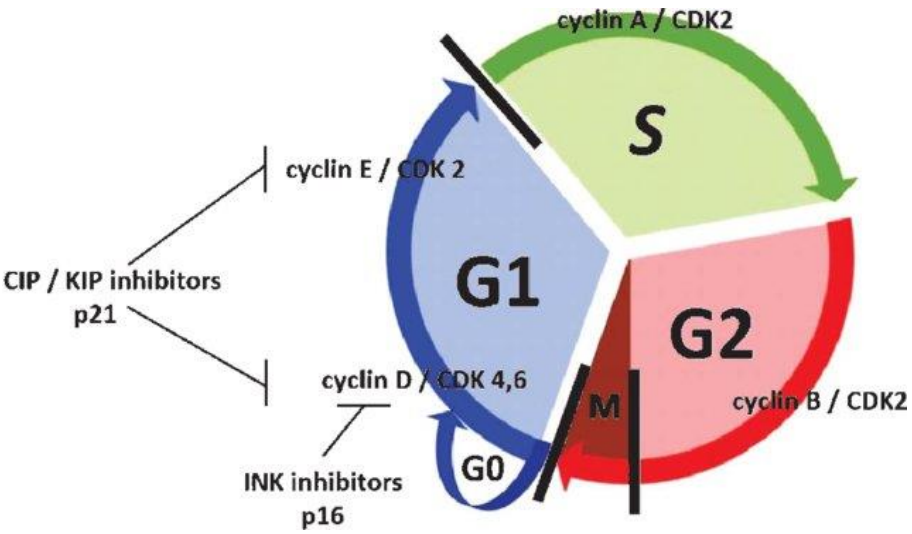

Figure3: Representation of cell cycle and its main regulators. Different CDK-cyclin complexes and the respective cyclin-dependent kinase inhibitors involved in the transition of cell cycle phases. p16INK4, member of INK4 family, specifically bind and inhibit CDK4/6-cyclin D complexes promoting cell cycle arrest in the G1 phase. The Cip/Kip proteins including p21CIP1/WAF governs cell-cycle arrest by counteracting with different spectrum of CDK-cyclin complexes and restrain cell-cycle both during early and late G1 phase by binding either CDK4/6-cyclin D or CDK2-cyclin E complexes. Also, impose a brake during the S-phase by binding CDK2-cyclin A complex (Adapted from Joanna Wojsiat et al., 2015).

Cyclin-dependent kinases 4 and 6 (CDK4/6) are serine–threonine kinases located in the 12q14.1 and 7q21.2 location of the chromosome, identified as a key driver in cell cycle progression from the G1 to the S phase. CDK4 and CDK6 are partners of D-type cyclins (D1, D2, and D3) that function in G1 before cyclin E in conjunction with CDK2. Once interaction

with cyclin D is activated, CDK4/6 phosphorylates a critical tumor suppressor called retinoblastoma protein (RB). RB is the product of the retinoblastoma tumor susceptibility gene (RB1) and the major function of RB is the inhibition of cell cycle progression exerted through repression of the E2F1 transcription factor. The hyperphosphorylation of RB1 by cyclin D in conjunction with CDK4/6 (and by cyclin E in conjunction with CDK2) allows the release of E2F and the transcription of genes required for S-phase entry, thus triggering the cell cycle cascade [Giacinti. C etal.,2006]. In each phase, the expression of cyclins varies along with the progression of the cycle, triggering the activation of their CDK partners. In addition to this canonical RB-dependent cell cycle transition, cyclin D1 involves in cellular migration, DNA damage response and repair [Fu M et al.,2004]. The deregulation of CDKs is predominately observed in different human disorders including cancer [M. Malumbres., 2014]. Emerging evidence indicates that abnormalities in the G1-S checkpoint due to overexpression or amplification of cyclin D and disruption of CDK4 and 6 can leads to tumorigenesis in many types of cancer including melanoma, stomach cancer, breast cancer, bladder cancer, skin cancer and lung cancer [Kalra S etal.,2017]. Besides, inhibitory/negative regulatory proteins, called endogenous CDK inhibitors (CKIs) are responsible for blocking the activity of CDKs.

1.2.1 Cell cycle and cancer

Despite innovations in health care technology, cancer continued to be one of the prime causes of mortality owing to various factors and approximately 10 million people died every year worldwide. The cell cycle is blocked in response to DNA damage-mediated cell cycle checkpoints, thereby initiating DNA repair before cell-cycle progression. The mitotic cell cycle regulation is a highly orchestrated process, which plays a vital role in tissue homeostasis. Cell-cycle checkpoints control the timing of cell-cycle phase transitions. The DNA damage signaling is detected mainly by key regulators such as ataxia telangiectasia mutated (ATM)/ataxia telangiectasia and Rad3-related (ATR), which then phosphorylate and activate transducer checkpoint kinases CHK2 (CHEK2 gene)/CHK1 (CHEK1 gene), respectively [Santo l etal.,2015]. The activated CHK2 induces the activation of p53, leading to p53-dependent early phase G1 arrest to allow time for DNA repair [Matsuoka S etal.,2000]. The activation of p53 induces the expression of p21CIP1, thereby causing the

inhibition of cyclin E/CDK2 complexes and downstream upregulation of DNA repair machinery. The cell faces apoptosis, induced by p53 if the damage cannot resolve successfully or the cells cannot respond to the stresses of viable cell-cycle arrest [Koniaras k etal.,2001]. The deregulation of cell cycle is a primary agenda leads to uncontrolled growth or evasion of apoptosis which is considered as major hallmarks of cancer. The cyclin-CDK4/6-Rb-E2F tumor suppressor pathway is dysregulated with overexpression of cyclin D in a diverse range of human cancers (approximately 90 %) [Shi C., 2019]. The defect might be caused by the gain-of-function mutations in the cyclin-dependent kinase (CDK) and cyclins or the loss of endogenous inhibitors expression and function, is relevant in different cancer types lead to a proliferative stimulus, and overexpression of cyclin D also a key driver in this mechanism. Understanding the factors that regulate cell division is a significant factor in drug development and clinical approaches for cancer therapy. It is well known that distinct signaling pathways connected with specific transcription factors in cell cycle regulation can trigger the shift of normal and cancer cells into different cell fates such as proliferation, quiescence, senescence, or apoptosis based upon the cell type, stimuli, and context.

1.2.2 INK4 and CIP/KIP proteins in cancer

In human cancer, the involvement of cell-cycle regulators has been extensively studied in the last years. The pRB as well as its regulators such as cyclins, CDKs and CKIs, which are frequently deregulated in cancer [Sherr C J.,2000; Malumbres M etal.,2001]. The activation of cyclins/CDKs is induced by mitogenic signals and inhibited by the activation of cell-cycle checkpoints in response to DNA damage. The cyclin/CDKs themselves are negatively regulated by CKIs. Two families of CKIs have been discovered, namely the INK4 and Cip/Kip protein families (Table1). The members of INK4 family, comprising p16(INK4a), p15(INK4b), p18(INK4c), and p19(INK4d), block the progression of the cell cycle by binding to either Cdk4 or Cdk6 and inhibiting the action of cyclin D. The members of CIP/KIP family comprising three proteins such as p21CIP1/WAF1, p27KIP1 and p57KIP2, shares sequence homology at the N-terminal domain allowing them to bind exclusively to both the cyclin and CDKs. They mainly engage in the binding and inhibition of G1/S and S-CDKs; also involves in activation/ stabilization of cyclin D- CDK4/6 complex.

Family of CKIs	Role	Family members	
INK4 family	**Inactivation of G1 CDK (CDK4 and CDK6).**	**p15**	**(INK4b)**
		p16	**(INK4a)**
		p18	**(INK4c)**
		p19	**(INK4d)**
CIP/KIP family	**Inactivation of G1 cyclin-CDK complexes and cyclin B-CDK1.**	**p21**	**(Waf1, Cip1)**
		p27	**(Kip2)**
		p57	**(Kip2)**

Table 1. CKIs bind to CDK alone or to the CDK-Cyclin complexes and regulate CDK activities.

Cell-cycle inhibitors of the Ink4 and Cip/Kip families have been classically viewed as tumor suppressors and are frequently inactivated in cancer by different mechanisms [Ruas M et al., 1998]. Although, overexpression of cyclin D or CDK4 and gain-of-function/ loss-of-function mutations in Rb are common events in human cancers. But complete loss of CIP/KIP function has not been observed in any cancer [Sherr C J etal.,1999]. Interestingly, elevated expression of p27 identified in tumours and is associated with increased tumour aggression and poor prognosis [Catzavelos C etal.,1997]. Further studies demonstrated that oncogene-induced senescence is dependent on p16/RB and TAp63/p21/RB pathways and suppress tumour growth [Guo X etal.,2009]. Moreover, the elevated expression of proteins such as p16INK4A, p21WAF1/CIP1and/or p27KIP1 involve in different senescence induction even without p53 [Osanai M etal.,2007].

1.3 CDK4/6 inhibitors: A trio of compounds

Cell cycle inhibitors have been approved as first-line therapy in ER+ metastatic BC. Earlier, these cancers were treated with systemic chemotherapy and endocrine therapy which causes hormone therapy associated resistance and tumor progression. The identification of a specific CDK4/6 inhibitor from approximately 20 different human CDKs were really challenging in the initial stage, and trials were problematic due to severe toxicity with pan-CDK inhibitors [Alvarez-Fernandez M etal.,2020]. Eventually, Palbociclib (PD0332991), a specific CDK4/6 inhibitor was discovered and able to induce G1 cell cycle inhibition in both cell lines and mouse models with functional RB [Fry DW et al.,2004; Toogood PL etal.,2005]. Later,

Ribociclib (LEE011) and Abemaciclib (LY2835219) have been identified [Gelbert L M etal., 2014]. As of today, Palbociclib, Abemaciclib and Ribociclib (figure4) have all been approved by the US Food and Drug Administration (FDA) and/or the European Medicines Agency (EMA), for breast cancer treatment that, in combination with the endocrine therapy in hormone-receptor positive (HR+) and HER2 negative metastatic breast cancer, dramatically improved the survival outcomes in clinical settings [Goetz MP etal.,2017; Cardoso F etal.,2020]. Ribociclib is structurally very similar to Palbociclib, whereas the structure of Abemaciclib is different from the two other compounds [Klein ME etal.,2018].

CDK4/6 inhibitors are orally available small molecules that interfere with the phosphorylation of RB. Endocrine resistance occurs due to the enhanced activity of cyclin D1-CDK4/6 complex. This reduction of phosphorylated RB leads to a cell cycle arrest between G1/S phase as a result endocrine therapy exhibits its anti-proliferative effect [Prall OW etal.,1997]. Evidence demonstrated that CDK4/6i preferentially inhibited luminal human breast cancer cell lines in both in vitro and in vivo experiments [Finn RS etal.,2016] and enhanced anti-tumor immunity in mice [Goel S etal.,2017]. Currently, numerous clinical trials are investigating the efficacy of CDK4/6 inhibitors alone or in combination to treat other cancer types.

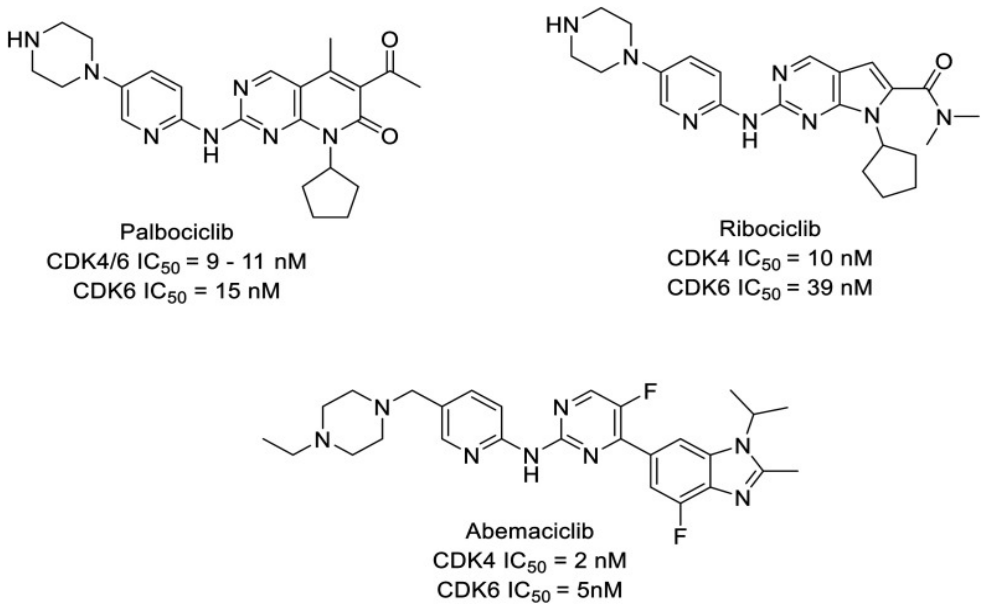

Figure4: The schematic diagram of FDA-approved three CDK4/6 inhibitiors: Palbociclib, Ribociclib and Abemaciclib [Adapted from Adon T etal.,2021].

1.3.1 Therapeutic application of CDK4/6 Inhibitors

Palbociclib (Ibrance®, Pfizer, New York, USA) received US FDA approval in 2015, with a recommended starting dosage of 125 mg once daily in a '3 weeks on and 1 week off' schedule in combination with an aromatase inhibitor (AI) or fulvestrant in pre and postmenopausal patients. Ribociclib (Kisqali®, Novartis, Basel, Switzerland) received US FDA approval in 2017, is a selective inhibitor of CDK4 and CDK6, with a recommended starting dosage of 600 mg once daily in a '3 weeks on/1 week off' schedule in combination with an AI in first-line treatment of post-menopausal patients with HR + HER2 − MBC [Novartis Kisqali.,2017]. Finally, abemaciclib (Verzenios®, Eli Lilly, Indianapolis, USA) received US FDA approval in 2017, with a recommended starting dosage of 150 mg twice daily in a continuous dosing schedule combined with fulvestrant in women with HR+/HER2− high risk early breast cancer [Johnston SRD etal.,2020] following endocrine therapy. It is also approved as a monotherapy administration with a starting dosage of 200 mg twice daily in patients with HR + HER2 − MBC who have previously received endocrine therapy and chemotherapy. Al together with palbociclib, ribociclib, or abemaciclib substantially prolonged progression-free survival with a consistent hazard ratio of around 0.5 among every phase III trial in first-line setting. The information of second-line setting were also quite consistent, with again a substantial progression-free survival demonstrated for fulvestrant together with all three compounds. The clinical efficacy across the three compounds seems similar.

In a clinical point of view, the relevance of CDK4/6 inhibitors is increasing due to their ability to induce a cytostatic clinical response in patients with manageable toxicities. The treatment with CDK4/6 inhibitors could undergo G0-G1 cell cycle exit in tumor cells especially with RB-positive cells. The G1 bypass mechanisms such as non-canonical cyclin D1-CDK2 complex formation, amplification of CDK6 or/and cyclin E1, loss of RB or p16Ink4a can be linked to intrinsic and acquired resistance with CDK 4/6i therapy. In therapy management, there are some differences across three CDK4/6i such as drug intake (1 dosing/day; 3 weeks on/1 week off) as well as side effect profile with neutropenia frequent among palbociclib and ribociclib. When it comes to abemaciclib, which is twice daily in a continuous manner and diarrhea, is its major side effect. Notably, abemaciclib has a lower incidence of neutropenia and a much greater incidence of all grades of diarrhea compared with the other two agents, making

diarrhea the key toxicity for abemaciclib. Also, abemaciclib is the only CDK4/6i demonstrated with substantial monotherapy activity and approved as a single agent. Abemaciclib inhibits CDK4 with 14-fold specificity for CDK4/Cyclin D1 over CDK6/Cyclin D3 complexes. Furthermore, clinically impressive efficacy makes these three CDK4/6 inhibitors an important improvement in armamentarium against HR+, HER2− breast cancer; however, their optimal use still needs to be established. Growing evidence showed that abemaciclib induce cell cycle arrest in ER + breast cancer cell lines and preferentially, able to induce senescence and apoptosis when continuously administered [Torres-Guzman R etal.,2017]. Mostly, treatment outcome depends upon the genomic alterations and phenotypes in different cancers.

1.3.2 Induction of senescence by CDK4/6 inhibitors

In the context of cancer, therapies such as irradiation, chemotherapy, and targeted anti-cancer drugs, including CDK4/6 inhibitors can induce senescence in different cancer types in vitro and in vivo [Petrova NV et al.,2016]. For instance, cancer cells have been found in the biopsies of breast and lung cancer patients who underwent neoadjuvant chemotherapy [Te Poele RH et al., 2002; Roberson RS etal.,2016]. Nevertheless, treatment with CDK4/6 inhibitors namely Palbociclib, Abemaciclib or Ribociclib does not exerts senescence in cancer cells uniformly. In addition to intrinsic or external factors, CDK4/6 inhibitors might create a senescence permissive status to influence cell fate (figure5).

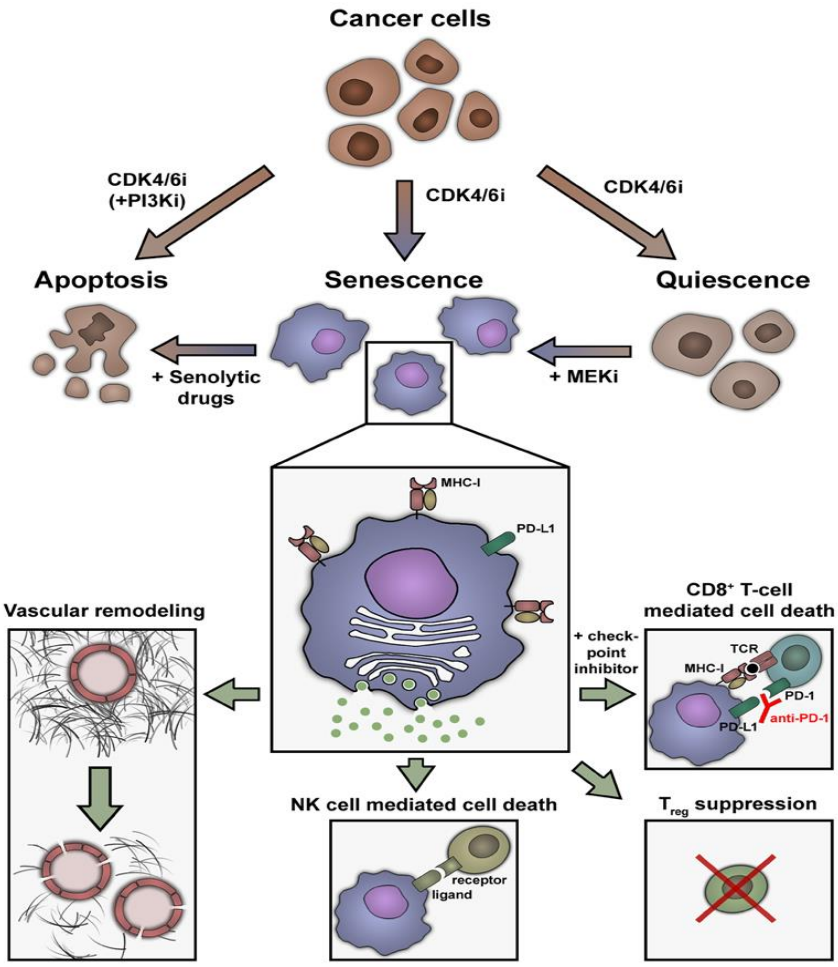

Figure5: The schematic representation of different cell fates caused by CDK4/6 inhibitors and treatment outcome. CDK4/6 inhibitors usually induce quiescence or senescence in functional RB positive cancer cells. The combination of a CDK4/6 inhibitor with a PI3K inhibitor causes apoptosis, which is rarely seen in a monotherapy setting. The SASP components promote vascular remodeling or recruitment of cytotoxic T cells into tumor microenvironment. CDK4/6 inhibitors enhance the activation of cytotoxic T cells through the expression of MHC-I complexes on cancer cells. Also, facilitate the immune-mediated clearance of senescent cancer cells in combination with checkpoint inhibitors [Adapted from Wagner V etal.,2020].

As of several studies, one of the leading causes of chemotoxicity is the premature and excessive induction of senescence in non-malignant cells [Demaria M etal.,2017; Baar M P etal.,2017].

Chapter2: Objectives

Prior work in the Demaria lab identified that CDK4/6i induces a premature state of senescence in non-malignant cells which is dependent on transcriptional activity of the tumor suppressor p53. Those CDK4/6i associated senescent program lacks NF-κB driven pro-inflammatory properties. Furthermore, CDK4/6i-induced senescent cells promote paracrine senescence without any pro-tumorigenic or/and detrimental effects. Owing to the complications/cytotoxicity associated with chemotherapeutic drugs and detrimental effect of senescence in tumor microenvironment due to TIS, we wondered how the nature of senescence when chemotherapeutic drug (doxorubicin) is in combination with CDK4/6i (Abemaciclib) and whether its nature is p53 or NF-κB dependent.

The purpose of this study was to characterize the senescence induction and phenotype of SASP depending upon the treatment regimens in nonmalignant cells.

- Evaluated the senescence induction and clarified whether it is p53 or NF-κB-dependent SASP factors in normal cells (MDF, p16-3MR and BJ) after therapy induced senescence using doxorubicin alone or in combination with abemaciclib.
- Analyzed the cytotoxic effect of Natural Killer (NK) cells on triple-negative breast cancer cell lines in the presence of treatment associated senescence in normal human fibroblast (BJ) using IncuCyte® S3 Live-Cell Analysis System.
- Performed the triple-negative breast cancer cell lines (MDAMB231 & BT549) proliferation assay in the presence of proliferating and senescent BJ and hTERT RPE-1 (after TIS) using IncuCyte® S3 Live-Cell Analysis System.
- By IncuCyte System, investigated the cancer cell proliferation in the presence of CM from proliferating and senescent BJ and hTERT RPE-1 cells.

Chapter3: Materials and Methods:

3.1 Cell culture and drug administration

MDFs (Mouse dermal fibroblasts; isolated from the dorsal skin of 3- month-old p53-null mice or wild-type littermates), 3MR (p16-3MR, these dermal fibroblasts were isolated from the novel mouse model (p16-3MR) (created by *Demaria etal*) which carries a transgene contains a trimodal reporter including functional domains of Renilla luciferase (LUC), monomeric red fluorescent protein (mRFP), and a truncated herpes simplex virus (HSV)-1 thymidine kinase (tTK) under the control of senescence-sensitive p16INK4a promoter), BJ (normal human fibroblast), hTERT RPE-1(hTERT- immortalized retinal pigment epithelial cell line), MDAMB231 (triple-negative breast cancer (TNBC) cell lines) and BT549 ((human ductal breast carcinoma) were cultured in DMEM- GlutaMAX (Thermo Fisher) medium supplemented with 10% fetal bovine serum (GE Healthcare Life Sciences) and 1% penicillin-streptomycin (Lonza) in 5% O2, 5% CO2, 37ºC incubator. Cell lines were regularly monitored (once per month) for mycoplasma contaminations.

For drug treatment experiment, MDFs, 3MR and BJ were seeded in T75 flask (0.75*106 cells/flask, around 50% confluence). The final concentration of doxorubicin hydrochloride (Tebu-bio, BIA-D1202-1) and abemaciclib (MedChemExpress, HY-16297) were 250nM and 1 µM respectively. Both drugs were prepared by dissolving in sterile milliQ water. The MDFs, 3MR and BJ were treated with vehicle (water - once for 24 hours) or doxorubicin (250 nM – once for 24 hours) and 6 days later with abemaciclib (1 µM – two treatments of 24 hours each). Cells were cultured in drug-free complete medium after doxorubicin treatment and the medium refreshed every 48-72 hours. Thereafter, cells from different groups were trypsinized, centrifuged at 300 g / 5 minutes and counted. The 2x105 cells from each group were used for RNA extraction (figure6).

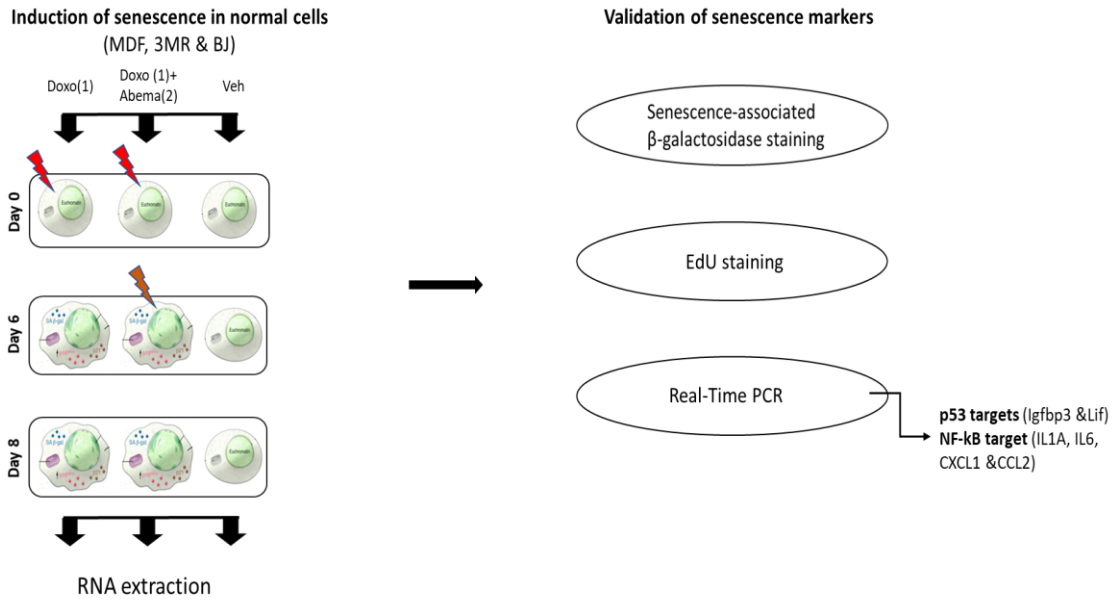

Figure6: Experimental design of the study. MDF, 3MR and BJ cell lines were treated with vehicle (water – once for 24 h) or doxorubicin (250nM – once for 24h) or abemaciclib (1µM – two treatments of 24h each) on 6th day of experiment. RNA was extracted from vehicle and treated cells, evaluated the mRNA level expression of gene of interests by qPCR. Cells were treated with above mentioned conditions, after drug withdraw, either replated for SA-β-gal staining or incubated with EdU staining.

3.2 Real-time PCR assay

RNA was isolated from cultured cells using an Isolate II RNA Mini Kit (Bioline). 200 ng of RNA was reverse transcribed into cDNA using the High-Capacity cDNA reverse transcription kit (Applied Biosystems). The qPCR reactions were performed using GoTaq system (Promega) and analyzed the data by delta-delta Ct method. Relative expressions of tubulin and Hypoxanthine-guanine phosphoribosyl transferase (hgprt) were used to normalize the expression of following genes: Insulin Like Growth Factor Binding Protein 3 (Igfbp3), Leukemia inhibitory factor (LiF), Interleukin-1 alpha (IL1alpha), Interleukin 6 (IL6), C-X-C Motif Chemokine Ligand 1 (CXCL1), C-C Motif Chemokine Ligand 2 (CCL2), CDKN1A (p21Cip1), CDKN2A (p16ink4a) and laminB1 (B-type nuclear lamin protein). Every biological replicate was analysed in duplicate.

Human #UPL probe number		
Tubulin #40	Forward	CTTCGTCTCCGCCATCAG
	Reverse	CGTGTTCCAGGCAGTAGAGC
HGPRT #73	Forward	TGACCTTGATTTATTTTGCATACC
	Reverse	CGAGCAAGACGTTCAGTCCT
p16 (INK4A) #67	Forward	GAGCAGCATGGAGCCTTC
	Reverse	CGTAACTATTCGGTGCGTTG
p21 (CDKN1A) #32	Forward	TCACTGTCTTGTACCCTTGTGC
	Reverse	GGCGTTTGGAGTGGTAGAAA
IGFBP3 #62	Forward	AACGCTAGTGCCGTCAGC
	Reverse	CGGTCTTCCTCCGACTCAC
LIF #51	Forward	TGAAGTGCAGCCCATAATGA
	Reverse	TTCCAGTGCAGAACCAACAG
IL1A #6	Forward	GGTTGAGTTTAAGCCAATCCA
	Reverse	TGCTGACCTAGGCTTGATGA
IL6 #45	Forward	CAGGAGCCCAGCTATGAACT
	Reverse	GAAGGCAGCAGGCAACAC
CXCL1 #83	Forward	CATCGAAAAGATGCTGAACAGT
	Reverse	ATAAGGGCAGGGCCTCCT
CCL2 #40	Forward	AGTCTCTGCCGCCCTTCT
	Reverse	GTGACTGGGGCATTGATTG
Lamin B1 #3	Forward	GTGCTGCGAGCAGGAGAC
	Reverse	CCATTAAGATCAGATTCCTTCTTAGC

Table2: Primers used for the qPCR reaction for human genes. The sequence of qPCR primers and catalog number of probes (UPL system) used in this study.

Mouse #UPL probe number		
Tubulin #89	Forward	CTGGAACCCACGGTCATC
	Reverse	GTGGCCACGAGCATAGTTATT
HGPRT #95	Forward	CCTCCTCAGACCGCTTTTT
	Reverse	AACCTGGTTCATCATCGCTAA
p16 (INK4A) #91	Forward	AATCTCCGCGAGGAAAGC
	Reverse	GTCTGCAGCGGACTCCAT
p21 (CDKN1A) #16	Forward	AACATCTCAGGGCCGAAA
	Reverse	TGCGCTTGGAGTGATAGAAA
IGFBP3 #63	Forward	GCAGCCTAAGCACCTACCTC
	Reverse	CTTTCCACACTCCCAGCATT
LIF #25	Forward	TGAAAACGGCCTGCATCTA
	Reverse	GACCTTCATTATGGGCTGGA
IL1A #52	Forward	TTGGTTAAATGACCTGCAACA
	Reverse	GAGCGCTCACGAACAGTTG
IL6 #6	Forward	GCTACCAAACTGGATATAATCAGGA
	Reverse	CCAGGTAGCTATGGTACTCCAGAA
CXCL1 #83	Forward	GACTCCAGCCACACTCCAAC
	Reverse	TGACAGCGCAGCTCATTG
CCL2 #62	Forward	CATCCACGTGTTGGCTCA
	Reverse	GATCATCTTGCTGGTGAATGAGT
Lamin B1 #15	Forward	GGGAAGTTTATTCGCTTGAAGA
	Reverse	ATCTCCCAGCCTCCCATT

Table3: Primers used for the qPCR reaction for mouse genes. The sequence of qPCR primers and catalog number of probes (UPL system) used in this study.

3.3 SA-β-gal (Senescence-associated β-galactosidase) staining

For staining of cells, drug-treated cells were re-plated in a 24-well plate (2*104 cells/well), and the SA- β-galactosidase staining was done as described previously (Hernandez-Segura et al., 2018a). In brief, cells were incubated O/N at 37 °C with 5% CO2 and 5% O2, washed twice with 500µL of PBS and fixed 10 min at room temperature using 500µL/well of 2% formaldehyde + 0.2% glutaraldehyde in PBS. After a second wash (two times with 500µL of PBS) cells were incubated in freshly prepared staining buffer (1 mg/ml X-gal (Thermo Fisher) in dimethylformamide, 40 mM citric acid/Na phosphate buffer, 5 mM potassium

ferrocyanide, 5 mM potassium ferricyanide, 150 mM sodium chloride and 2 mM magnesium chloride) in 37 ºC incubator without CO2 for 12hrs in dark condition. After incubation, washed with 500µL of PBS, images were acquired at 10× magnification and quantification performed using the ImageJ software. Every biological replicate was stained in triplicate, and the number of positive cells were counted manually in blind.

3.4 EdU (5-ethynyl-2'-deoxyuridine) staining

Drug-treated cells were re-seeded on coverslip in a 24-well plate (4*104 cells/well) and cultured for 24 hours in the presence of EdU (10 µM), then fixed with 4% formaldehyde in PBS for 10 mins, incubated 5 min in 100 mM Tris (pH 7.6) and permeabilized 10 min in PBS + 0.1% Triton X-100. After 3 washes with PBS, cells were incubated with 50µl/coverslip of label mix (PBS: 44.45 µl, Cu (II)SO4: 0.5 µl, sulfo-Cy3-azide: 0.05 µl, Sodium ascorbate: 5 µl) 30 min in the dark. After 3 washes with PBS, 400µl of DAPI solution (2mg/ml) was added and incubated for 10 minutes at room temperature. Coverslips were mounted with mounting media (Prolong TM Gold antifade reagent; Invitrogen (Thermo Fisher Scientific) onto glass slides and keep it dry overnight. Images were acquired at 10x magnification with a fluorescent microscope (Leica). Every biological replicate was stained in triplicate, and counting was made in blind using software ImageJ.

3.5 Immune and cancer cell co-culture experiments

NK cell cytotoxicity assay was performed using the MDAMB231 as a model system. To measure NK cell cytotoxicity using IncuCyte®Zoom live-cell analysis system, BJ cells either proliferating (Vehicle) or treated (doxorubicin alone (Doxo) or in combination with doxorubicin plus abemaciclib (D+A)/(Doxo+Abema)) were plated with MDAMB231 cells in a 96 well plate. The ratio between cancer cells and BJ are 1000 and 5000 per well respectively. On every next day, NK cells were added (10,000 cells/well) into the plate and those NK cells were activated by IL-2. Cell Tox Green dye (Promega) was added to determine the cytotoxicity. Proliferation of red fluorescent MDAMB231 cells were measured based on red fluorescent intensity (RCU) using IncuCyte®Zoom live-cell analysis system. The

incubation time for this experiment was 48 hours. We used the IncuCyte® imaging system to study the killing potential of natural killer cells on cancer cell line. The IncuCyte system tracks living cells, labelled by a red fluorescent protein (a lentiviral construct expressing nuclear localized mcherry red fluorescent protein to stably label cancer cells) and cell death, as indicated by the cell tox green dye, which generates a green, fluorescent signal.

3.6 Cancer cell proliferation assay

The MDAMB231 and BT549 along with proliferating (Vehicle) or treated (doxorubicin alone (Doxo) or abemaciclib alone (abema) or combination with doxorubicin plus abemaciclib (D+A)) BJ or hTERT RPE-1 (5000 cells/well) were plated in a 96-well plate). The ratio between cancer cells and BJ/ hTERT RPE-1 were 1000 and 5000 per well respectively. Proliferation of red fluorescent MDAMB231 cells were measured based on red fluorescent intensity using IncuCyteS3 live-cell analysis system. The incubation time was 48 hours.

3.7 Conditioned media (CM) collection and analyses

BJ fibroblasts and hTERT RPE-1 were treated with vehicle (water-8 times in 24 h; 1 in 1,000), doxorubicin (250nM—1 time 24 h), or and 6 days later with abemaciclib (1µM – two treatments of 24 hours each. After the treatment, cells from different groups were trypsinized and counted, and 10*6 cells from each group were replated and incubated with serum-free medium for 24 h. Then, the CM was collected and centrifuged at 300 g/5 min to remove any floating cell or debris and added 100µl of CM into 96 well plate which already plated with either MDAMB231 or BT549 cell lines for incuCyteS3 experiment to perform cancer cell proliferation assay.

3.8 Statistics

GraphPad Prism 9 was used for the statistical analyses and detailed information was provided in each figure legend.

Chapter4: Results

4.1 Therapy- induced senescence and elevated relative expression of SASPs in wild-type MDF, 3MR and BJ.

Based on previous studies from Demaria's lab (Demaria et al., 2017), we induced senescence by using 250nM of doxorubicin hydrochloride for 24 hours. After reaching senescence, cells were then treated with abemaciclib 2 times 24 hours each. Cells either treated with doxorubicin only or with a combination of doxorubicin and abemaciclib showed the induction of the CDK inhibitors, p16 and p21 and loss of laminB1(figure7), indicating the entrance into senescence state.

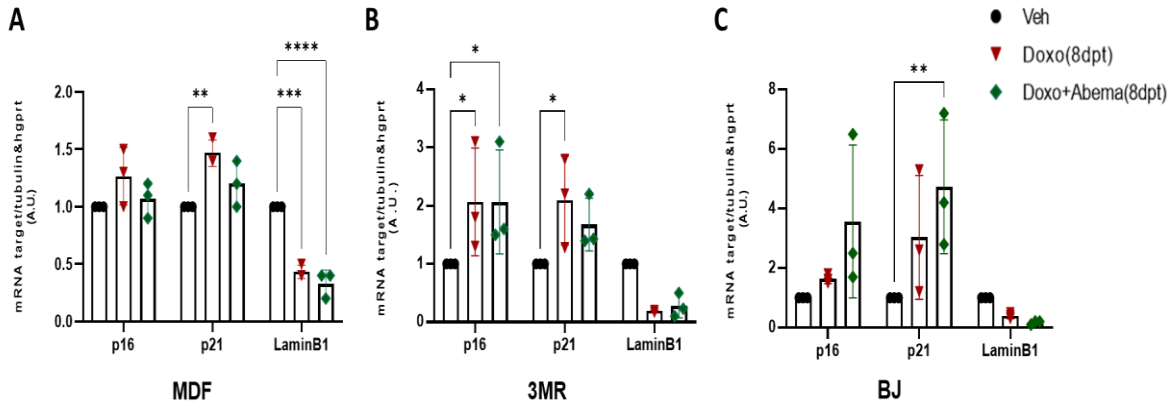

Figure7:Representative image showing the relative expression of p16, p21 and laminB1 in (A)MDF, (B)3MR and (C)BJ cell lines. Quantification was performed by qPCR with three biological replicates. Data in means ± SD. Two-way ANOVA used. *P < 0.05, **P < 0.01,***P < 0.001 &****P < 0.0001. Only displayed P values less than or equal to 0.05.

To further evaluate senescence induction, we stained cells for SA-β-gal (figure8), a lysosomal enzyme strongly senescence-associated, and with EdU (figure9), a fluorescent dye that labels actively replicating DNA. SA-β-gal- positive cells were noted in both doxorubicin treated and doxorubicin plus abemaciclib treated cell lines.

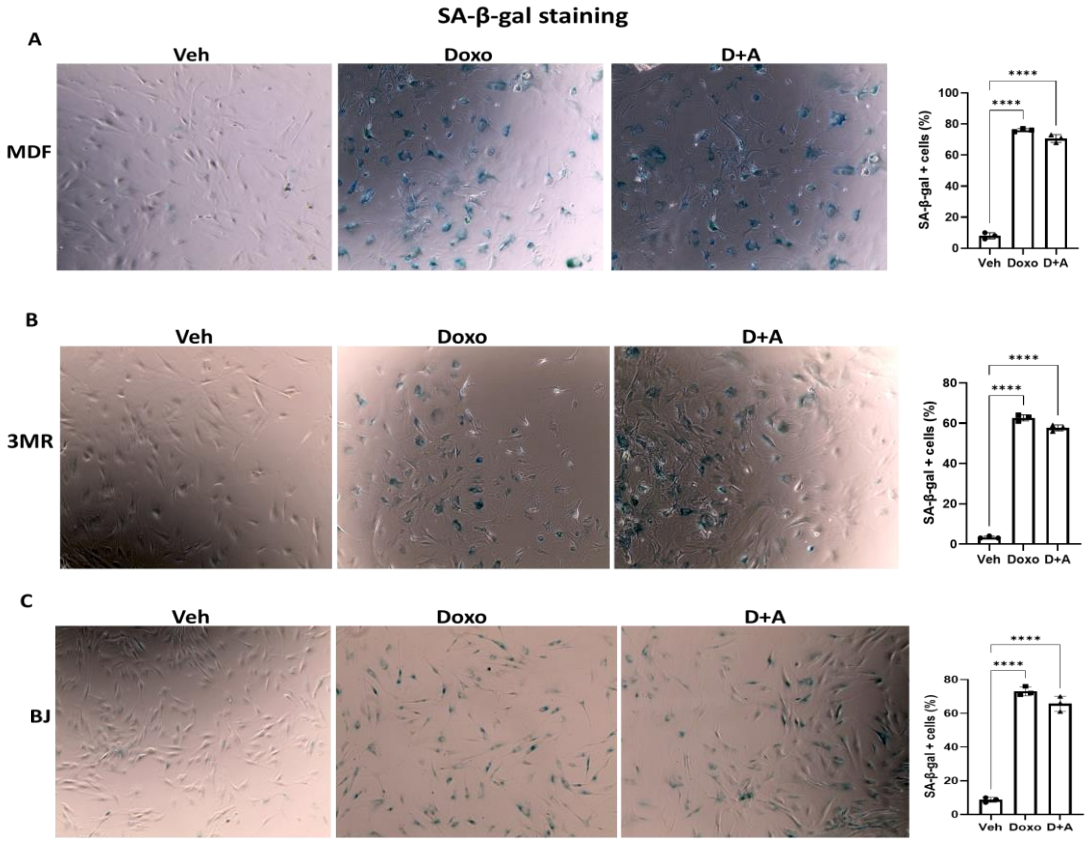

Figure8: Representative results for the SA-β-gal staining in (A)MDF, (B)3MR and (C)BJ. Graph showing thepercentage of SA-β-gal positive cells in the untreated and treated samples of MDFs, 3MR and BJ fibroblast. One-way ANOVA used. ****P < 0.0001. Only displayed P values less than or equal to 0.05.

EdU (5-ethynyl-2'-deoxyuridine) is an analog of the nucleoside thymidine, that efficiently incorporatedinto replicating DNA (Salic A et al.,2008). The incorporation of EdU into DNA has visualized after performing the Copper-Catalyzed Azide-Alkyne cycloaddition (CuAAC) to the EdU, reaction was not based on regular thymidine because it lacks the alkyne group. A Sulfo-Cy3-azide was used in this protocol. If the coupling of the azide to the alkyne has taken place, cells will display fluorescence undera Cy3 filter (figure9).

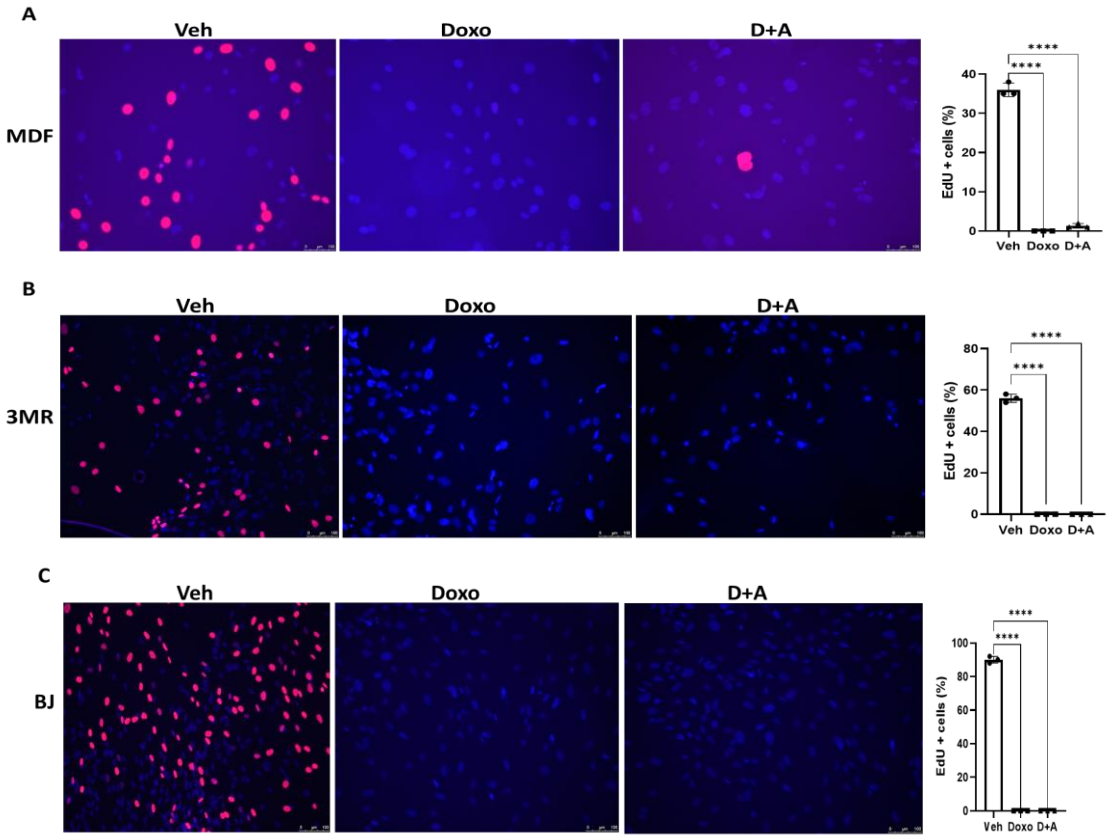

Figure9: Detection of EdU incorporated into the DNA of proliferating (A)MDF, (B)3MR & (C)BJ [(Veh), treated (doxorubicin alone (Doxo) and combination with doxorubicin plus abemaciclib (D+A)] after 8dpt by fluorescence microscopy and quantification of EdU positive cells among 100 cells in total per each replicate. One-way ANOVA used. ****P < 0.0001. Only displayed P values less than or equal to 0.05.

After validating successfully, the induction of senescence in both doxorubicin and doxorubicin plus abemaciclib groups, we then measured mRNA level expression of various SASP factors. The 'Igfbp3 and 'LiF' are predicted to be p53 target (Fischer, 2017) (figure10) and observed that these two genes were upregulated and there was no significant difference in their relative expression between the doxorubicin alone or in combination with abemaciclib groups.

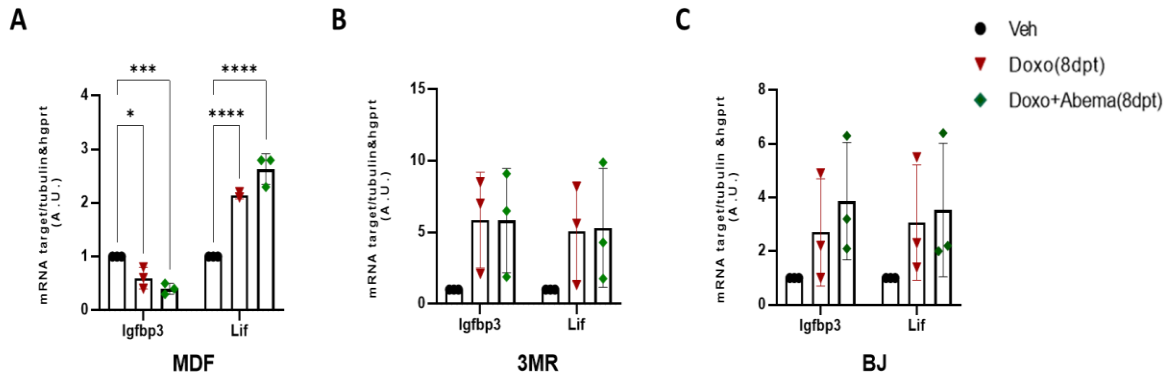

Figure10: Expression of p53-associated SASP factors in (A)MDF, (B)3MR and (C)BJ. Quantification by qPCR and the relative fold gene expression of samples were analysed using 2–ΔΔCt method. Data in means ± SD. Two-way ANOVA used. *P < 0.05, **P < 0.01, and ***P < 0.001. Only displayed P values less than or equal to 0.05.

The activation of NF-κB signalling in normal cells are one of the characteristic senescence-associated features and we observed that only genotoxic drug, but not CDK4/6i, were able to promote the production and secretion of factors, which are part of the NF-κB-Associated Secretory Phenotype (NASP) such as IL1A, IL6, CXCL1 and CCL2 (figure11).

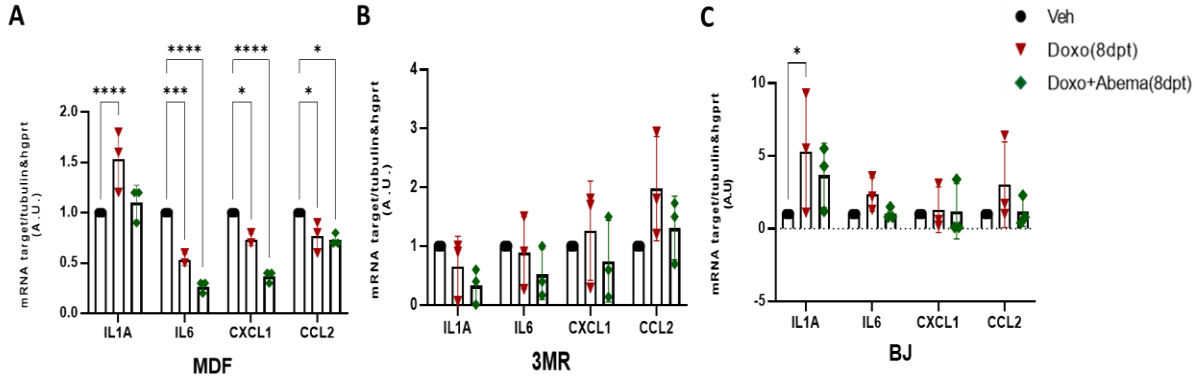

Figure11: Expression of NF-κB-associated SASP factors in (A)MDF, (B)3MR and (C)BJ. Quantification by qRT-PCR and the relative fold gene expression of samples were analysed using 2–ΔΔCt method. Data in means ± SD. Two-way ANOVA used. *P < 0.05, **P < 0.01, and ***P < 0.001. Only displayed P values less than or equal to 0.05.

4.2 Utilizing the IncuCyte® Zoom live-cell analysis system to quantify Natural Killer cell- mediated cytotoxic responses of cancer cell line in real-time.

We used the Sartorius IncuCyte® system to examine the dynamics of immune cell (NK)

killing of cancer cell line in culture (figure12). Using this system, we cultured nuclear localized red fluorescent labelled MDAMB231 breast cancer cells along with proliferating BJ (Vehicle) or treated doxorubicin alone (Doxo) or combination with doxorubicin plus abemaciclib (D+A) and co-cultured with NK cells. We used 1000 red fluorescent MDAMB231 cells, 5000 treated or non-treated BJ and 10,000 NK cells were cultured per well. We found that the proliferation of MDAMB231 cells reduced in the presence of doxorubicin plus abemaciclib (D+A) treated BJ when compared with the other conditions, indicating that abemaciclib might have role in the reduction of MDAMB231 proliferation (figure12).

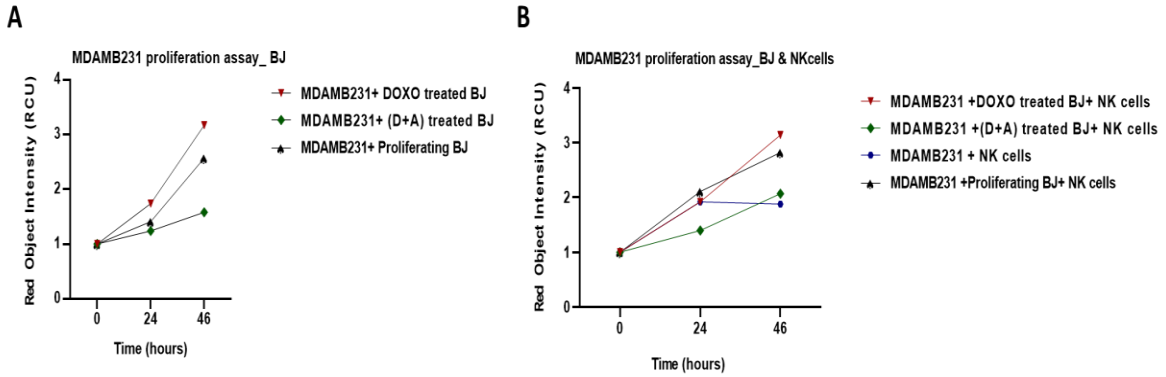

Figure12: The IncuCyte® live-cell analysis system to study immune cell kill responses of cancer cell line in real-time. The graph on the left (A) compares the red object intensity in the absence of NK cells and the graph on the right (B) compares the red object intensity in the presence of NK cells. Two-way ANOVA used. Only displayed P values less than or equal to 0.05.

4.3 MDAMB231 and BT549 proliferation assay with BJ fibroblast by IncuCyte S3 live-cell analysis system in real-time.

The previous results demonstrated that the proliferation of MDAMB231 was less in the presence of doxorubicin plus abemaciclib (D+A) treated BJ when compared with other conditions. So, we were curious to verify it was because of abemaciclib treatment or not. So, we added one more condition, abemaciclib treatment for 48 hours (short term treatment) in BJ fibroblast and analysed the red object intensity (RCU) of red fluorescent MDAMB231 cells along with other conditions (figure13). The MDA-MB-231 and BT-549 cell lines are characterized as triple-negative/basal B mammary carcinoma. Research evidence stated that BT549 was completely devoid of RB1 expression. So, that cell line is resistant to abemaciclib treatment. At 48 h of incubation, there was an increase in both cancer cell lines

proliferation in the presence of senescent BJ fibroblast induced by doxorubicin treatment. Also, the proliferation of both MDAMB231 and BT549 cell lines were less in the presence of doxorubicin plus abemaciclib (D+A) treated senescent BJ and abemaciclib (abema) short term (48hours) treated BJ (figure13).

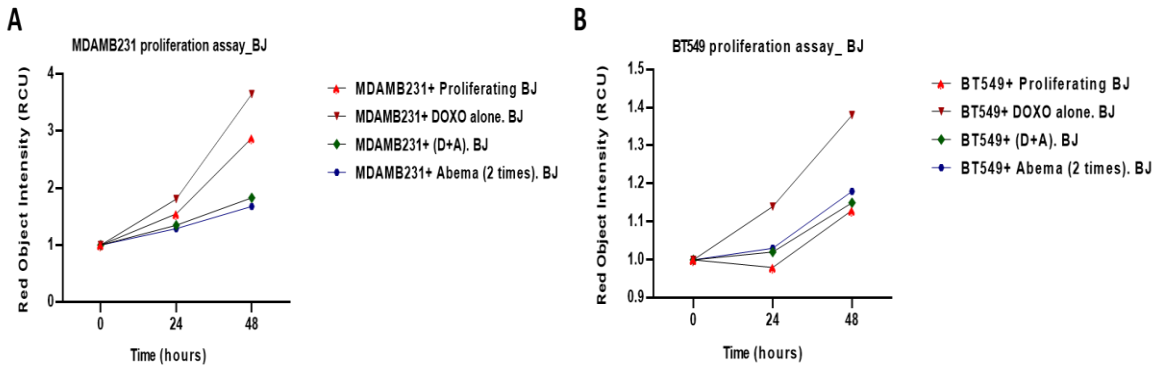

Figure13: Cancer cell lines (MDAMB231 & BT549) proliferation assay by IncuCyte®S3 live-cell analysis system. (A)The graph illustrates the red object intensity of red fluorescent MDAMB231 cells in the presence of proliferating (Vehicle) or doxorubicin(doxo) treated senescent or in combination with doxorubicin plus abemaciclib (D+A) treated senescent or abemaciclib(abema) short term(48hours) treated BJ. (B) The graph shows the red object intensity of red fluorescent BT549 cells in the presence of proliferating (Vehicle) or doxorubicin(doxo) treated senescent or in combination with doxorubicin plus abemaciclib (D+A) treated senescent or abemaciclib(abema) short term(48hours) treated BJ. Two-way ANOVA used. Only displayed P values less than or equal to 0.05.

4.4 MDAMB231 and BT549 proliferation assay with hTERT RPE-1 (RPE) by IncuCyte S3 live-cell analysis system in real-time.

To verify whether the effect of treatment on cancer cell proliferation is likely dependent on cell type or not. We added another cell type; hTERT RPE-1 and the results demonstrated that both MDAMB231 and BT549 proliferation was not dependent on cell type because MDAMB231 and BT549 cells were less in the presence of abemaciclib (48hours) treated RPE when compared with other conditions (figure14), indicating that abemaciclib might have role in the reduction of cancer proliferation neither depend on senescent status nor cell type.

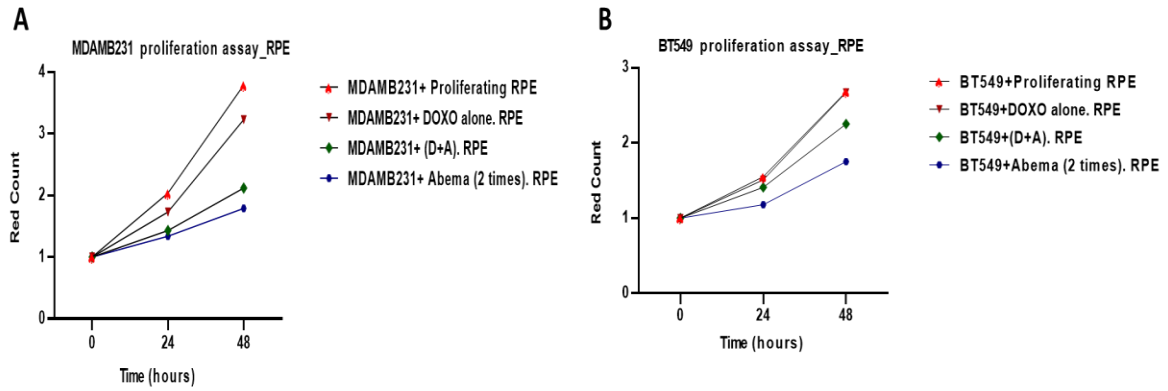

Figure14: MDAMB231 & BT549 proliferation assay with hTERT RPE-1 by IncuCyte®S3 live- cell analysis system. (A)The graph shows the red count of red fluorescent MDAMB231 cells in the presence of proliferating(Vehicle) or doxorubicin(doxo) treated senescent or in combination with doxorubicin plus abemaciclib (D+A) treated senescent or abemaciclib(abema) short term(48hours) treated RPE. (B)The graph shows the red count of red fluorescent BT549 cells (CCs) in the presence of proliferating (Vehicle) or doxorubicin(doxo) treated senescent or in combination with doxorubicin plus abemaciclib (D+A) treated senescent or abemaciclib(abema) short term(48hours) treated RPE. Two-way ANOVA used. Only displayed P values less than or equal to 0.05.

4.5 MDAMB231 and BT549 proliferation assay with conditioned media (CM) of BJ fibroblast and RPE by IncuCyteS3 live- cell analysis system in real-time.

To determine SASP secreted from treated BJ fibroblast/ RPE have influence on the cancer proliferation, we collected CM from doxorubicin(doxo) treated senescent or in combination with doxorubicin plus abemaciclib (D+A) treated senescent or abemaciclib(abema) short term(48hours) treated BJ fibroblast/ RPE. The results (figure15) indicated that the proliferation of MDAMB231 was less in the presence of CM from doxorubicin plus abemaciclib treated and abemaciclib alone treated conditions in BJ and RPE cell lines. Same results observed even in the case of BT549 in the presence of CM from senescent RPE induced by both doxorubicin plus abemaciclib treated and abemaciclib alone but not in BJ fibroblast case, which might be due to some external stress stimuli manifests distinctive SASP components.

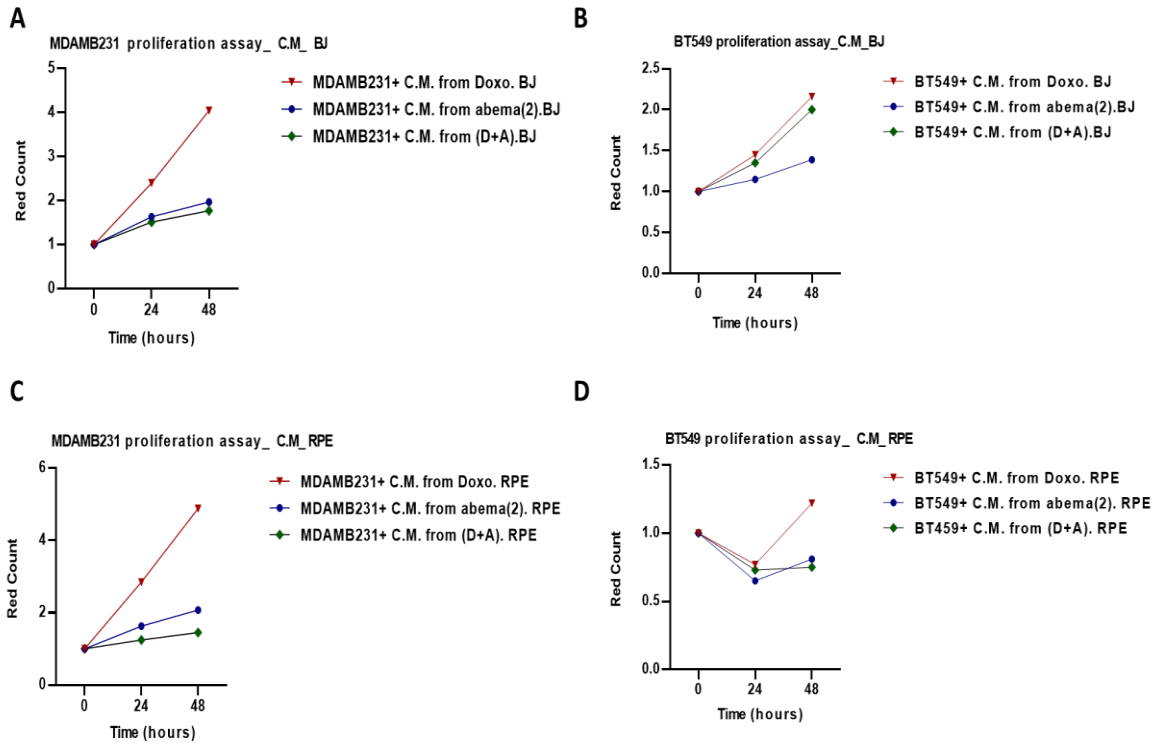

Figure15: MDAMB231 & BT549 proliferation assay with conditioned media (C.M) of BJ fibroblast or hTERT RPE-1 by IncuCyte®S3 live-cell analysis system. (A)The graph illustrates the red count of red fluorescent MDAMB231 cells in the presence of C.M from doxorubicin(doxo) treated senescent or in combination with doxorubicin plus abemaciclib (D+A) treated senescent or abemaciclib(abema) short term(48hours) treated BJ fibroblast. (B)The graph shows the red count of red fluorescent BT549 cells in the presence of C.M from three conditions of BJ fibroblast. (C)The graph shows the red count of red fluorescent MDAMB231 cells in the presence of C.M from three conditions of RPE. (D)The graph shows the red count of red fluorescent BT549 cells in the presence of C.M from three conditions of RPE. Two-way ANOVA used. Only displayed P values less than or equal to 0.05.

Chapter5: General Discussion

My PhD thesis involved two studies in which senescence is a common denominator. The 1st study was a non-interventional observational study, investigated the presence of senescent T lymphocytes in peripheral blood of early breast cancer patients in response to neoadjuvant chemotherapy, based upon their biological subtype and validated whether it had a predictive role or not. Thereby, may allow the early detection of those patients who are unlikely to benefit from NAT. Additionally, evaluated the percentage of peripheral sub populations of MDSCs, some immune inflammatory biomarkers such as SII and PIV and plasma associated metabolomics.

The 2nd study was conducted in prof. Marco Demaria laboratory in ERIBA, University of Groningen, Netherlands during my visiting period. This work was a continuation of one of their main projects about CDK4/6i-induced premature senescence in nonmalignant cells. They have observed that CDK4/6i-induced senescence is p53 dependent and exhibited a p53-associated secretory phenotype not the NF-kB-associated secretory phenotype in their previous work. In my study, we mainly focused on the nature of SASP after therapy induced senescence using doxorubicin alone or in combination with abemaciclib in both mouse and human fibroblast cell lines (MDF, p16-3MR and BJ) and this study was completed on in vitro. The first study was about neoadjuvant chemotherapy induced senescence in breast cancer patients whereas CDK4/6i induced senescence in normal cell lines were investigated in the second study.

Cells are always subject to cellular damage throughout their lifetime, evolve in several maintenance mechanisms to respond in a timely manner to various triggers and activate pathways to repair DNA damage and maintain homeostasis. Cellular senescence is a molecular program with a unique phenotypic outcome. This stress program is triggered by replicative, oxidative, oncogenic, and genotoxic stresses. It is also linked to a wide range of physiological declines and disease disorders including cancer. Cells undergo senescence in response to several cancer therapeutics termed TIS. TIS has been proposed to contribute several adverse reactions to cancer treatments including relapse and metastasis [Luo X etal.,2016; Baar MP etal.,2017]. However, there is limited evidence on senescence induction

in response to NAT in clinical cancer and its contribution to disease outcomes. In the 1st work, patients with histologically or cytologically confirmed early BC were included and the primary end point was overall response rate (ORR) of four months' sequential administration of anthracyclines and taxanes in patients. Traditionally, NAT is considered as a standard approach in patients with locally advanced and inflammatory breast cancer, allows the reduction in disease volume which increases the chance of successful resection and might reduce the recurrence and distant metastasis. NAT is now extended to use in patients with early-stage breast cancer, especially HER-2 positive and triple negative tumors and patients who desire breast conservation [Rastogi P etal.,2008; Van der Hage JA etal.,2001]. Mounting evidence demonstrated that patients who achieve pCR have a better outcome in response to NAT. As a result, better assessment is necessary to understand the degree of response to NAT because it has a major impact on selection of patient, management of follow-up of each patient and defines patient outcome.

Achieving a pathologic complete response after neoadjuvant chemotherapy is associated with improved prognosis in breast cancer. Accordingly, 55% (33/60) of patients who achieved pCR and the remaining patients having residual disease (RD) or incomplete clinical response after NAT among our study participants. Six patients had relapse so far. The KATHERINE trial showed the effectiveness of trastuzumab-emtansine (TDM1) as adjuvant therapy in HER2-positive patients having RD after NAT. A significant benefit of capecitabine therapy has been demonstrated by CREATE-X trial in HER2-negative patients with RD after neoadjuvant chemotherapy, especially those with triple-negative breast cancer who had residual invasive disease after NAT. In our study, all HER2-positive and HER2-negative patients who did not achieve a pathologic complete response, had taken trastuzumab-emtansine (TDM1) and capecitabine after NAT respectively, for prolonging disease-free survival.

Several markers are commonly used in vitro for the identification of senescence induction [Gorgoulis V etal.,2019]. To examine if TIS is a component of the partial or incomplete clinical response to NAT, we assessed the expression of TIS-associated protein markers in CD3+ve T cells in blood samples of patients who received NAT prior to surgery at two time points; at baseline (PRE) and after NAT (POST. The investigated biomarkers include p16INK4 and p21CIP1, two CDKIs involved in the regulation of the senescent growth arrest by RTPCR [Kreis

NN etal.,2019]. Importantly, many studies have suggested that p16INK4 and p21CIP1 are key drivers in TIS [Chang BD etal.,1999; Demaria M etal.,2017], and in consequence, p21CIP1 is widely used in preclinical models as senescence markers [González-Gualda E etal.,2020]. Out of 90, only 60 patients were included in the final analysis. There was no significant difference in relative expression of p16INK4a and p21CIP1 at baseline and after NAT in patients who achieved pCR. However, patients having RD had a statistically higher significance in p16INK4a and p21CIP1 expression after NAT. These findings suggest that the above-mentioned senescence markers were not correlated with pCR status, at least in our study cohort and the propensity to increase p16INK4a or p21CIP1 expression might be dependent on the baseline expression in each candidate due to the severity of disease. Notably, high basal level expression of peripheral p16INK4a and p21CIP1 were associated with increased risk of relapse, and these results might be useful to categorize the high-risk patients. Our data in this study demonstrated that there was no positive correlation between p16INK4a and p21CIP1 expression. One explanation is activation of p53-p21CIP1 pathway has been involved in senescence induction, though only at the early stage [Stein et al., 1999]. When it comes to p16, frequently induced late after senescence induction, represents more established and durable response [Alcorta DA etal.,1996; Kohli J etal.,2021].

There is a convincing evidence indicating that senescent cells co-operate with MDSCs in inflammation and tumor progression via SASP. To understand the effect of baseline MDSC and its subsets percentage in response to pCR in BC patients, we analyzed these cells using different markers by Flow Cytometry. Our data indicated that the percentage of MDSCs, its subsets: M-MDSCs and PMN-MDSCs and a small subpopulation of PMN-MDSCs, which is LOX1-positive (LOX1 positive PMN-MDSCS) was not considerably changed among pCR and RD group.

Cancer related inflammation seems to be involved in the pathogenetic pathways of BC. To predict the outcome of NAT, the methods such as imaging, positron emission tomography, and gene expression profiling such as PIK3CA mutation can be used. However, those are expensive and not conducive to general clinical practices. Blood based IIB, is based on the counts of peripheral blood cells. Importantly, it is a simple and inexpensive procedure. Blood based IIB has been reported to be closely related to prognosis in many tumors, including breast. However, the predictive value of pretreatment blood based IIB such as SII and PIV on

pCR rates in patients with breast cancer treated with NAT is unknown. Our study examined the correlation between blood based IIB and pCR in BC patients and we provided evidence that SII and PIV were independently predictive factors of pCR. Compared to SII, PIV is more comprehensive because monocytes were also included in this index. The pathophysiological functions of peripheral blood cells in cancer-associated inflammation includes, neutrophils could alter tumor progression through the production of chemokines, cytokines, matrix-degrading proteases and reactive oxygen species, platelets play an important role in tumorigenesis, monocytes act as a mediator of inflammation and cause tumor initiation and finally, lymphocytes induce cytotoxic cell death and blocks tumor cell proliferation and migration [Mantovani A etal.,2008;Olingy CE etal.,2019]. Notably, the levels of increased circulating cytokine concentrations reflect the host's immune response to tumors. These reasons may explain why patients with higher SII and PIV have lower pCR rate.

In a holistic approach, one of the challenges of translational research is to integrate the clinical data with genomic, proteomic, transcriptomic and metabolomic information. In this regard, metabolomics is useful for the detection of molecular changes resulting from physical-pathological processes including in cancer. We observed a strong association between the increased presence of specific molecules and the failure of NAT. The plasma-associated metabolomic profiling of patients who achieved pCR have a different profile than those who have residual disease. Notably, patients having RD had baseline elevated upregulation of unsaturated fatty acids such as (8Z,11Z,14Z)-Icosatrienoate, 9-Decenoic acid and 17-Octadecynoic acid. These small molecules not only involve in cancer progression but also cause reduction in drug metabolism and trigger inflammation through immune cells recruitment [Powell WS etal.,2013; Luzardo-Ocampo I etal.,2020]. Also, we observed some downregulated fatty acids in RD patients such as hexadecenoic acid (or palmitoleic acid), Doconexent and 9(E),11(E)-Conjugated linoleic acid might involve in ferroptosis and aerobic metabolism in tumor cells, sensitivity of chemotherapy, and downregulation of some signaling pathways in BC [Liu J etal.,2005; Newell M etal.,2019]. Furthermore, the association of metabolomics with clinical data might be helpful to understand the molecular level of BC, prediction of treatment outcome including adverse effects, and final implementation of new strategies towards more personalized medicine. Nonetheless, monitoring TIS as biomarkers to limit toxicities of standard chemotherapy may provide additional valuable information to

build a circulating “pCR-likely” profile and possibly improve the health of patients with cancer.

One potential limitation of our study was a smaller sample size (60 patients in total). Larger studies will improve the quantification of senescence markers induced by different chemotherapy regimens in NAT. Furthermore, evaluating more senescence markers improves knowledge about invivo senescence and thereby elucidates its contribution to therapy outcomes and paves the way for the utilization of potential cancer therapy. For plasma associated metabolites, we used an untargeted approach in our study design and less sample size makes it difficult to elucidate whether these metabolites could be useful in future BC screening and characterization.

In the 2nd study, we assessed the impact of CDKi-induced cellular senescence and nature of SASPs in non-malignant cells. Growing evidence demonstrated that the advent of CDK4/6 inhibitors has been a major milestone in different cancer treatments including breast cancer. However, senescence induction because of CDKi is beneficial or detrimental not fully known yet. Based on their previous results, Prof. Demaria group had considerable interest in validating how senescence induction pattern and SASP nature after treatment together with doxorubicin and CDK4/6 inhibitor in non-malignant cells. We found that fibroblast cells in culture readily displayed hallmark features of cellular senescence (expression of p16INK4a, p21CIP1 and loss of LaminB1) when treated with both doxorubicin alone and in combination with abemaciclib. Interestingly, NF-κB-targeted genes (IL1A, IL6, CXCL1 and CCL2) expression was observed only on genotoxic drug alone treatment, but not on combination with CDK4/6i. When it comes to p53 targets, there was no significant difference in their relative expression among the two groups.

As innate immune effectors, NK cells are one of the major infiltrating immune cells in breast cancer and able to recognize nascent transformed cells to prevent tumorigenesis and subsequent metastasis [Dewan MZ etal.,2007; Mamessier E etal.,2011]. We evaluated the cytotoxic effect of human Natural Killer (NK) cells on triple-negative breast cancer cell lines (MDAMB231) in the presence of treatment-associated senescent BJ using IncuCyte® S3 Live-Cell Analysis System. We found out that MDAMB231 proliferation decreased in the presence of doxorubicin plus abemaciclib treated BJ when compared with the other conditions,

indicating that abemaciclib might have role in the reduction of MDAMB231 proliferation. Further research is necessary to understand the mechanism behind this outcome.

Further, performed the triple-negative breast cancer cell lines (MDAMB231 & BT549) proliferation assay in the presence of proliferating and senescent BJ / hTERT RPE-1 (after TIS) using IncuCyte to mimic in vivo condition. In the presence of senescent BJ fibroblast induced by doxorubicin treatment, a significant increase observed in both cancer cell lines proliferation. Notebly, proliferation is less in the presence of doxorubicin plus abemaciclib treated senescent BJ and abemaciclib short term (48hours) treated BJ. Altogether, our results demonstrated that reduction of cancer proliferation in abemaciclib treatment was neither depend on senescent status nor cell type.

Overall, our results demonstrated that regulators of senescence-associated toxicities mainly associated with NF-κB associated SASPs. The short-term treatment of cancer cells with CDK4/6 inhibitor induces RB-dependent G1 arrest and this might be a reason for the reduction of cancer cell proliferation in the presence of CDK4/6 inhibitor. There are still many gaps in our understanding of how CDK4/6 inhibitors affect tumor and normal cells, and why their impact differs in different cancer types.

Chapter6: Conclusion

In the war on cancer, the main goal is to achieve cure through complete eradication. However, this goal is not that easy. A promising approach to induce cytostasis in tumor cells is TIS. However, in an oncogenic context, TIS can have different consequences depends on the type and nature of therapy. Accumulating data indicate that cellular senescence, which is recognized as a central component of TIS in both normal and tumor cells independent of direct genomic damage. TIS is highly heterogeneous and context dependent such as tissue of origin, trigger and so on. The acquisition of plasticity, stemness, tumorigenic, and aggressive growth phenotypes may occur due to the escape or bypass of some senescent cells from growth arrest. Additionally, therapy can modulate both tumor cells and normal tissues via specific SASP, resulting in inhibition and/or promotion of tumorigenesis.

Through better understanding of TIS, we can anticipate a steady pipeline of novel biomarkers and development of robust senescence-inducing agents, and continued investigations of the biological implications of senescence in both cancerous and non-cancerous microenvironment, as effectively as possible to achieve better outcomes for cancer patients.

A novel transcriptomic-based classifier for senescent cancer cells

Feba Mariam Varughese and Marco Demaria

The inability to unequivocally identify senescent cancer cells is hindering the development of novel anti-cancer therapies using senolytic compounds. In a recent study in Cell Reports, *Jochems et al.* used a machine-learning approach to generate a classifier for senescent cancer cells based on transcriptional signatures.

Cellular senescence is a state of stable and generally irreversible growth arrest distinct from quiescence or terminal differentiation [Gorgoulis V etal.,2019]. It is induced by several stressors, including telomere shortening, exposure to genotoxic agents, nutrient deprivation, oxidative stress, or oncogene overexpression [Hernandez-Segura A etal.,2018]. In addition to losing proliferative capacity, senescent cells undergo various and heterogeneous morphological, structural, and functional changes. These changes include flattened shape, increased cellular volume, altered composition of the plasma membrane, metabolic reprogramming, chromatin rearrangements, autophagy modulation, enhanced lysosomal activity, and a hypersecretory phenotype (senescence-associated secretory phenotype; SASP) [Gorgoulis V etal.,2019]. Due to the lack of a universal, senescence-specific marker, multiple markers are normally combined to identify senescent cells: (i) upregulation of the cyclin-dependent kinase (CDK) inhibitors p16INK4a and p21CIP1; (ii) enhanced activity of the lysosomal senescence-associated β-galactosidase (SA-β-gal); (iii) expression and secretion of SASP factors, such as proinflammatory cytokines and chemokines; (iv) presence of senescence-associated heterochromatin foci (SAHF); and (v) loss of the nuclear lamina protein laminB1 [Borghesan M etal.,2020]. However, some of these markers can be identified in non-senescent cells and are not homogenously present in all senescence subsets [Hernandez-Segura A etal.,2018]. Both normal and cancer cells are capable of activating a senescent program in response to excessive genotoxic stress, such as upon exposure to high doses of radio- or chemotherapy [Wang B etal.,2020]. Cancer cells can enter a senescent state because of direct therapy-driven genotoxic damage or paracrine interactions promoted by the SASP produced by neighboring therapy-induced senescent normal cells. The activation of the senescence-associated growth arrest then

restricts tumor growth. Moreover, the SASP of senescent normal and cancer cells can lead to activation of immunosurveillance mechanisms, further reinforcing tumor suppression. However, persistence of therapy-induced senescent (TIS) cells can also have detrimental and protumorigenic effects [Wang B etal.,2020]. Chronic secretion of SASP factors from TIS normal cells might interfere with immunosurveillance and remodel the microenvironment favoring tumor progression [Demaria M etal.,2017; Murali B etal.,2018]. In addition, senescent cancer cells acquire stem-like features and might be able to escape proliferative arrest and contribute to cancer relapse [Milanovic M etal.,2018]. For this reason, Bernards and colleagues suggested that combining prosenescence (chemo- or radiotherapy) with antisenescence (senolytic) therapies, the so-called 'one-two punch' approach, would have superior efficacy and reduced adverse effects [Wang C etal.,2019]. However, because of the heterogeneity of the senescence state, it remains difficult to identify senescent cancer cells unequivocally. Moreover, because senolytics target specific senescence-associated vulnerabilities, the efficacy of the antisenescence punch is dependent on which phenotypes are displayed by the senescent subpopulation. For these reasons, it is challenging to understand which populations of patients with cancer could benefit from the one-two punch approach. In a recent study in Cell Reports, Jochems et al. performed a comprehensive characterization of the transcriptional profiles of various senescent cancer cells [Jochems F etal.,2021]. The authors initially induced senescence in 13 different cell lines (MCF-7, T47D, MDA-MB-231, SUM159, A549, PC9, H358, HCT116, LoVo, RKO, Huh7, Hep3B, and HepG2) from four tissues (breast, colon, lung, and liver cancer) using the chemo-therapeutic agents alisertib or etoposide. The senescence phenotype was validated based on morphology, SA-β-gal activity, and seven other protein markers of senescence, including retinoblastoma protein (RB) phosphorylation, p53, p53 phosphorylation, laminB1, p21CIP1, p16INK4A, and γ-H2AX. The authors additionally performed RNA-sequencing and the data were assessed with single-sample gene set enrichment analysis (ssGSEA) for four gene sets associated with senescence, which demonstrated high variability in the expression of these transcriptional senescence-associated signatures.

Senescent cells often become resistant to apoptosis because of the transcriptional upregulation of BCL2 antiapoptotic family proteins [Borghesan M etal.,2020]. Along this line, exposure to the pan-BCL2 inhibitor ABT-263 (navitoclax) is toxic to several senescent

cell types [Zhu Y etal.,2016; Chang J etal.,2016]. However, the sensitivity of the panel of senescent cancer cells, uncovered by Jochems et al., toward ABT-263 showed remarkable divergence. While senescent LoVo cells were resistant to ABT-263, possibly to due to biallelic frame-shift mutations in the proapoptotic gene BAX, the divergent response of other cell lines did not correlate to the expression and state of pro or antiapoptosis-related genes. Senescence-associated transcriptomic signatures are heterogeneous and dependent on various factors, including the stressor, time point, tissue of origin, and cell type [Hernandez-Segura etal.,2017]. The signatures of alisertib- and etoposide-induced senescence resulted in highly overlapping expression profiles, suggesting that, at least in this context, senescence-associated gene expression is independent of the inducer. Similar results were obtained by analyzing additional common senescence inducers, such as doxorubicin and palbociclib. By contrast, several differentially expressed genes were identified in alisertib-treated cells on Day 7 versus Day 14 post treatment, suggesting that the transcriptome of senescent cancer cells, similar to senescent normal cells [12], is highly dynamic. Even more remarkable was the observation that the senescence-associated transcriptomic signature relies on the cell type and tissue of origin. Expression levels of classical SASP factors, such as IL-6 and IL-8, varied between cell lines, with some cells expressing high levels at baseline and nonsignificant upregulations upon treatment. Additional differences were observed when focusing on the tissue of origin. Overall, these results support the notion that transcriptomic profiles of senescent cancer cells are dynamic and heterogeneous, and that a major contributor to transcriptional diversity is the tissue of origin. Importantly, chromatin state and mutations in key genes for the senescence program (p53, NFkB, and C/EBPs) could also influence the gene expression profile.

While different studies have attempted to define core transcriptomic signatures of normal senescent cells, transcripts similarly differentially regulated in different senescent cancer models remain largely unknown. To overcome this limitation, the authors established a machine-learning approach to define whether a transcriptomic profile could be used as a classifier for cancer senescence. The SENCAN classifier selected 137 genes that included known senescence-associated genes, such as p21CIP1 and HMGB1, genes involved in mRNA processing, interferon-response genes, histone variants, and the telomere regulator RTEL1. SENCAN was able to classify different cancer cell lines and human tumors as senescent, and

to discriminate between senescence and quiescence. Interestingly, SENCAN remains applicable to cancer specimens only, because it was not able to correctly classify senescence in different normal cell strains.

In summary, the study by Jochem et al. not only strengthens the concept of senescence heterogeneity, but also presents a robust classifier that allows the detection of senescent cancer cells based on their transcriptome. It is now key to understand the sensitivity of the classifier for the detection, quantification, and characterization of senescent cells in malignant tissues. Moreover, in consideration of the increasing number of available senescence transcriptomic data sets, classifiers for different subsets of normal and cancer senescent cells should be developed. The development of subset-specific classifiers could help to further understand and predict the heterogeneity of the biological functions of senescent cells in vivo. In addition, these classifiers could provide a potent tool for the development of personalized senolytic interventions based on subset-specific vulnerabilities (Figure 1).

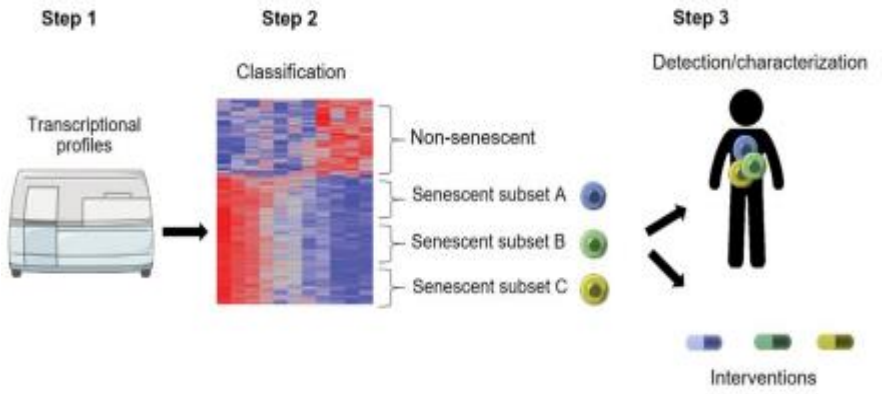

Figure1: Development and application of senescence subset-specific classifiers. There are numerous transcriptional data sets generated from whole-transcriptome sequencing of different normal and cancer senescent cells. These data can provide a unique profile for the different senescence subsets (Step 1). The profiles can be then used to generate classifiers that not only distinguish senescent versus nonsenescent cells, but also describe specific senescent subsets (Step 2). Subset-specific classifiers will help to identify and characterize the different subpopulations of senescent cells present in certain tissues and conditions, and to develop tailored senolytic approaches targeting such subpopulations (Step 3).

Chapter7: References

1. Albert R. Davalos, Jean-Philippe Coppe, Judith Campisi, and Pierre-Yves. Senescent cells as a source of inflammatory factors for tumor progression. Cancer Metastasis Rev. 2010; 29(2): 273–283.

2. Seluanov, et al. Change of the death pathway in senescent human fibroblasts in response to DNA damage is caused by an inability to stabilize p53. Mol. Cell. Biol., 21 2001, pp. 1552-1564.

3. Alcorta DA, Xiong Y, Phelps D, Hannon G, Beach D, Barrett JC. Involvement of the cyclin-dependent kinase inhibitor p16 (INK4a) in replicative senescence of normal human fibroblasts. Proc Natl Acad Sci U S A. 1996;93(24):13742–7.

4. Alix-Panabières C, Pantel K. Liquid Biopsy: From Discovery to Clinical Application. Cancer Discov. 2021;11(4):858–73.

5. Alvarez-Fernandez M, Malumbres M. Mechanisms of Sensitivity and Resistance to CDK4/6 Inhibition. Cancer Cell. 2020 ;37:514–529.

6. Arina A, Beckett M, Fernandez C, et al. Tumor-reprogrammed resident T cells resist radiation to control tumors. Nature communications 2019;10(1):3959.

7. B.Y. Lee, et al. Senescence-associated β-galactosidase is lysosomal β-galactosidase. Aging Cell, 5 2006, pp. 187-195.

8. Baar MP, Brandt RMC, Putavet DA, Klein JDD, Derks KWJ, Bourgeois BRM, Stryeck S, Rijksen Y, van Willigenburg H, Feijtel DA et al.Targeted apoptosis of senescent cells restores tissue homeostasis in response to chemotoxicity and aging. Cell 2017; 169: 132–147.

9. Dewan MZ, Terunuma H, Takada M, Tanaka Y, Abe H, Sata T, et al Role of natural killer cells in hormone-independent rapid tumor formation and spontaneous metastasis of breast cancer cells in vivo. Breast Cancer Res Treat 2007;104:267–75.

10. Mamessier E, Sylvain A, Bertucci F, Castellano R, Finetti P, Houvenaeghel G, et al Human breast tumor cells induce self-tolerance mechanisms to avoid NKG2D-

mediated and DNAM-mediated NK cell recognition. Cancer Res 2011;71:6621–32.

11. Bennecke, M.; Kriegl, L.; Bajbouj, M.; Retzlaff, K.; Robine, S.; Jung, A.; Arkan, M.C.; Kirchner, T.; Greten, F.R. Ink4a/Arf and oncogene-induced senescence prevent tumor progression during alternative colorectal tumorigenesis. Cancer Cell 2010, 18, 135–146.

12. Bernal-Estevez DA, Garcia O, Sanchez R, Parra-Lopez CA. Monitoring the responsiveness of T and antigen presenting cell compartments in breast cancer patients is useful to predict clinical tumor response to neoadjuvant chemotherapy. BMC Cancer. 2018; 18(1):77.

13. Borghesan, M. et al. A sewanescence-centric view of aging: implications for longevity and disease. Trends Cell Biol. 2020; 30, 777–791.

14. Bruni E, Cazzetta V, Donadon M, et al. Chemotherapy accelerates immune senescence and functional impairments of Vdelta2(pos) T cells in elderly patients affected by liver metastatic colorectal cancer. Journal for immunotherapy of cancer 2019;7(1):347.

15. C. Shi , Q. Wang and X. Liao , *et al.*, Discovery of 6-(2-(dimethylamino)ethyl)-N-(5-fluoro-4-(4-fluoro-1-isopropyl-2-methyl-1H-benzo[d]imidazole-6-yl)pyrimidin-2-yl)-5,6,7,8-tetrahydro-1,6-naphthyridin-2-amine as a highly potent cyclin-dependent kinase 4/6 inhibitor for treatment of cancer, *Eur. J. Med. Chem.*, 2019, 178, 352 —364.

16. C.J. Sherr, J.M. Roberts. CDK inhibitors: positive and negative regulators of G1-phase progression. Genes Dev., 13 1999, pp. 1501-1512.

17. Campisi, J. & d'Adda di Fagagna, F. Cellular senescence: when bad things happen to good cells. Nat. Rev. Mol. Cell Biol. 2007; 8, 729–740.

18. Cardoso F, Paluch-Shimon S, Senkus E, Curigliano G, Aapro MS, Andreí F, et al. 5th ESO-ESMO international consensus guidelines for advanced breast cancer (ABC 5). Ann Oncol 2020; 31:1623–49.

19. Carlomagno C, Perrone F, Lauria R, de Laurentiis M, Gallo C, Morabito A, Pettinato G, Panico L, Bellelli T, Apicella A, et al: Prognostic significance of necrosis, elastosis, fibrosis, and inflammatory cell reaction in operable breast cancer. Oncology 52: 1995; 272-277.

20. Catzavelos C, Bhattacharya N, Ung YC, Wilson JA, Roncari L, Sandhu C, Shaw P, Yeger H, Morava-Protzner I, Kapusta L, Franssen E, Pritchard KI, Slingerland JM. "Decreased levels of the cell-cycle inhibitor p27Kip1 protein: Prognostic implications in primary breast cancer". Nature Medicine.1997; 3 (2): 227–230.

21. Chang B.D., Xuan Y., Broude E.V., Zhu H., Schott B., Fang J.et al. Role of p53 and p21(waf1/cip1) in senescence-like terminal proliferation arrest induced in human tumor cells by chemotherapeutic drugs. Oncogene 18, 1999; 4808–4818.

22. Chang, J. etal. Clearance of senescent cells by ABT263 rejuvenates aged hematopoietic stem cells in mice. Nat. Med. 2016; 22, 78–83.

23. Cheang MCU, van de Riin M, Nielsen TO. Gene expression profiling of breast cancer. Annu Rev Pathol Mech Dis. 2008; 3: 67– 97.

24. Childs, B.G., Baker, D.J., Kirkland, J.L., Campisi, J., and Deursen, J.M. Senescence and apoptosis: dueling or complementary cell fates? EMBO 2014; Rep. 15, 1139–1153.

25. Collado, M., Gil, J., Efeyan, A., Guerra, C., Schuhmacher, A.J., Barradas, M., Benguría, A., Zaballos, A., Flores, J.M., Barbacid, M., et al. Tumour biology: Senescence in premalignant tumours. Nature 2005; 436, 642.

26. Coppe J.P., Kauser K., Campisi J., Beausejour C.M. Secretion of vascular endothelial growth factor by primary human fibroblasts at senescence. J. Biol. Chem. 2006;281:29568–29574.

27. Davaapil H., Brockes J.P., Yun M.H. Conserved and novel functions of programmed cellular senescence during vertebrate development. Development. 2017;144:106–114.

28. De Giorgi U, Mego M, Scarpi E, Giordano A, Giuliano M, Valero V, Alvarez RH, Ueno NT, Cristofanilli M, Reuben JM. Association between circulating tumor cells and peripheral blood monocytes in metastatic breast cancer. Ther Adv Med Oncol. 2019;11:1758835919866065.

29. Debacq-Chainiaux F, Erusalimsky JD, Campisi J, Toussaint O. Protocols to detect senescence-associated beta-galactosidase (SA-betagal) activity, a biomarker of senescent cells in culture and in vivo. Nat Protoc. 2009;4(12):1798–806.

30. Demaria M, O'Leary MN, Chang J, Shao L, Liu SU, Alimirah F, Koenig K, Le C, Mitin N, Deal AM et al. Cellular senescence promotes adverse effects of chemotherapy and cancer relapse. Cancer Discov. 2017; 7: 165–176.
31. Demaria M. etal. Cellular senescence promotes adverse effects of chemotherapy and cancer relapse. Cancer Discov. 2017; 7, 165–176.
32. Di Mitri D, Toso A, Chen JJ, Sarti M, Pinton S, Jost TR, D'Antuono R, Montani E, Garcia-Escudero R, Guccini I, et al. Tumour-infiltrating Gr-1+ myeloid cells antagonize senescence in cancer. Nature. 2014; 515: 134–137.
33. Dimri GP, et al. A novel biomarker identifies senescent human cells in culture and in aging skin in vivo. Proceedings of the National Academy of Sciences of the United States of America. 1995;92:9363–9367.
34. Dimri GP, Lee X, Basile G, Acosta M, Scott G, Roskelley C, et al. A biomarker that identifies senescent human cells in culture and in aging skin in vivo. Proc Natl Acad Sci U S A. 1995;92(20):9363–7.
35. Dolan RD, Lim J, McSorley ST, Horgan PG, McMillan DC. The role of the systemic inflammatory response in predicting outcomes in patients with operable cancer: Systematic review and meta-analysis. Sci Rep. 2017; 7:16717.
36. Eggert T, Wolter K, Ji J, Ma C, Yevsa T, Klotz S, Medina-Echeverz J, Longerich T, Forgues M, Reisinger F, et al. Distinct functions of senescence-associated immune responses in liver tumor surveillance and tumor progression. Cancer Cell. 2016; 30: 533–547.
37. El Daker, S., Sacchi, A., Tempestilli, M., Carducci, C., Goletti, D., Vanini, V., Colizzi, V. et al., Granulocytic myeloid derived suppressor cells expansion during active pulmonary tuberculosis is associated with high nitric oxide plasma level. PLoS One. 2015. 10: e0123772.
38. el-Deiry WS, Tokino T, Velculescu VE, Levy DB, Parsons R, Trent JM, et al. WAF1, a potential mediator of p53 tumor suppression. Cell. 1993; 75:817–825.
39. Evangelou K, Lougiakis N, Rizou SV, Kotsinas A, Kletsas D, Muñoz-Espín D, et al. Robust, universal biomarker assay to detect senescent cells in biological specimens. Aging Cell. 2017;16(1):192–7.
40. Faget, D. V., Ren, Q. & Stewart, S. A. Unmasking senescence: context-dependent effects of SASP in cancer. Nat. Rev. Cancer. 2019; 19, 439–453.

41. FDA. Pathological Complete Response in Neoadjuvant Treatment of High-Risk Early-Stage BreastCancer: Use as an Endpoint to Support Accelerated Approval. https://www.fda.gov/drugs/guidance-compliance-regulatory information/ guidances-drugs (2022).

42. Finn RS, Martin M, Rugo HS, Jones S, Im SA, Gelmon K, et al. Palbociclib and letrozole in advanced breast cancer. N Engl J Med. 2016;375(20):1925–36.

43. Fry DW, Harvey PJ, Keller PR, Elliott WL, Meade M, Trachet E, et al. Specific inhibition of cyclin-dependent kinase 4/6 by PD 0332991 and associated antitumor activity in human tumor xenografts. Mol Cancer Ther. 2004;3:1427–1438.

44. Fu M, Wang C, Li Z, Sakamaki T, Pestell RG. Cyclin D1: normal and abnormal functions. Endocrinology. 2004; 145:5439-47.

45. Fucà G, Guarini V, Antoniotti C et al (2020) The pan-immune-inflammation value is a new prognostic biomarker in metastatic colorectal cancer: results from a pooled-analysis of the Valentino and TRIBE first-line trials. Br J Cancer 123:403–409.

46. Fuca G, Guarini V, Antoniotti C, Morano F, Moretto R, Corallo S, et al. The Pan-Immune-Inflammation Value Is a New Prognostic Biomarker in Metastatic Colorectal Cancer: Results From a Pooled-Analysis of the Valentino and TRIBE First-Line Trials. Br J Cancer 2020; 123(3):403–9.

47. Gabrilovich D.I. Myeloid-Derived Suppressor Cells. Cancer Immunol. Res. 2017; 5:3–8.

48. Gelbert LM, Cai S, Lin X, Sanchez-Martinez C, Del Prado M, Lallena MJ, et al. Preclinical characterization of the CDK4/6 inhibitor LY2835219: in-vivo cell cycle-dependent/independent anti-tumor activities alone/in combination with gemcitabine. Invest New Drugs. 2014;32:825–837.

49. Georgiannos SN, Renaut A, Goode AW, Sheaff M. The immunophenotype and activation status of the lymphocytic infiltrate in human breast cancers, the role of the major histocompatibility complex in cell-mediated immune mechanisms, and their association with prognostic indicators. Surgery 134: 827-834, 2003.

50. Giacinti, C.; Giordano, A. RB and cell cycle progression. Oncogene 2006, 25, 5220–5227.

51. Goel S, DeCristo MJ, Watt AC, BrinJones H, Sceneay J, Li BB, et al. CDK4/6 inhibition triggers anti-tumour immunity. Nature. 2017;548(7668):471–5.
52. Goetz MP, Toi M, Campone M, Treídan O, Bourayou N, Sohn J, et al. MONARCH 3: Abemaciclib as initial therapy for advanced breast cancer. J Clin Oncol 2017; 35(32):3638–46.
53. González-Angulo A.M., Ferrer-Lozano J., Stemke-Hale K., Sahin A., Liu S., Barrera J.A., Burgues O., Lluch A., Chen H., Hortobagyi G.N., et al. PI3K Pathway Mutations and PTEN Levels in Primary and Metastatic Breast Cancer. Mol. Cancer Ther. 2011; 10:1093–1101.
54. González-Gualda E., Baker A.G., Fruk L. and Muñoz-Espín D. A guide to assessing cellular senescence in vitro and in vivo. FEBS J. 2020; 288, 56–80.
55. Gorgoulis V., Adams P.D., Alimonti A., Bennett D.C., Bischof O., Bishop C.et al. Cellular senescence: defining a path forward. Cell 2019; 179, 813–827.
56. Grivennikov SI, Greten FR, Karin M. Immunity, inflammation, and cancer. Cell 2010; 140(6):883–899.
57. Guo, X. et al. TAp63 induces senescence and suppresses tumorigenesis in vivo. Nat. Cell Biol. 2009; 11, 1451–1457.
58. Haile LA, Gamrekelashvili J, Manns MP, Korangy F, Greten TF. CD49d is a new marker for distinct myeloid-derived suppressor cell subpopulations in mice. J Immunol. 2010;185(1):203–10.
59. Hao Z, Li R, Wang Y, Li S, Hong Z, Han Z. Landscape of myeloid-derived suppressor cell in tumor immunotherapy. Biomark Res. 2021;9(1):77.
60. Henson, S.M., Riddell, N.E and Akbar, A.N. Properties of end-stage human T cells defined by CD45RA re-expression. Current Opinion in Immunology. 2012; Vol. 24 No. 4, pp. 476–81.
61. Hernandez-Segura, A. et al. Unmasking transcriptional heterogeneity in senescent cells. Curr. Biol. 2017; 27, 2652–2660.
62. Hernandez-Segura, A. et al. Hallmarks of cellular senescence. Trends Cell Biol. 2018; 28, 436–453.
63. Herranz, N. & Gil, J. Mechanisms and functions of cellular senescence. J. Clin. Invest.2018; 128, 1238–1246.

64. https://acsjournals.onlinelibrary.wiley.com/doi/10.3322/caac.21763
65. https://www.aiom.it/tumori-nel-2022-in-italia-stimati-390-700-nuovi-casi-14-100-in-2-anni-post-covid-piu-screening-ma-e-allarme-per-gli-stili-di-vita-scorretti/
66. https://www.breastcancer.org/facts-statistics
67. https://www.cancer.org/cancer/breast-cancer/about/how-common-is-breastcancer.html
68. Huang, S. etal. EZH2 inhibitor GSK126 suppresses antitumor immunity by driving production of myeloid-derived suppressor cells. Cancer Res 2019; 79, 2009–2020.
69. Hui-Ling Ou, Reuben Hoffmann, Cristina González-López, Gary J. Doherty, James E. Korkola, Daniel Muñoz-Espín. Cellular senescence in cancer: from mechanisms to detection. Molecular Oncology15 2021;2634–2671.
70. J.A. Ewald, J.A. Desotelle, G. Wilding, D.F. Jarrard. Therapy-induced senescence in cancer. J. Natl. Cancer Inst., 102 2010; pp. 1536-1546.
71. J.C. Jeyapalan, M. Ferreira, J.M. Sedivy, U. Herbig. Accumulation of senescent cells in mitotic tissue of aging primates. Mech. Ageing Dev., 128 (1) 2007; pp. 36-44.
72. James, E.L., Michalek, R.D., Pitiyage, G.N., De Castro, A.M., Vignola, K.S., Jones, J., 189 Mohney, R.P., et al. Senescent human fibroblasts show increased glycolysis and redox homeostasis with extracellular metabolomes that overlap with those of irreparable DNA damage, aging, and disease, Journal of Proteome Research, 2015; Vol. 14 No. 4, pp. 1854–71.
73. Jochems, F. etal. The Cancer SENESCopedia: a delineation of cancer cell senescence. Cell Rep. 2021; 36, 109441.
74. Johnson CH, Ivanisevic J, Siuzdak G. Metabolomics: beyond biomarkers and towards mechanisms. Nat Rev Mol Cell Biol. 2016;17(7):451–9.
75. Johnston SRD, Harbeck N, Hegg R, Toi M, Martin M, Shao ZM, et al. Abemaciclib combined with endocrine therapy for the adjuvant treatment of HR+, HER2-, node-positive, high-risk, early breast cancer (monarchE). J Clin Oncol 2020; 38(34):3987–98.
76. Jun J and Lau LF. The matricellular protein CCN1 induces fibroblast senescence and restricts fibrosis in cutaneous wound healing. Nature Cell Biology, 2010; Vol. 12 No. 7, pp. 676–85.

77. Kalra S. Joshi G. Munshi A. Kumar R. Structural insights of cyclin dependent kinases: implications in design of selective inhibitors. Eur. J. Med. Chem. 2017; 142:424–458.

78. Kang, T. W. et al. Senescence surveillance of pre-malignant hepatocytes limits liver cancer development. Nature 2011; 479, 547–551.

79. Klein ME, Kovatcheva M, Davis LE, Tap WD, Koff A. CDK4/6 Inhibitors: The Mechanism of Action May Not Be as Simple as Once Thought. Cancer Cell. 2018; 34:9–20.

80. Kohli J, Wang B, Brandenburg SM, Basisty N, Evangelou K, Varela-Eirin M, et al. Algorithmic assessment of cellular senescence in experimental and clinical specimens. Nat Protoc. 2021; 16(5):2471–98.

81. Koniaras K., Cuddihy A.R., Christopoulos H., Hogg A., O'Connell M.J. Inhibition of Chk1-dependent G2 DNA damage checkpoint radiosensitizes p53 mutant human cells. Oncogene. 2001;20:7453–7463.

82. Kreienberg R, Albert U S, Follmann M et al. Interdisciplinary GoR level III guidelines for the diagnosis, therapy and follow-up care of breast cancer: short version – AWMF Registry No.: 032-045OL AWMF-Register-Nummer: 032-045OL – Kurzversion 3.0, Juli 2012. Geburtsh Frauenheilk. 2013; 73:556–583.

83. Kreis N.N., Louwen F. and Yuan J. (2019) The multifaceted p21 (Cip1/Waf1/CDKN1A) in cell differentiation, migration and cancer therapy. Cancers (Basel) 2019; 11, 1220.

84. Krizhanovsky, V., Yon, M., Dickins, R.A., Hearn, S., Simon, J., Miething, C., Yee, H., et al, "Senescence of Activated Stellate Cells Limits Liver Fibrosis", Cell,2008; Vol. 134 No. 4, pp. 657–67.

85. Kuchenbaecker, K. B. et al. Risks of breast, ovarian, and contralateral breast cancer for BRCA1 and BRCA2 mutation carriers. JAMA 2017; 317, 2402–2416.

86. Kuilman T, Michaloglou C, Mooi WJ, Peeper DS. The essence of senescence. Genes Dev. 2010;24(22):2463–2479.

87. Kuilman, T. et al. Oncogene-induced senescence relayed by an interleukin-dependent inflammatory network. Cell 2008; 133, 1019–1031.

88. Kuilman, T., Michaloglou, C., Vredeveld, L.C.W., Douma, S., van Doorn, R., Desmet, C.J., Aarden, L.A., Mooi, W.J., and Peeper, D.S. Oncogene-Induced Senescence Relayed by an Interleukin-Dependent Inflammatory Network. Cell 2008; 133, 1019–1031.

89. Kumar V. The Nature of Myeloid-Derived Suppressor Cells in the Tumor Microenvironment. Trends Immunol. 2016; 37:208–220.

90. L. Hayflick, P. Moorhead. The serial cultivation of human diploid cell strains. Exp. Cell Res., 25 1961; pp. 585-621.

91. L. Hayflick. The limited in vitro lifetime of human diploid cell strains. Exp Cell Res. 1965; 37, 614–636.

92. Lécuyer L, Dalle C, Lyan B, Demidem A, Rossary A, Vasson MP, et al. Plasma metabolomic signatures associated with long-term breast cancer risk in the SU.VI.MAX prospective cohort. Cancer Epidemiol Biomarkers Prev. 2019; 28(8):1300–7.

93. Lécuyer L, Victor Bala A, Deschasaux M, Bouchemal N, Nawfal Triba M, Vasson MP, etal. NMR metabolomic signatures reveal predictive plasma metabolites associated with long-term risk of developing breast cancer. Int J Epidemiol. 2018; 47(2):484–94.

94. Lee BY, Han JA, Im JS, Morrone A, Johung K, Goodwin EC, etal. Senescence-associated beta-galactosidase is lysosomal beta-galactosidase. Aging Cell. 2006; 5(2):187–95.

95. Lee, S. & Schmitt, C. A. The dynamic nature of senescence in cancer. Nat. Cell Biol. 2019; 21, 94–101.

96. Liantao Guo, Deguang Kong, Jianhua Liu, Ling Zhan, Lan Luo, Weijie Zheng, Qingyuan Zheng, Chuang Chen and Shengrong Sun. Breast cancer heterogeneity and its implication in personalized precision therapy. Experimental Hematology & Oncology 2023; 12:3.

97. Liqin Wang, Lina Lankhorst & René Bernards. Exploiting senescence for the treatment of cancer. Nature Reviews Cancer 2022; volume 22, pages340–355.

98. Liu J, Sidell N. Anti-estrogenic Effects of Conjugated Linoleic Acid through Modulation of Estrogen Receptor Phosphorylation. Breast Cancer Research and Treatment 2005 94:2 2005; 94: 161–9.

99. Luzardo-Ocampo I, Campos-Vega R, Gonzalez de Mejia E, Loarca-Piña G. Consumption of a baked corn and bean snack reduced chronic colitis inflammation in CD-1 mice via downregulation of IL-1 receptor, TLR, and TNF-α associated pathways. Food Research International 2020; 132.

100. Malumbres M. Cyclin-dependent kinases, Genome Biol., 2014, 15 1-10.

101. M. Serrano, A.W. Lin, M.E. McCurrach, D. Beach, S.W. Lowe. Oncogenic ras provokes premature cell senescence associated with accumulation of p53 and p16INK4a. Cell, 1997; 88 (5), pp. 593-602.

102. M.P. Baar, R.M.C. Brandt, D.A. Putavet, J.D.D. Klein, K.W.J. Derks, B.R.M. Bourgeois, S. Stryeck, Y. Rijksen, etal. Targeted apoptosis of senescent cells restores tissue homeostasis in response to chemotoxicity and aging. Cell, 169 (1) 2017; pp. 132-147.

103. Malumbres M, Barbacid M. To cycle or not to cycle: a critical decision in cancer. Nat Rev Cancer 2001; 1: 222–231.

104. Mantovani A, Allavena P, Sica A, Balkwill F. Cancer-related inflammation. Nature. 2008; 454(7203):436–444.

105. Mantovani, A., Allavena, P., Sica, A. & Balkwill, F. Cancer-related inflammation. Nature 2008; 454, 436–444.

106. Martínez-Sáez O., Chic N., Pascual T., Adamo B., Vidal M., González-Farré B., Sanfeliu E., Schettini F., Conte B., Brasó-Maristany F., et al. Frequency and spectrum of PIK3CA somatic mutations in breast cancer. Breast Cancer Res. 2020; 22:45.

107. Massimo Di Maio, Diego Serraino. I NUMERI DEL CANCRO IN ITALIA 2022.

108. Mastio J, Condamine T, Dominguez G, Kossenkov AV, Donthireddy L, Veglia F, et al. Identification of monocyte-like precursors of granulocytes in cancer as a mechanism for accumulation of PMN-MDSCs. J Exp Med. 2019; 216(9):2150–69.

109. Matsuoka S., Rotman G., Ogawa A., Shiloh Y., Tamai K., Elledge S.J. Ataxia telangiectasia-mutated phosphorylates Chk2 in vivo and in vitro. Proc. Natl. Acad. Sci. USA. 2000; 97:10389–10394.

110. McHugh D, Gil J. Senescence and aging: Causes, consequences, and therapeutic avenues. J Cell Biol. 2018; 217:65–77.

111. Michaloglou, C., Vredeveld, L.C.W., Soengas, M.S., Denoyelle, C., Kuilman, T., Van Der Horst, C.M.A.M., Majoor, D.M., Shay, J.W., Mooi, W.J., and Peeper, D.S. (2005). BRAFE600-associated senescence-like cell cycle arrest of human naevi. Nature 436, 720–724.

112. Michaloglou, C.; Vredeveld, L.C.; Soengas, M.S.; Denoyelle, C.; Kuilman, T.; van der Horst, C.M.; Majoor, D.M.; Shay, J.W.; Mooi, W.J.; Peeper, D.S. BRAFE600-associated senescence-like cell cycle arrest of human naevi. Nature 2005, 436, 720–724.

113. Mieog JS, van der Hage JA, van de Velde CJ. Preoperative chemotherapy for women with operable breast cancer. Cochrane Database Syst Rev. 2007; 18(2):CD005002.

114. Milanovic, M. et al. (2018) Senescence-associated reprogramming promotes cancer stemness. Nature 2018; 553, 96–100.

115. Muñoz-Espín, D. and Serrano, M. Cellular senescence: From physiology to pathology, Nature Reviews Molecular Cell Biology, 2014; Vol. 15 No. 7, pp. 482–96.

116. Muñoz-Espín, D., Cañamero, M., Maraver, A., Gómez-López, G., Contreras, J., MurilloCuesta, S., Rodríguez-Baeza, A., et al. Programmed cell senescence during mammalian embryonic development, Cell, 2013; Vol. 155 No. 5, pp. 1104–18.

117. Murali, B. etal. Inhibition of the stromal p38MAPK/MK2 pathway limits breast cancer metastases and chemotherapy-induced bone loss. Cancer Res. 2018; 78, 5618–5630.

118. Murphy B.L., Day C.N., Hoskin T.L., Habermann E.B. and Boughey J.C. Neoadjuvant chemotherapy use in breast cancer is greatest in excellent responders: triple-negative and HER2+ subtypes. Ann. Surg. Oncol. 2018; 25, 2241–2248 10.1245/s10434-018-6531-5.

119. Murthy P, Zenati MS, Al Abbas AI, Rieser CJ, Bahary N, Lotze MT, Zeh HJ 3rd, Zureikat AH, Boone BA. Prognostic Value of the Systemic Immune Infammation Index (SII) after neoadjuvant therapy for patients with resected pancreatic cancer. Ann Surg Oncol. 2020; 27(3):898–906.

120. Nardella, C., Clohessy, J. G., Alimonti, A. & Pandolfi, P. P. Pro-senescence therapy for cancer treatment. Nat. Rev. Cancer 2011; 11, 503–511.

121. Newell M, MacKey JR, Bigras G, et al. Comparing docosahexaenoic acid (DHA) concomitant with neoadjuvant chemotherapy versus neoadjuvant chemotherapy alone in the treatment of breast cancer (DHA WIN): protocol of a double-blind, phase II, randomised controlled trial. BMJ Open 2019; 9: e030502.

122. Nikolaou K, Sarris M, Talianidis I. Molecular Pathways: The Complex Roles of Inflammation Pathways in the Development and Treatment of Liver Cancer. Clin Cancer Res 2013; 19(11):2810–6.

123. Noren Hooten N, Evans MK. Techniques to induce and quantify cellular senescence. J Vis Exp. 2017; (123). 10.3791/55533.

124. Novartis Kisqali (ribociclib, LEE011) receives FDA approval as first-line treatment for HR +/HER2 − metastatic breast cancer, 2017.

125. Olingy CE, Dinh HQ, Hedrick CC. Monocyte heterogeneity and functions in cancer. J Leukoc Biol. 2019; 106(2):309–322.

126. Onyema OO, Decoster L, Njemini R, et al. Shifts in subsets of CD8+ T-cells as evidence of immunosenescence in patients with cancers affecting the lungs: an observational case-control study. BMC cancer 2015; 15:1016.

127. Osanai, M. et al. Occludin-mediated premature senescence is a fail-safe mechanism against tumorigenesis in breast carcinoma cells. Cancer Sci. 2007; 98, 1027–1034.

128. Ostrand-Rosenberg S, Sinha P. Myeloid-derived suppressor cells: linking inflammation and Cancer. J Immunol. 2009;182(8):4499–506.

129. P. Spallarossa, et al. Doxorubicin induces senescence or apoptosis in rat neonatal cardiomyocytes by regulating the expression levels of the telomere binding factors 1 and 2. Am. J. Physiol. Circ. Physiol., 297 2009, pp. H2169-H2181.

130. Pak AS, Wright MA, Matthews JP, Collins SL, Petruzzelli GJ, Young MR. Mechanisms of immune suppression in patients with head and neck cancer: presence of CD34(+) cells which suppress immune functions within cancers that secrete granulocyte-macrophage colony-stimulating factor. Clin Cancer Res. 1995;1(1):95–103.

131. Pan H., Gray R., Braybrooke J., Davies C., Taylor C., McGale P.et al. 20-year risks of breast-cancer recurrence after stopping endocrine therapy at 5 years. N. Engl. J. Med. 2017; 377, 1836–1846.

132. Pérez-Mancera, P.A., Young, A.R.J. and Narita, M, Inside and out: The activities of senescence in cancer, Nature Reviews Cancer, 2014; Vol. 14 No. 8, pp. 547– 58.

133. Petrova NV, Velichko AK, Razin SV, Kantidze OL. Small molecule compounds that induce cellular senescence. Aging Cell. 2016;15:999–1017

134. Pluquet O., Pourtier A., Abbadie C. The unfolded protein response and cellular senescence. A review in the theme: Cellular mechanisms of endoplasmic reticulum

stress signaling in health and disease. Am. J. Physiol. Cell Physiol. 2015;308:C415–C425.

135. Powell WS, Rokach J. The eosinophil chemoattractant 5-oxo-ETE and the OXE receptor. Progress in Lipid Research. 2013; 52: 651–65.

136. Prall OW, Sarcevic B, Musgrove EA, Watts CK, Sutherland RL. Estrogen-induced activation of Cdk4 and Cdk2 during G1-S phase progression is accompanied by increased cyclin D1 expression and decreased cyclin-dependent kinase inhibitor association with cyclin E-Cdk2. J Biol Chem. 1997;272(16):10882–94.

137. Punglia RS, Hughes ME, Edge SB, et al. Factors associated with guideline-concordant use of radiotherapy after mastectomy in the NCCN. Int. J. Radiat. Oncol. Biol. Phys.2008; 72, 1434–1420.

138. Rastogi P, Anderson SJ, Bear HD, et al. Preoperative chemotherapy: Updates of national surgical adjuvant breast and bowel project protocols B-18 and B-27. J Clin Oncol 2008; 26:778-85.

139. Rhei, E. et al. Molecular genetic characterization of BRCA1-and BRCA2-linked hereditary ovarian cancers. Cancer Res.1998; 58, 3193–3196.

140. Rinschen MM, Ivanisevic J, Giera M, Siuzdak G. Identification of bioactive metabolites using activity metabolomics. Nat Rev Mol Cell Biol. 2019; 20(6):353–67.

141. Roberson RS, Kussick SJ, Vallieres E, Chen SY, Wu DY. Escape from therapy-induced accelerated cellular senescence in p53-null lung cancer cells and in human lung cancers. Cancer Res. 2005; 65:2795–2803.

142. Rodier, F.; Campisi, J. Four faces of senescence. J. Cell Biol. 2011, 192, 547–556.

143. Ruas M, Peters G. The p16INK4a/CDKN2A tumor suppressor and its relatives. Biochim Biophys Acta 1998; 1378: F115–F177.

144. Ruhland, M. K. & Alspach, E. Senescence and immunoregulation in the tumor microenvironment. *Front. Cell Dev. Biol.* 9, 754069 (2021).

145. Ruscetti, M. et al. NK cell-mediated cytotoxicity contributes to tumor control by a cytostatic drug combination. *Science* 362, 2018; 1416–1422.

146. Salama R., Sadaie M., Hoare M., Narita M. Cellular senescence and its effector programs. Genes Dev. 2014;28:99–114.

147. Salminen A, Kauppinen A, Kaarniranta K. Emerging role of NF-kappaB signaling in the induction of senescence-associated secretory phenotype (SASP) Cell. Signal. 2012; 24:835–845.

148. Santo L., Siu K.T., Raje N. Targeting Cyclin-Dependent Kinases and Cell Cycle Progression in Human Cancers. Semin. Oncol. 2015; 42:788–800.

149. Schnitt SJ. Will molecular classification replace traditional breast pathology? Int J Surg Pathol. 2010; 18 (3): 162S– 166S.

150. Shelton, D. N., Chang, E., Whittier, P. S., Choi, D. & Funk, W. D. Microarray analysis of replicative senescence. Curr. Biol. 1999; 9, 939–945.

151. Sherr CJ, Roberts JM (1999). "CDK inhibitors: positive and negative regulators of G1-phase progression". Genes & Development. 13 (12): 1501–1512.

152. Sherr CJ. The Pezcoller lecture: cancer cell cycles revisited. Cancer Res 2000; 60: 3689–3695.

153. Siravegna G, Marsoni S, Siena S, Bardelli A. Integrating liquid biopsies into the management of cancer. Nat Rev Clin Oncol. 2017;14(9):531–48.

154. Smith-Garvin, J. E., Koretzky, G. A. & Jordan, M. S. T cell activation. Annu. Rev. Immunol.2009; 27, 591–619.

155. Stein, G. H. , Drullinger, L. F. , Soulard, A. , & Dulic, V. Differential roles for cyclin-dependent kinase inhibitors p21 and p16 in the mechanisms of senescence and differentiation in human fibroblasts. Molecular and Cellular Biology, 1999; 19, 2109–2117. 10.1128/mcb.19.3.2109.

156. Suzuki E, Kapoor V, Jassar AS, Kaiser LR, Albelda SM. Gemcitabine selectively eliminates splenic Gr-1+/CD11b+ myeloid suppressor cells in tumor-bearing animals and enhances antitumor immune activity. Clin Cancer res. 2005; 11:6713–6721.

157. Te Poele R.H., Okorokov A.L., Jardine L., Cummings J., Joel S.P. DNA damage is able to induce senescence in tumor cells in vitro and in vivo. Cancer Res. 2002; 62:1876–1883.

158. Te Poele RH, Okorokov AL, Jardine L, Cummings J, Joel SP. DNA damage is able to induce senescence in tumor cells in vitro and in vivo. Cancer Res. 2002; 62:1876–1883.

159. Tenzin Adon, Dhivya Shanmugarajan, and Honnavalli Yogish Kumar. CDK4/6 inhibitors: a brief overview and prospective research directions. RSC Adv. 2021 Sep 1; 11(47):

29227–29246.

160. Tischkowitz M, Xia B. PALB2/FANCN: recombining cancer and Fanconi anemia. Cancer Res 2010; 70(19):7353–7359.

161. Toogood PL, Harvey PJ, Repine JT, Sheehan DJ, VanderWel SN, Zhou H, et al. Discovery of a potent and selective inhibitor of cyclin-dependent kinase 4/6. J Med Chem. 2005;48:2388–2406.

162. Torres-Guzman R, Calsina B, Hermoso A, Baquero C, Alvarez B, Amat J, et al. Preclinical characterization of abemaciclib in hormone receptor positive breast cancer. Oncotarget. 2017;8(41):69493–507.

163. V. Probin, Y. Wang, A. Bai, D. Zhou. Busulfan selectively induces cellular senescence but not apoptosis in WI38 fibroblasts via a p53-independent but extracellular signal-regulated kinase-p38 mitogen-activated protein kinase-dependent mechanism. J. Pharmacol. Exp. Ther., 319, 2006; pp. 551-560.

164. van der Hage JA, van de Velde CJ, Julien JP, et al. Preoperative chemotherapy in primary operable breast cancer: results from the European Organization for Research and Treatment of Cancer trial 10902. J Clin Oncol 2001; 19:4224-37.

165. Van Deursen J.M. The role of senescent cells in ageing. Nature. 2014; 509:439–446.

166. Van Deursen JM. The role of senescent cells in ageing. Nature. 2014;509:439–446.

167. Veglia, F.; Sanseviero, E.; Gabrilovich, D.I. Myeloid-derived suppressor cells in the era of increasing myeloid cell diversity. Nat. Rev. Immunol. 2021.

168. Vuk-Pavlović S, Bulur PA, Lin Y, Qin R, Szumlanski CL, Zhao X, Dietz AB. Immunosuppressive CD14+HLA-DRlow/−monocytes in prostate cancer. Prostate. 2010; 70(4):443–455.

169. Waks AG, Winer EP. Breast Cancer Treatment: A Review. JAMA - Journal of the American Medical Association. 2019; 321: 288–300.

170. Wang D, DuBois RN. Immunosuppression associated with chronic inflammation in the tumor microenvironment. Carcinogenesis 2015; 36:1085–1093.

171. Wang, B. etal. Senescent cells in cancer therapy: friends or foes? Trends Cancer 2020; 6, 838–857.

172. Wang C. etal. Inducing and exploiting vulnerabilities for the treatment of liver cancer. Nature 2019; 574, 268–272.

173. Wu, H., Zhen, Y., Ma, Z., Li, H., Yu, J etal., Arginase-1-dependent promotion of TH17 differentiation and disease progression by MDSCs in systemic lupus erythematosus. Sci. Transl. Med. 2016; 8: 331ra40.

174. X. Luo, Y. Fu, A.J. Loza, B. Murali, K.M. Leahy, M.K. Ruhland, M. Gang, X. Su etal., Stromal-initiated changes in the bone promote metastatic niche development. Cell Rep 2016; 14 (1), pp. 82-92.

175. Xu M., Pirtskhalava T., Farr J.N., Weigand B.M etal. Senolytics improve physical function and increase lifespan in old age. Nat. Med. 2018; 24:1246–1256.

176. Xue, W. et al. Senescence and tumour clearance is triggered by p53 restoration in murine liver carcinomas. Nature 2007; 445, 656–660.

177. Yang L, Zhu Y, Tian D, Wang S, Guo J, Sun G, et al. Transcriptome Landscape of Double Negative T Cells by Single-Cell RNA Sequencing. J Autoimmun 2021; 121:102653.

178. Yang Z, Guo J, Weng L, Tang W, Jin S, Ma W. Myeloid-derived suppressor cells-new and exciting players in lung cancer. J Hematol Oncol. 2020; 13(1):10.

179. Zhang K, Hua YQ, Wang D, Chen LY, Wu CJ, Chen Z, Liu LM, Chen H. Systemic immune-infammation index predicts prognosis of patients with advanced pancreatic cancer. J Transl Med. 2019; 17:30.

180. Zhu, Y. et al. Identification of a novel senolytic agent, navitoclax, targeting the Bcl-2 family of anti-apoptotic factors. Aging Cell 2016; 15, 428–435.

Acknowledgements

In this unique journey that I was blessed to have, I would like to extend my gratitude to many supportive and caring individuals who selflessly aided me in completing this project. First and foremost, I would like to thank my supervisor, Prof. Alessandra Gennari, for giving me this fantastic opportunity and believing in my abilities to carry this work. Thank you, Veronica Martini, my tutor, for her guidance and support throughout my PhD, especially during Covid-19 times. She always helped me to overcome the obstacle that could impede my research.

During my phD, I got the opportunity to work around 14 months with Prof. Marco Demaria group in ERIBA, University of Groningen, Netherlands. His passion for research has been inspiring and your encouragement helped keep me motivated during difficult times. Our meeting and discussion were insightful and helped me push my thesis work forward.

Also, I would like to thank all my labmates who either assisted with this project or other aspects during my phD career. Your help in collecting data and general presence in the lab made the time pass much more quickly. I am happy to have crossed paths with all of you and I look forward to seeing what you do in your future careers!

To my parents, Mr. V.K Varughese and Mrs. Elsy Varughese, this work is dedicated to you. You are the ones who believed in my dreams and helped me to make them true. Without you, I would never be here. To my brother, Mr. Febin K Varughese, your inspiration and your visits were the ones that helped me move forward and I am so grateful for that.

Last but not least, Mr. Boby Kurian, my husband, you joined me in the most challenging times of my PhD. You endured my ugly mood swings and my stress. You are always there whenever I need you, thank you so much for being there for me.